MODELING OF PROSPECTIVITY FOR LODE–AU MINERALIZATION IN THE KIBARAN OF UGANDA

M.E. MSECHU

FEBRUARY, 2011

SUPERVISORS:
Dr. E.J.M. Carranza
Dr. F. J. A van Ruitenbeek
Dr. S. Barrit

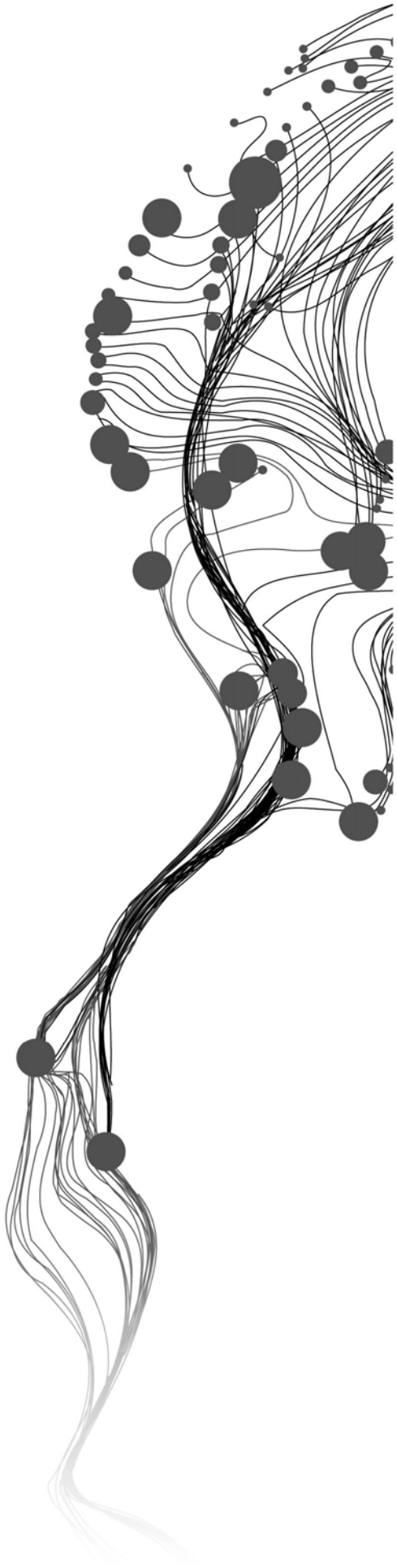

MODELING OF PROSPECTIVITY FOR LODE–AU MINERALIZATION IN THE KIBARAN OF UGANDA

MARUVUKO ELISAMIA MSECHU
ENSCHEDE, THE NETHERLANDS, FEBRUARY, 2011

Thesis submitted to the Faculty of Geo-Information Science and Earth Observation of the University of Twente in partial fulfilment of the requirements for the degree of Master of Science in Geo-information Science and Earth Observation.
Specialization: Applied Earth Sciences

SUPERVISORS:
Dr. E.J.M. Carranza
Dr. F. van Ruitenbeek
Dr. S. Barrit

THESIS ASSESSMENT BOARD:
Prof. Dr. van der Meer (Chair)
Dr. P. M. van Dijk (External Examiner, ITC, University of Twente)
.

ABSTRACT

Accurate prediction of potential zones for the occurrence of new mineral deposits requires an understanding of geological processes that controlled the existing deposits. Understanding these geological controls means understanding the geological processes that were active during the formation and preservation of the deposits sought. Quartz-vein hosted gold mineralization, typical of orogenic gold deposit model occurs in the south-western part of Uganda in which the study area lies. Geologically, it is characterized by deformed and metamorphosed Karagwe Ankole Belt (KAB) lithologies consisting predominantly of biotite gneisses, amphibolites, intebedded schist, metasediments, granites and mafic volcanics.

In order to understand geological processes that are conceived to control mineralization, airborne magnetics and radiometric methods were employed. In addition, digital elevation model (DEM) outlined several surficial deformation features that were in turn used to infer structural conduits related to transportation and preservations of gold bearing fluids. Interpretations of these structural features were to some extent supported by the presence of existing ground structural measurements. Otherwise, standard procedures used to interpret magnetic and radiometric datasets were used.

The results of this study show that the indicative geological features/processes that control mineralization include 1) age of mineralization (Neoproterozoic) 2), proximity to NW-trending faults/shear airborne 3) proximity to NE-trending faults/shear and 4) proximity to anticlines. On the other hand, the results of the analyses of magnetic and radiometric datasets were further used to study and understand lithological variations of existing lithological units. Contrasts within the magnetic dataset are related to either variations within similar/different lithological units or major structural sutures. This understanding led to the identification of new deformation zones and lithological units and subsequently added value to the geological map of the area.

Knowledge-guided data-driven wildcat modeling of mineral prospectivity was used to generate predictor maps independent of existing deposits but based on improved wildcat predictor scores through 5-percentile intervals of distances to the above mentioned evidential features (except for age of mineralization). The resultant scores maps were later integrated using principal component analysis in order to generate prospectivity map of the study area. The prospectivity map was further re-classified based on 5-percentile classes and pixels above 85 percentile, i.e. mean+1SD were considered prospective. Of the total 10 mineral deposits tested, 50% were correctly predicted. In addition, 20% of the area tested, i.e. 132265 out of 661085 pixels, is considered prospective. These prospective zones can be used as potential corridors for strategic mineral exploration programmes of the area.

Keywords: Geology, Orogenic, Karagwe Ankole Belt (KAB)

ACKNOWLEDGEMENTS

I am very grateful to Dr. John Carranza (first supervisor) for his constructive criticisms and innovative ideas. Throughout the whole thesis period, he has been very keen to make sure that the arguments made in this work are scientific and are critically constructed. Your guidance is also highly appreciated. To Dr Frank van Ruitenbeek (second supervisor); I really appreciate your in-depth evaluation of everything I wrote. I remember in one stage of the thesis you commented in one of my arguments, "The idea here is shallow" In this way you built the modality of backing up scientific arguments once presented. I am also cordially appreciating the time and effort shown by Dr. Sally Barrit (third supervisor), to improve this work. You are currently out of ITC, but still you were willingly coming to ITC and spare your time to step by step evaluate and provide technical support/opinion to improve the thesis. Otherwise, the generally responsibilities of this thesis, including its pitfalls and ambiguities, remains mine.

I would also like to extend my sincere gratitude to Dr. Nigel Stack from Fugro together with Dr. Sally Barrit (my third supervisor) who works with Geowitch who helped to have the airborne geophysical available for research. Also I thank the Department of Geological Survey and Mines (DGSM) for their permission to use the airborne geophysical dataset.

On the other hand I truly appreciate the financial support from Joint Japan/World Bank Graduate Scholarship Program (JJ/WBGSP) that made this work possible. The program is really fundamental towards supporting individuals, who in turn can use the knowledge acquired to accelerate sustainable development of their respective nations.

I would also like to extend my gratitude to Drs. Tom Loran, Program Director of AES for accepting my request to come for the second time to pursue MSc. Studies. In addition, I would like to forward my sincere gratitude to Dr. A. B. Westerhof, who far away back in 2005 on top of the of stromatolitic limestone outcrop, NW Tanzania encouraged me to join ITC, and successfully did in 2006. I am as well expressing my appreciation to Drs. J. B. de Smeth for his moral and technical support during my 2006/7post-graduate studies to this end. Special thanks should also go to all other staff/instructors of AES department for their tireless efforts to make sure that fundamental GIS and remote sensing skills are diligently acquired.

I am indebted to Prf. A. Mruma, my employer and chief executive officer of geological survey of Tanzania (GST) for his recommendations that made it possible for me to be accepted and pursue MSc. studies here at ITC. I am also thankfully to all my colleagues and management of GST for all their support. Special gratitude should be conveyed to Mr. E. B. Temu (Director of geology-GST), Mr. A. Minde (Director-data base management-GST), Dr. P. Semkiwa (Manager-applied geology-GST), E. G Kanza (Manager – regional mapping –GST) as well as Mr. J. Kashabano, F. Mosses, A Myumbilwa, P. Nyanda and R. S Kajara, all principal geologists at GST.

I am also thankful to all my classmates in AES whom we share the same cluster during critical phases of thesis writing, including Husin Setia Nugraha and Darwin Edmund Riguer. The memories of cluster 5.056 in the ITC building will remain forever.

Lastly, but not least in order of importance, I would like extend my heartfelt gratitude to my wife-Rehema and my lovely son-Brian. The daily communications made the studying environment here in the Netherlands quite pleasant.

TABLE OF CONTENTS

Contents

LIST OF FIGURES

LIST OF TABLES

APPENDIX

1. INTRODUCTION

1.1. Background to the Research

Understanding of geological controls on mineralization, by studying the characteristics of existing deposits of a certain type, in order to locate prospective zones where undiscovered mineral deposits of the same type are likely to occur is one of the prime foci for the sustainable development in the mining industry. Understanding the geological controls on mineralization means understanding the geological processes that were involved in the formation and distribution of mineral deposits in space and time by adopting a mineral system approach (McCuaig et al., 2010). This approach is based on the fact that mineral deposits are small manifestations of larger-scale geological processes. McCuaig et al. (2010) proposed this four-step approach towards understanding and translating a mineral system into 'effective exploration targeting systems' such as predictive modeling of mineral prospectivity (Fig. 1).

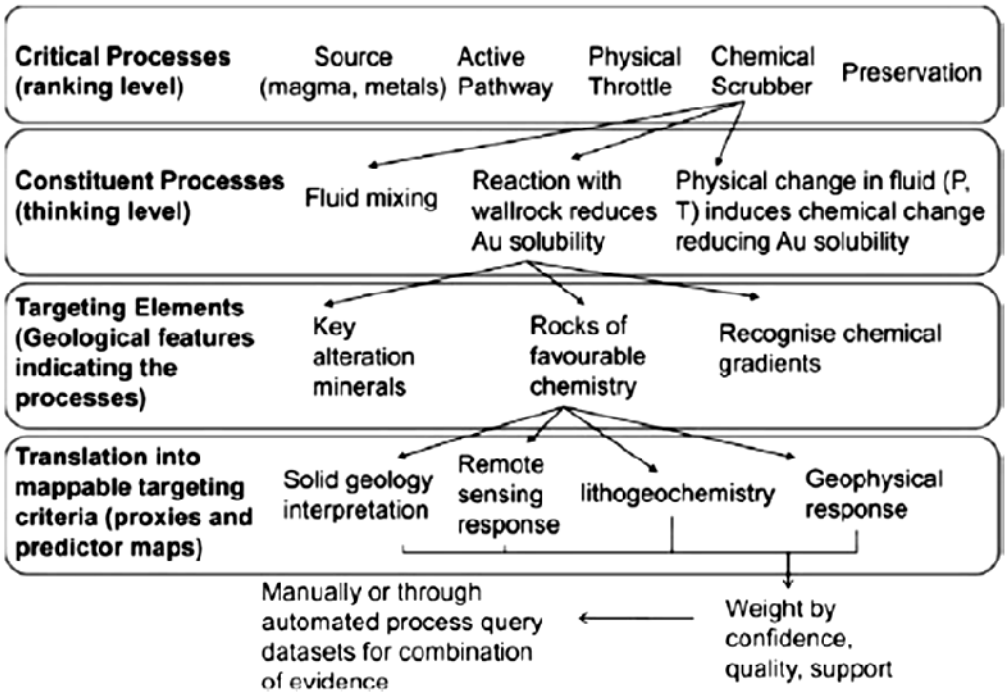

Fig 1: Critical and constituent processes, targeting elements and mappable targeting criteria for orogenic gold mineral system (*from McCuaig et al. 2010*).

Understanding of geological processes is fundamental to mineral prospectivity mapping using GIS (Knox-Robinson and Wyborn, 1997). Having a sound knowledge of the genesis of the existing deposits is a prime prerequisite in predicting the favourability for occurrence of undiscovered deposits in mineral prospectivity modeling (Bonham-Carter, 1994). Whenever a new geological understanding of mineral deposit formation has been proposed, mineral prospectivity modeling must be adapted to accommodate that new understanding. The former has happened in south-western Uganda, where the study area of this research lies. In the past, gold mineralization in the area was considered to be associated with post-Kibaran Event (Brinckmann et al., 1994; Pohl, 1994; Pohl and Günther, 1991), which was considered to be of a protracted character. Based on the recent studies by Tack et al. (2010), the above assumptions are

no longer valid and that the 'Kibaran Event' is now considered to be a short lived but prominent tectono-magmatic event between 1380 Ma to 1370 Ma. In the past, the event was considered to occur between 1400-950 Ma (Pohl, 1987). The mineralization is now considered to be post Lomanian Orogeny (1Ga-950Ma), (Pohl, 1987) tectonically associated with tin granites at 986 Ma (Tack et al., 2010). The mineralization is hosted in the quartz vein i.e. quartz-vein hosted type of gold deposits (Pohl and Günther, 1991)

However, mineral deposits are non-renewable resources. This means that mineral deposits of whatever sizes may eventually be depleted. Therefore exploration for the discovery of new mines is vitally important for the sustainable development of mining industry. GIS can effectively be used in predicting prospective grounds for the discovery of new deposits by studying the spatial association of the existing deposits and their related geological features based on geo spatial datasets (Hosseinali and Alesheikh, 2008; Scott, 2000)

In the search for favourable mineral exploration targets, analysis of geoscientific data to determine areas most likely to contain mineral deposits is becoming increasingly common in the mining industry. The approach is based on characterizing areas known to contain mineral deposits and seeking similar areas elsewhere (Holden et al., 2008). Based on the qualitative and quantitative examinations of available geospatial datasets involving the knowledge of spatial associations between various geological features and existing mineral deposits, GIS can assist in deriving better prediction of new potential sites of the respective minerals under investigation(Bonham-Carter, 1994).

There are two main approaches followed in using GIS to predict prospective areas for undiscovered mineral deposits based on the existing ones, namely knowledge- and data-driven approaches (Bonham-Carter, 1994). In applying the knowledge-driven approach to mineral prospectivity mapping, preferences are based on the 'expert knowledge' about the spatial associations between certain geological features/processes and the type of mineral deposits sought. In addition, substantial field experiences in understanding genetic characteristics of the deposits under investigation is of prime prerequisite in this approach (Carranza, 2008). On the other hand, this subjectivity in the knowledge-driven approach is minimized, if not avoided, in the data-driven approach. As the name stands, data-driven approach to mineral prospectivity mapping involves systematic execution and evaluation of reliable spatial datasets that are used to determine geo-spatial features related to known mineralization (Hosseinali and Alesheikh, 2008).

Based on either data- or knowledge-driven knowledge approach, several methods have been developed and are applied to produce predictive mineral prospectivity maps of a given area. Carranza and hale (2000) applied a data-driven approach based on Bayesian probability known as weights-of-evidence modeling by combining binary patterns of geological features to predict and locate gold prospective areas in the Baguio district of the Philippines. Hosseinali and Alesheikh (2008) employed six methods namely logistic regression, weights-of-evidence and artificial neural networks (ANN) (as data-driven methods) as well as analytical hierarchy process (AHP), Delphi and ratio estimation (RE) (as knowledge-driven methods) to assess and rate/weight predictors of copper mineralization and then produce copper prospectivity maps of the Ali-Abad area, central Iran. Several other authors have applied predictive modeling techniques to predict, model and map prospective sites of particular types of mineral deposits (Asadi and Hale, 2001; Scott, 2000).

This research aims at addressing the application of improved wildcat modeling of mineral prospectivity (Carranza, 2010) to determine prospectivity zones for undiscovered gold deposits in south-western Uganda. According to Carranza (2010), improved wildcat modeling of mineral prospectivity (WMMP) is in fact a knowledge-driven data-guided method that determines optimum distances to indicative geological

features i.e. anticlines, without incorporating locations of existing deposits (presumed non –existing). These optimum distances are considered as zones where a mineral deposit can occur. Unlike data driven method of mineral prospectivity, WMMP does not need training data of mineral deposits to be used as input in quantifying them with their respective indicative geological features. Therefore, with this characteristic, WMMP is a plausible method in regions, like this study area, where there are few existing mineral occurrence. The few deposits existing are only used to validate the mineral prospectivity map generated.

1.2. Research Problem

The south-western (SW) corner of Uganda, where the study area lies, contains several mineral deposits of valuable wealthy, including gold (Hester et al., 2006; Kogre and Afilaka, 1988). Understanding the geological processes related to the genesis of each of the known types of mineral deposits is a prime prerequisite towards predicting the favourability of occurrence of undiscovered deposits of each of those deposit types. In this study the focus is gold mineralization.

In the past, as stated earlier, gold deposits in the area were postulated to be associated with post 'Kibaran Event' that was portrayed to be an extended orogenic event occurring between 1400-900 (Pohl and Günther, 1991) with successive extensional and compressional phases (e.g., Pohl, 1994; Rumvegeri, 1991) Therefore, the protracted nature of the then Kibaran Event in conjunction with its associated extensional tectonic regimes hampered the emplacement of the gold mineralization into orogenic deposit model. The recent studies by Tack et al. (2010) refuted this protracted nature of the Kibaran Event. The Kibaran Event is now postulated to be associated with narrow but prominent tectono-magmatic event that occurred between 1380 Ma to 1370 Ma (Tack et al., 2010). Having this understanding in place, gold mineralization in SW Uganda can now be firmly conceived to be associated with orogenic deposit model with Lomanian orogeny being a possible compressive event around 1000-950Ma (Pohl, 1987) and that the mineralization is tectonically associated with tin granites (Pohl and Günther, 1991) at 986±10 Ma (Tack et al., 2010).

However, the study area has got few gold deposits. The challenge is now to adapt the recently developed geological understanding associated with the mineralization of the area in order to predict new zones of undiscovered deposits. In addition, indicative geological features controlling the gold deposits in the study area, which are important components in predictive modelling, have not been established.

1.3. Research Objectives

The main objective of this research is to study, determine and outline the indicative geological processes/features associated with gold mineralization in SW Uganda based on the new geological understanding of the area and utilize computer-based prospectivity modeling technique guided by lithology, digital elevation model (DEM) and airborne geophysical datasets in order to delineate favourable zones for the occurrence of undiscovered deposits. To address this objective properly, the following sub objectives have been formulated:

1. To identify the genetic characteristics of gold mineralization in SW Uganda based on the recently developed geological understanding of the area.

2. To study, determine and outline favourable zones for the occurrence of undiscovered gold deposits in SW Uganda.

1.4. Research Questions

1. How can geophysical and geological spatial variables/features existing in SW Uganda be applied to study, understand and map the geological processes related to gold mineralization?

2. How can the current knowledge of geological processes/features associated with gold mineralization in SW Uganda be used to determine and predict viable and plausible sites potential for the undiscovered deposits?

1.5. General Methodology

In order to achieve the objectives of this study, literature review was carried out in order to understand general geology, gold mineralization and geodynamic evolution of the area. Understanding the geology of the area and its associated gold mineralization was a vital step towards developing a mineral deposit conceptual model.

Conceptual model constitute typical characteristics of mineral deposit sought. These characteristics were used to extract indicative geological features guided by geological map, airborne magnetics, radiometric and DEM. Based on improved version of wildcat modeling of mineral prospectivity (WMMP), which is a knowledge-guided data-driven technique (Carranza, 2010), predictor maps were created using the indicative geological features. During the creation of predictor maps, the mineral deposits are considered non-existing. In addition, all the predictor maps were re classified based on the age of mineralization i.e. Neoproterozoic

Finally, principal component analysis was applied to integrate the predictor maps in order to generate the mineral potential map of the area. Furthermore, the mineral deposits that were previously considered non-existing were then used to validate the mineral potential map already created. The flow chart for the methodology is presented in Fig 1.5.

1.6. Expected Results and Thesis Outline

1.6.1. Research Output

This research is expected to provide mineral potential map of the study area, delineating favourable zones for the occurrence of undiscovered deposits. In addition, these zones are considered to be potential sites for strategic mineral exploration programmes covering the study area.

1.6.2. Thesis Structure

This thesis is comprised of six chapters. Chapter one introduces the background to the research, problem definition, objectives, questions and general methodology. General literature study on geology and characteristics of lode gold mineralization as well as deposit conceptual model are emphasized in chapter two to be followed by datasets and methodology used in this research and its implementation (chapter three). Chapter four is comprised of the results of data analysis and interpretation. Indicative geological features, generation of predictor maps and spatial data Integration for predictive mineral mapping are discussed and presented in chapter five. Chapter six: deals with general conclusions and recommendations.

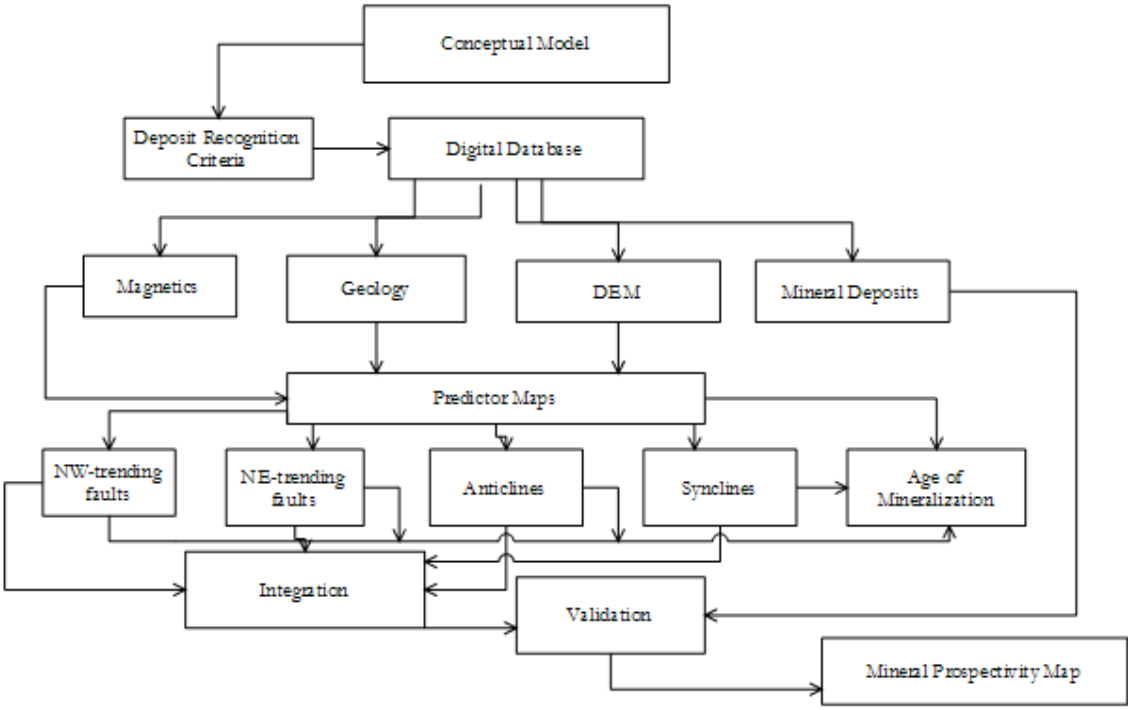

Fig 1.5 Flow chart for the Methodology of Mineral Prospectivity Map

2. THE STUDY AREA

2.1. Location, Accessibility and Mining History

The study area is situated in the south-western part of Uganda. Uganda is located in east Africa and it shares common frontiers with Kenya to the east, Tanzania and Rwanda to the south, the Democratic Republic of Congo (DRC) to the west, and Sudan to the north (Fig. 2.1). Except for few areas of elevated ground altitude, the greater part of the study area consists of an average altitude of about 1500 m (Hester et al., 2006). The mean high temperature varies between 25ºC and 30ºC with a mean low temperature of about 15ºC (Hester et al., 2006). The study area can be accessed from Kampala via the Kampala – Kasese road or the Kampala – Masaka – Mbarara road (Fig. 2.1). Several airstrips exist at Kasese, Mbarara, Kabala and Kisoro. The area can also be reached via the railway line from Kampala to Kasese. The history of mining and prospecting in the area began in the mid-1920s with tin and gold, and expanded to include other minerals such as beryllium, bismuth, copper, cobalt, etc. (Hinde and Peters, 2007).

Fig 2.1: Location of the study area (*after Hester et al., 2006*)

2.2. General Geology Geodynamic Evolution and Gold Mineralization

The study area lies within the previously portrayed single and continuous Mesoproterozoic Kibaran orogenic belt, which extends for more than 1500 km from the triple junction of DRC, Angola and Zambia, and trends NE-SW all the way to Burundi, Rwanda, NW Tanzania and SW Uganda (Buchwaldt et al., 2008; Rumvegeri, 1991; Tack et al., 1994). The Kibaran belt is characterized mainly by deformed metavolcanics and metasediments (Hester et al., 2006; Rumvegeri, 1991; Tack et al., 1990), which consist of amphibolites, dolomitic limestone, red mudstone, amygdaloidal lava, banded chert and ironstones (Hester et al., 2006).

However, the recent studies based on satellite imagery done by Tack et al. (2010) have revealed a break in the continuation of the previously thought single and continuous Kibaran orogenic belt. The belt has now been interpreted to be crosscut by the Palaeproterozoic Ubende and Rusizian terranes of Tanzania and DRC, respectively (Fig. 2.2). Hence, the Kibaran orogenic belt is now separated into two distinct belts (Fig. 2.2): (1) the Karagwe Ankole Belt (KAB), comprising the NE-extension of the Ubende-Rusizian terranes formerly known as North-eastern Kibaran Belt (Tack et al., 1994); and (2) the Kibara Belt (KIB), comprising the SW extension of the Ubende-Rusizian terranes.

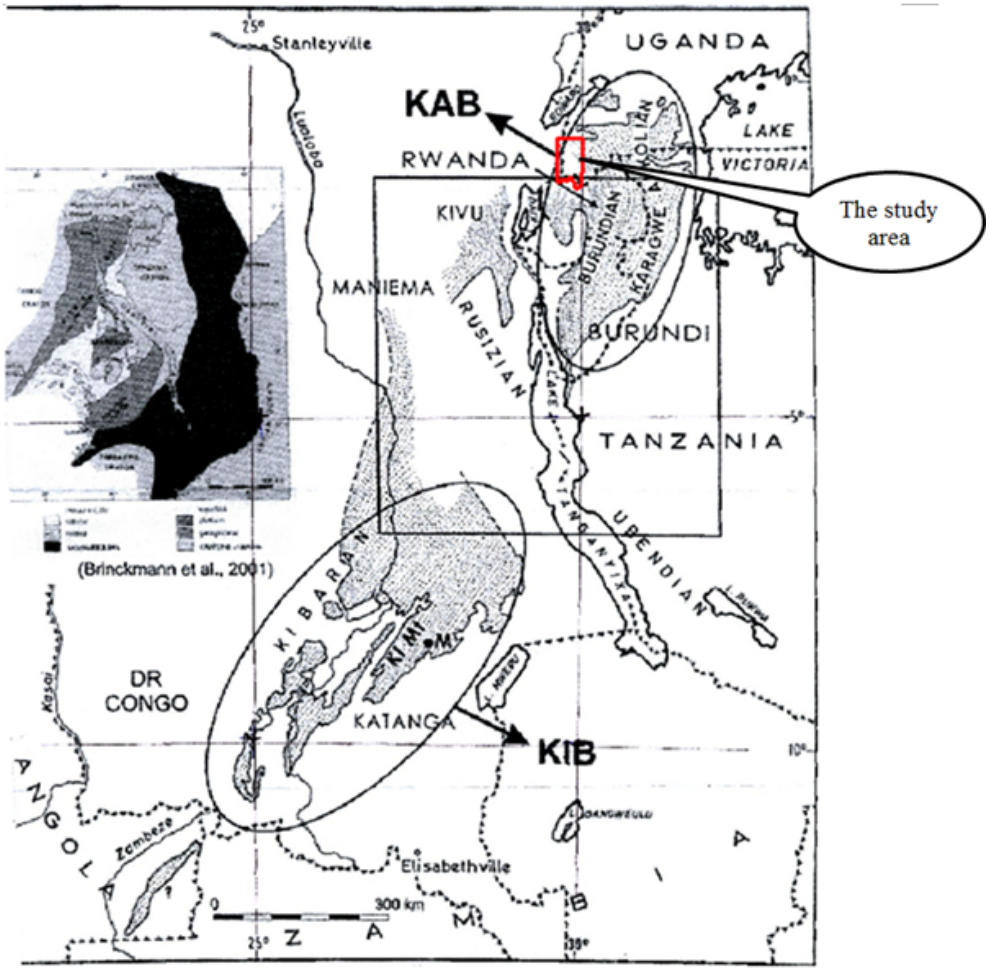

Fig 2.2: Geographical location of Kibara Belt (KIB) and Karagwe Ankole Belt (KAB) (*after Tack et al., 2010*)

The newly redefined NE-SW trending Mesoproterozoic KAB has been further subdivided into two domains, namely, the Western and Eastern Domains, Fig 2.3. The Western Domain (WD), where the

study area is situated (Fig 2.3), has been intensely deformed and highly metamorphosed. According to Tack et al. (2010), it is composed of deformed greenschist to amphibolite facies Mesoproterozoic metasedimentary rocks and subordinate, inter-layered metavolcanic units. The Eastern Domain (ED) overlies the less deformed Archaean gneissic basement of the Tanzania Craton (Fig 2.3), (Tack et al., 2010).

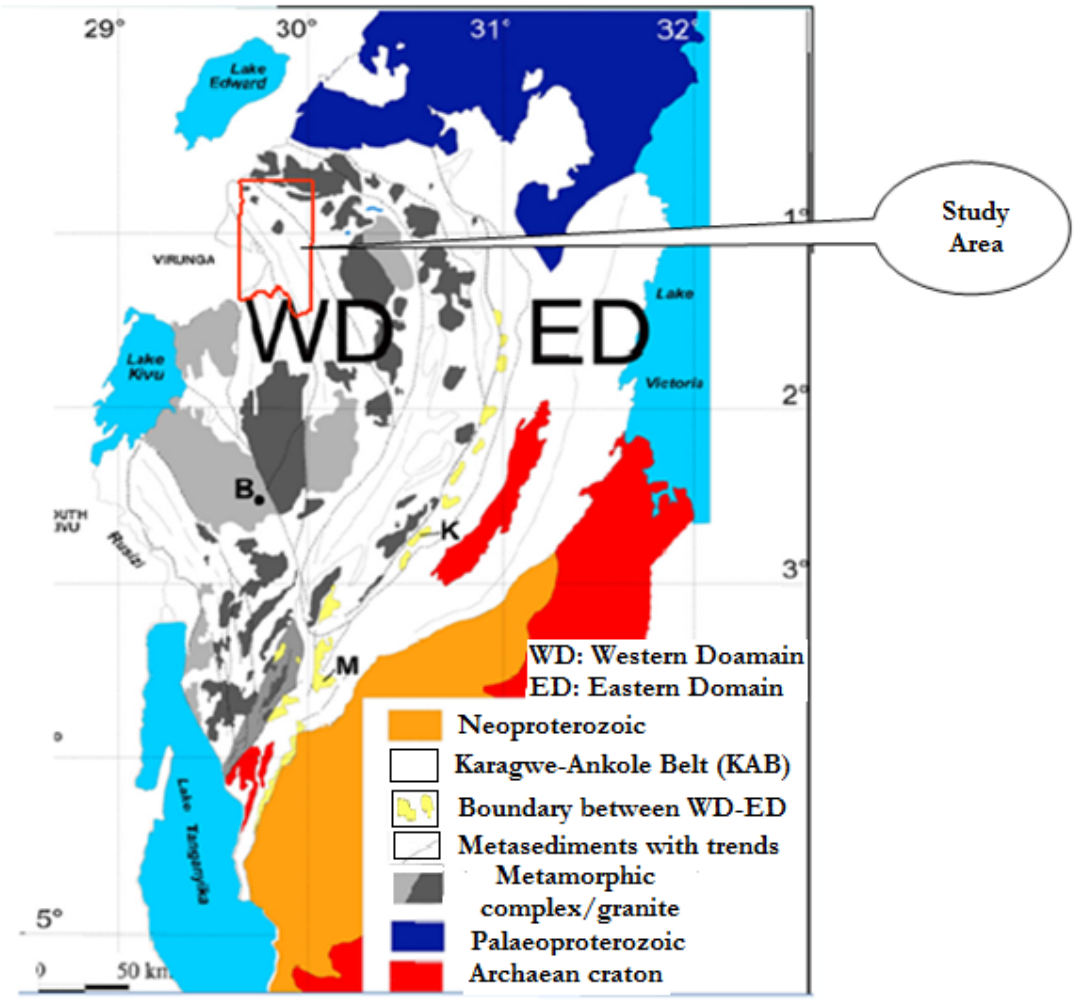

Fig 2.3: Sketch map of the Karagwe-Ankole belt with WD (Western Domain) separated from the ED (Eastern Domain) by a boundary zone comprising the Kabanga-Musongati (KM) alignment of mafic and ultramafic layered complexes (after Tack et al., 2010). K = Kabanga massif. M = Musongati massif. B = Butare town. The boundary between WD and ED is marked by the presence of KM (ultra)mafic complexes. (*after Tack et al., 2010*)

Magmatism in the KAB was postulated to have occurred around 1275 Ma (Tack et al., 1990; Tack et al., 1994). On the other hand, the new findings by Tack et al. (2010) show that magmatism in KAB occurred earlier and was associated with profuse emplacement of bimodal intrusions between 1380 Ma and 1370 Ma (Table 2.1). These bimodal intrusions consist of about 350-km long and NE-SW trending Kabanga-Musongati (KM) mafic-ultramafic layered intrusions (Fig 2.3) associated with Ni-Cr-Cu-V-Fe-Ti and PGE (Rumvegeri, 1991; Tack et al., 1994). The KM mafic-ultramafic intrusions are postulated to be coeval with S-type granitoids and both are said to originate from an enriched lithospheric mantle source (Tack et al., 2010). The geological setting related to the early phase of magmatic intrusions in KAB is now considered to be associated with an extensional regime in a regional-scale intra-cratonic setting, creating permissive

conduits for the emplacement KM mantle-derived magmatism (Tack et al., 2010). In addition, the mantle-derived magmas initiated 'concomitantly large-scale, crustal melting preferentially of the Palaeoproterozoic basement under extension at 1375 Ma and characterized by the absence of a thick lithospheric profile in contrast to the nearby Achaean Craton' (Tack et al., 2010). According to Tack et al. (2010), the short-lived but prominent tectono-magmatic event was followed by A-type granitoid intrusions at 1205 Ma and a later on invasion by tin granites at 986 Ma (Table 2.1).

Table 2.1: Geodynamic evolution of KAB, observe the difference between age of emplacement of KM bimodal magmatism as postulated by Tack et al. (1994:1990) and Tack et al. (2010).

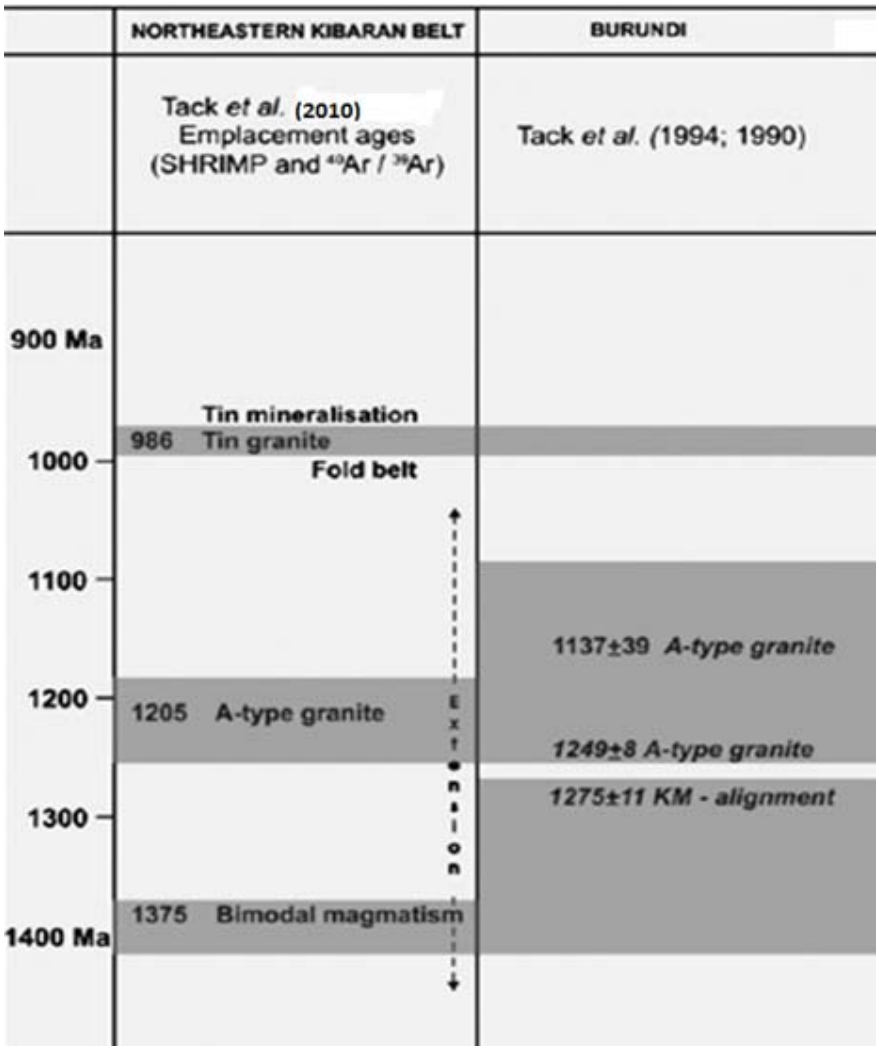

Pohl and Günther (1991) studied the genetic relationship between the Sn-W mineralization associated with the above 986 Ma granitic intrusion and the gold quartz vein deposits on the north-eastern part of the then Kibaran belt (now KAB). The 986 Ma granitic intrusion may have been observed to be spatially unrelated to gold mineralization; however, they are both postulated to result from deep crustal thickening processes similar to the Sn-W mineralization (Fig. 2.4). The faults created earlier during the geodynamic evolution of the Kibara Belt (now KAB) acted as the conduits, which were used as channels for the advection of deep crustal ore bearing fluids (Pohl and Günther, 1991). The general tectonic setting and resulting alteration products associated with gold mineralization in KAB is further emphasized in the

coming sections. The style of gold mineralization is typical of orogenic gold deposit model as proposed by Groves et al. (1998).

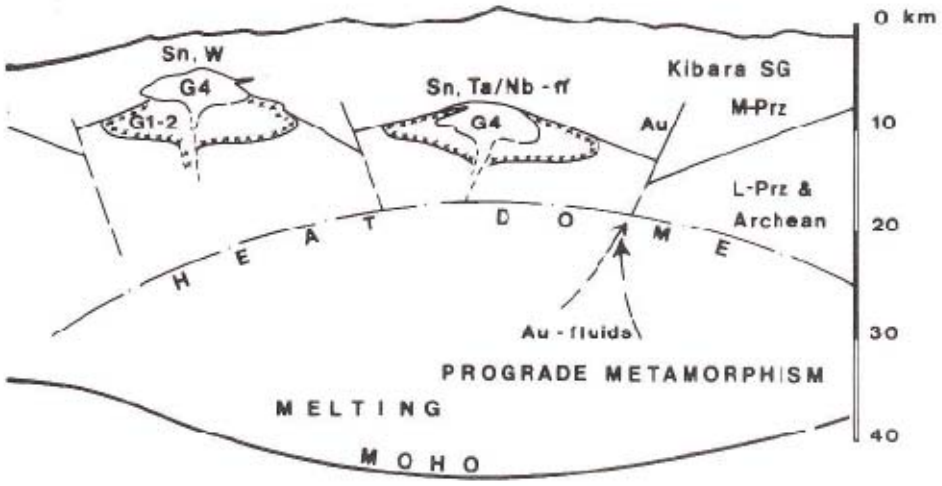

Fig 2.4: Conceptual model of Sn-W and Au mineralizations. G1-2: adamellitic granites; G3: alkaline biotite granite; G4: pegmatitic granite (*Pohl et al., 1991*).

2.3. Orogenic Gold Deposits in General

Several studies have been conducted to determine and quantify the generally common characteristics of epigenetic gold deposits (Arehart, 1996; Hedenquist and Lowenstern, 1994; Lang and Baker, 2001; Sewell and Wheatley, 1994; Sillitoe, 1997). The quantification of these characteristics as evidenced in Table 2.2, are based on tectonic setting, temperature of formation, depth of emplacement, ore fluids composition as well as the resultant alteration types (Campbell and Kerrich, 1998; Groves et al., 1998; Hedenquist and Lowenstern, 1994). The style of gold mineralization discussed in this report is associated with deformed metamorphic and intensely altered lithological units and hosted in quartz veins.

Several terms such as metamorphic gold, mesothermal gold, shear-zone-hosted gold, gold quartz vein, stockworks, structurally-controlled deposits as well as greenstone-hosted gold mineralization have been used to describe similar mineralization styles (Cox et al., 1991; Eisenlohr et al., 1989; Fan et al., 2003; Pal and Mishra, 2002; Zhu et al., 2007)). On the other hand, there has been a confusion associated with the misuse of the original definitions of some of these mineralization styles. For instance, the depth of emplacement of mesothermal gold deposit is characteristically between 1.2 and 3.6 km (e.g., Groves et al., 1998) in contrary to the characteristics of other gold mineralization styles mentioned above. To avoid the confusion, Groves et al. (1998) proposed orogenic gold deposit model, whose general characteristics are summarized in Table 2.2.

Orogenic gold deposits are postulated to be both lithologically and structurally controlled (Groves et al., 1998). Lithologically and based on the favourability of mineral geochemistry of the host rocks, the deposits can occur in any type of rock, although most deposits have been confirmed to occur in metamorphic terranes of all ages (Groves et al., 1998), associated with sub-greenschist and amphibolite to granulite metamorphic facies conditions (Campbell and Kerrich, 1998; Groves, 1993).

Table 2.2 Characteristics of some common epigenetic gold deposits (*after Groves et al., 1998*). Note the common geological features associated with orogenic gold deposits.

Deposit type	Tectonic setting	Depth of emplacement (km)	Alteration type	Important geological features
Orogenic	**Continental margin; compressional to transpressional regime; veins typically in metamorphic rocks on seaward side of continental arc**	**2-20**	**carbonation, sericitization, sulfidation; skarn-like assemblages in higher temperature deposits**	**hosted in metamorphic terranes; spatial association with transcrustal fault zones and granitic magmatism**
Sedimentary -rock hosted	back-arc extension and thinning of continental crust	2-3	intense silicification; some kaolinization	Very fine grained gold in intensely silicified rock; dissolution of surrounding carbonate
Gold rich skarn	Oceanic or continental arc; subduction related but often associated with extension environment	1-5	garnet-pyroxene-epidote-chlorite-calcite	most occur as calsic exoskarns; typically associated with mafic, low silica, very reduced plutons
Submarine exhalative	Back-arc rift basins (Kuroko-type) or mid-oceanic seafloor spreading (Cyprs-and Besshi-type)	On or near seafloor	Quartz-talc-chlorite is most common associated with illite;anhydrite or barite cup in some places	Laminated, banded or massive fine-grained sulphides; exhalative and synsedimentary replacement textures

According to Groves et al. (1998), orogenic gold deposits are mineralogically associated with quartz veins with significant amount of sericites, sulphides and carbonates. In addition, albite, mica, chlorite, scheelite and tourmaline have been observed to occur as gangue minerals (Groves et al., 1998).

Structurally, most of orogenic gold deposits are formed proximal to terrane-boundary deformation structures zones associated with extensive hydrothermal plumbing systems (Campbell and Kerrich, 1998) and syn-to post-peak metamorphism. They are normally characterized by high fluid fluxes along fault or shear zones structural controls (Campbell and Kerrich, 1998; Cassidy et al., 1998). These structural controls are always of second to third order suture zones near large-scale compressional to transpressional tectonic regimes associated with convergent plate corridors (Groves et al., 1998). According to Groves et al. (1998), the ore forming fluids associated with orogenic gold deposits are postulated to be generated as a result of subduction-related thermo-tectonic event resulting from multiple phases of magmatism and metamorphism of ore-bearing lithological units at depth.

A summary of the general tectonic setting of epigenetic gold deposits is presented in Fig 2.5. Hence, by reviewing the geodynamic history of KAB as proposed by Tack et al. (2010), the quartz-vein hosted gold mineralization of the study area has a genetic relationship with granitic magmatism under compressional tectonic regime (Pohl and Günther, 1991). The host geological environment includes deformed meta-

sedimentary terranes that are spatially associated with transcrustal structural zones dominated by folding and thrusting (Pohl and Günther, 1991). Along with the alteration products (see section 2.4), the gold mineralization style in the study area is therefore considered to be typical of the orogenic gold deposit model as proposed by Groves et al (1998) (Table 2.2) and outlined in Fig 2.5.

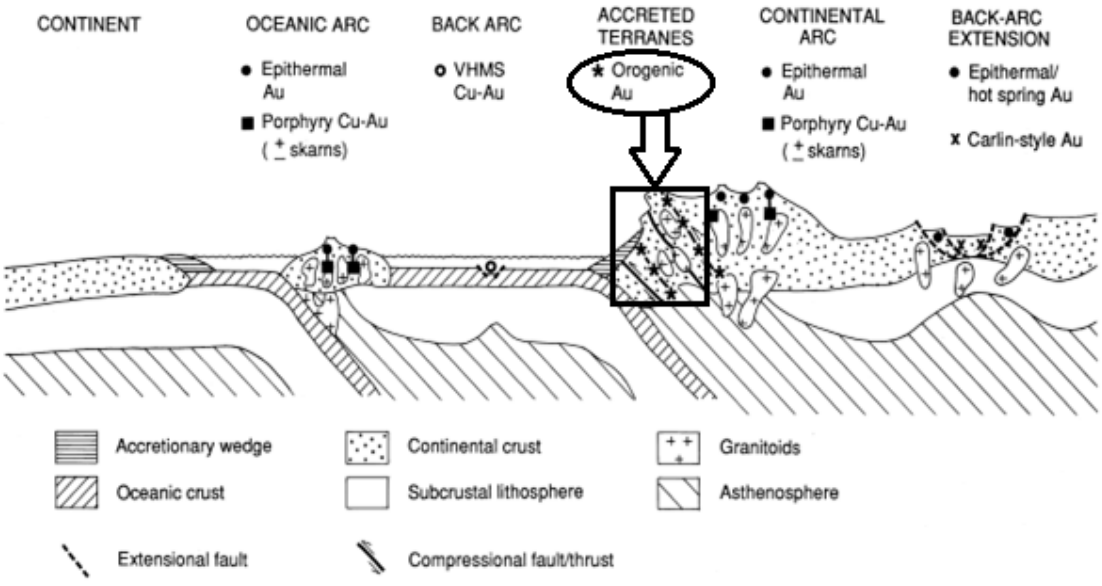

Fig 2.5: General tectonic setting of gold-rich epigenetic mineral deposits showing orogenic gold deposits associated with compressional structures under convergent plate margins in deformed accretionary belts adjacent to continental magmatic arcs typical of gold mineralization in the study area (*after Groves et al., 1998*)

2.4. Gold Mineralization in the KAB

The gold-bearing fluid associated with the quartz-vein gold deposits in KAB is postulated to be generated at depth as a final consequence of crustal thickening (Pohl and Günther, 1991). The ore forming fluid was channelled along compressional deformation systems, composed of regional crustal-scale fault zones, and was trapped by favourable lithologies and structures. These structures are mostly controlled within syn-to post-peak metamorphism and in the transition zone between ductile and brittle structural levels. The general structural trends are mainly vertical shear zones orienting NW-SE to NE-SW associated with faulting and mylonitization.

Lithologically, the lode gold mineralization in the KAB is controlled within mafic rocks, metasediments and greenstone lithologies of volcanic origin (Pohl and Günther, 1991). The host rocks have been subjected to various metamorphic conditions ranging from greenschist to amphibolitic facies conditions along regional-scale shear-zone hydrothermal corridors where they are hosted by various favourable lithologies. These host rocks include amphibolites, mudstones, shales and siltstones (Pohl and Günther, 1991). The hydrothermal alterations associated with lode gold mineralization include carbonitization, pyritization, chloritization and argillation (for greenstones) and sericitization, silicification, pyritization and tourmalization (for metasediments), (Pohl and Günther, 1991).

2.5. Implication of the Current Geological Knowledge to Lode Gold Mineralization in the KAB

For many decades the 'Kibaran Event' was portrayed as an extended orogenic event that affected the then Kibaran belt (now separated and known as KAB and KIB) before 1370 Ma to 1310 Ma, and that the tin granite intrusions and its associated quartz-vein gold mineralization was postulated to post-date this event (Brinckmann et al., 1994; Pohl, 1994; Pohl and Günther, 1991).

Based on the recent studies by Tack et al. (2010), the above assumptions as well as the geodynamic evolution of the whole belt are no longer valid (see section 2.2 of this report). Hence, by reviewing the tectonic history of KAB as proposed by Tack et al. (2010) (see also Table 2.1), the following assumptions are made: 1) the bi-modal magmatism from an enriched lithospheric mantle origin together with other subduction-related thermal processes could have contributed to the initiation of deep structural break-ups, 2) zones of deep structural break-ups controlled by compressive deformation and associated with deep-crustal metamorphism resulted into: a) anatexis that resulted into tin-granite intrusion (Pohl and Günther, 1991) and b) crustal thickening that cause the generation of fluid-forming gold deposits (Pohl and Günther, 1991). In addition, Pohl and Günther (1991) emphasized that the structural break-ups acted as channels to trap and transport deep crustal gold-bearing fluids to favourable host lithologies. On the other hand, the presence of a Palaeproterozoic basement has been proven to underlie WD of KAB (Tack et al., 2010). This has been a very positive discovery because Pohl and Günther (1991) earlier demonstrated the broad correlation between this basement underlying KAB and source of gold mineralization. Furthermore, the KM mantle-derived magmatism emplacement is now confirmed to be intruding KAB earlier than previously thought (Table 2.1), which justifies its role in the formation of deep structural break-ups. Hence, the existence of mafic lithologies in conjunction with predominant NE-SW to NW-SE structural trends of the study area also justifies the potential extension of permissive conduits favourable for the discovery of zones of undiscovered deposits, which is the prime focus of this study.

2.6. Local Geology

The existing geological map of the study area (Fig. 2.6) was compiled from the 1:100.000 scale geological maps of Rukungiri and Kabale, which were published in 1960 and 1965 respectively. Therefore, these geological maps were helpful in deriving geological explanations of the study area.

The basement of the area is characterized by gneisses (refoliated gneisses) of Palaeproterozoic age (probably Toro System) dominating the northern part of the study area. These basement rocks are associated with lenses of amphibolite and quartzites. Lithostratigraphically, the basement is also postulated to be unconfomably overlain by intebedded schists and gneisses. According to the 1960 published geological map of Rukingiri, the age of intebedded schists and gneisses is uncertain, but it can generally be perceived as Mesoproterozoic.

On the other hand, it should be noted that most of the rocks in the study area are comprised of complex metasedimentary units. Therefore, based on their associations with felspathic grits, quartzite, sandstone and also conglomerates, these metasediments have further been subdivided into lower, middle and upper series.

The lower series is dominated by biotite gneisses and migmatites. In addition, mudstones and phyllites with occasional arenaceous horizons are present in the lower series. Other dominant lithologies in this series include minor quartzites, felspathic grits and quartz-rich schist with biotite lenses.

The middle series consists of arenaceous-dominated metasediments. The arenaceous shift is preferential, with mudstones, shales and ferruginous siltstone dominating the east and central parts of the study area,

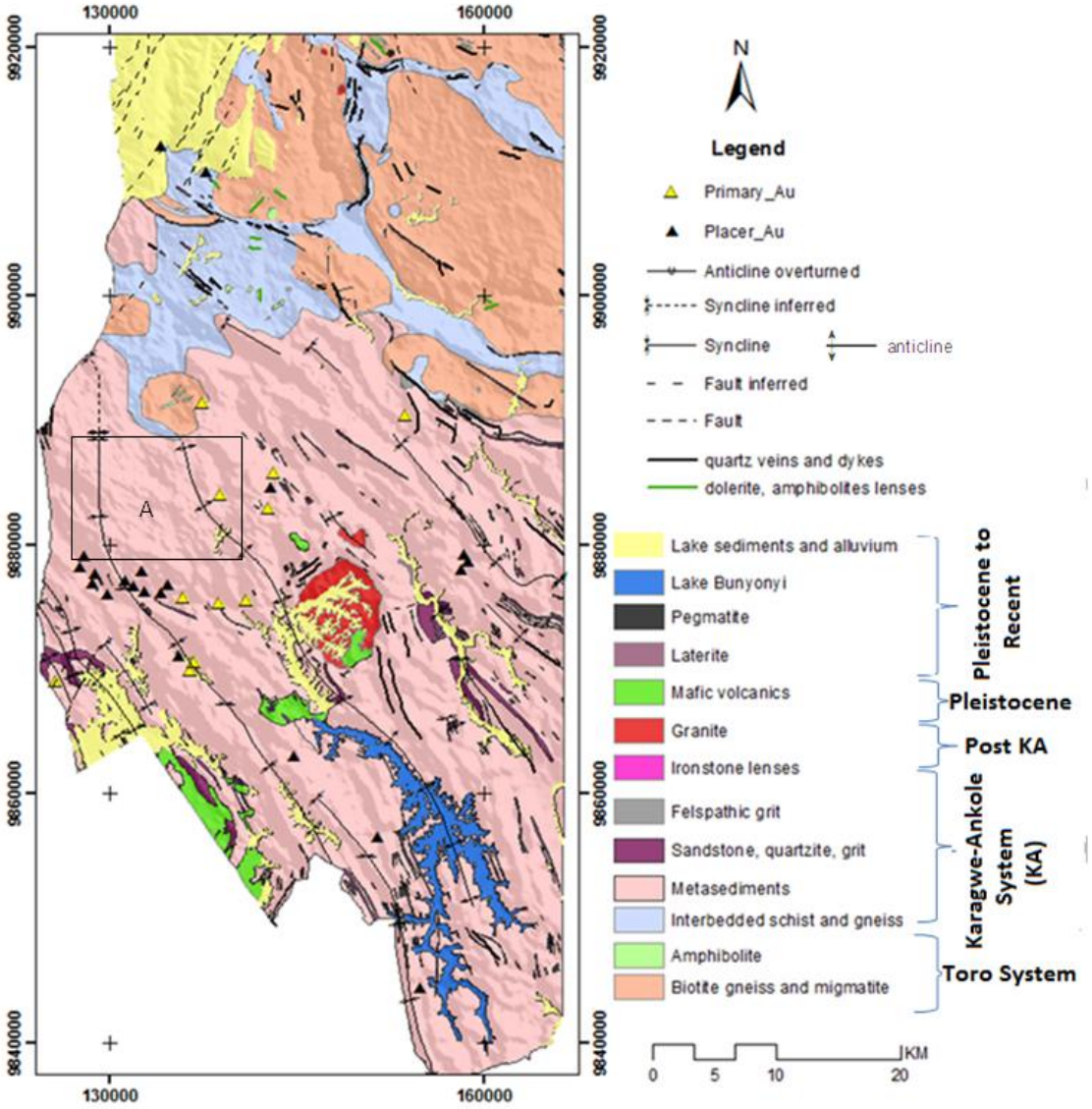

Fig 2.6: The existing geological map of the study area. (*digitized from the geological map of Rukingiri (1960) and Kabale (1965)*)

which became progressively arenaceous towards the southwest. Concomitantly, numerous ironstone lenses have been recognized and proved to be present within quartzites, grits and mudstones. The ironstone lenses are commonly specular and sometimes massive, consisting chiefly of hematite which is occasionally limonitic.

The upper series is somehow distinctive to both lower and upper series characterizing the study area. In addition to the presence of mudstones, shales and siltstones, conglomerates, possibly polymictic, are also present. It is not yet clear which kind of unconformity these conglomerates signify. However, where the conglomerates appear to be polymictic, which can be considered to be the case here, they can signify erosional unconformity (Pohl, 1987). Otherwise, the units in this series are often ferruginous with impersistent sandstone and quartzites.

Magmatic activity in the study area is evidenced by the presence of the unfoliated coarse-grained biotite granite, which intruded the metasediments in the central part (Fig. 2.6). Other acidic intrusions postulated to be of similar composition have been observed to intrude the schists and gneiss in the northern part. The same type of intrusions, considered to be of calc-alkaline tendency, have been reported to intrude the metasediments in Burundi (Radulescu, 1982). Other magmatic activities are confined to the extreme end of the south-western part of the study area. These magmatic activities are represented by the Pleistocene to Recent mafic volcanics chiefly dominated by basalts and andesites.

The dominant superficials include late Pleistocene to recent undifferentiated swamps and alluvium occupying the northern, central and western parts of the study area. Other superficials related to lacustrine deposits mostly occupy the central and southern parts of the study area. They include laterites, boulder deposits, sands, clays and gravels.

2.6.1. Metamorphism

Generally, the metamorphic grade that affected the Kibaran (now KAB), in which the study area lies, is significantly low (Pohl, 1987) . The degree of metamorphism is very low within the synclinoria i.e. location A and increase progressively to reach the amphibolite facies towards large batholithic granites i.e. location B and anticlinal basement (Pohl, 1987). On the other hand, Pohl (1987) also emphasizes that where amphibolite facies metamorphism is attained, migmatite also occurs. Hence, the existence of synclinoria, migmatite and granitic intrusion signify the presence of low to amphibolite facies metamorphism in the study area.

2.6.2. Structures

According to Pohl (1987), most of the then Kibaran (now KAB) rocks are characterized by wide anticloria and significantly narrow synclinoria. In other words, the synclines are generally tightly folded (Radulescu, 1982). The folds are generally upright and are cylindrical in shape characterized by varied fold axes (Pohl, 1987). Two prominent deformation trends are present in the study area. These deformation trends can be vital toward understanding the relationship between the deposits formations and their associated tectonic events. The deformation corridors are typical of faulting and shearing, locally thrusted and running approximately NW-SE and NE-SW. In addition, the dominant fold axes in the study area trend approximately NW-SE.

2.6.3. Mineral Deposits

In the study area, 11 quartz-hosted gold and 22 placer deposits are present in the study area. The dominant lithologies that have been currently recognized to host the primary gold-rich quartz veins in the study area are the metasediments (Pohl, 1994). The primary deposits are considered to be the source of gold placers occupying the present day valleys (Pohl, 1987). The characteristics features of primary deposits such as the source of fluids and metal as well as their associated structural features and alteration products are discussed in section 2.7 below.

2.7. Conceptual Model

Understanding the principal characteristics associated with the geological processes of existing mineral deposits is fundamental towards predicting prospective zones for undiscovered deposits in mineral prospectivity modeling. These characteristics are vital and are presented in an idealized model called conceptual model of a mineral deposit (Bonham-Carter, 1994). Defining a conceptual model of mineral prospectivity is the first, basic and crucial step towards mineral prospectivity modeling (Fig. 2.7). It

provides information on the geological processes related to the deposits under investigation as well as 'how' and 'where' the deposits can occur (Carranza, 2008). The model involves the interpretation of fundamental geological processes responsible for the formation and preservation of deposit sought (Carranza, 2008). The spatial associations of the respective geological processes are later translated into evidential features/layers in a GIS environment (Bonham-Carter, 1994). These features act as guidelines delineating favourable zones for undiscovered deposits.

In this study, the focus is on the prediction of favourable zones for the occurrence of undiscovered lode gold deposits based on the lithology, geophysical and existing deposit datasets. This style of mineralization is typical of orogenic gold deposit (section 2.3). Hence, based on the understanding of geological processes associated with orogenic gold deposit (Fig. 2.5), as summarized in Table 2.2, the following conceptual model has been developed:

1. According to Pohl and Günther (1991) and Pohl (1994), crustal shortening and thickening processes (Fig 2.4), associated with prograde metamorphism resulting from thermal equilibration of the crust and radiogenic heating are considered to be the primary processes for the gold-ore formation. These processes commenced with anatexis and crustal thickening processes within the lower levels of the crust (Pohl and Günther, 1991). Pohl and Günther (1991) further emphasizes that the later processes are considered responsible for the generation of fluid-forming gold deposits. Gold-bearing fluids are postulated to be extracted either from Archean greenstones or Proterozoic mafic rocks (Pohl, 1994; Pohl and Günther, 1991). The gold-bearing fluids were later transported along the earlier-formed structural corridors generated during the geodynamic evolution of the KAB (Tack et al., 2010) and reactivated later during Lomanian Orogeny (1000 – 900Ma). Based on the fluid inclusion studies by Pohl and Günther (1991), gold formed at relatively high temperatures of about 450°C and at a pressures of about 4 kbars from fluids with an original salinity of about 8 wt% NaCl equiv at depths ranging between 6 and 12 km (Pohl and Günther, 1991). On the other hand, some of the fluid inclusions resulted in abnormal elevated salinity of about 34 wt% NaCl equiv (Table 2.7) (Pohl and Günther, 1991). Such elevated salinity contradicts typical salinities of orogenic gold, which are less than 10 wt% NaCl equiv (Campbell and Kerrich, 1998; Groves et al., 1998). Such abnormality was attributed to retrograde metamorphism (Bennett and Barker, 1992) associated with crustal thickening (Pohl and Günther, 1991).

Table 2.7: Homogenization temperatures (T_H) of fluid inclusions in quartz (Pohl et al., 1991)

Inclusion type	wt% NaCl equiv.	T_H °C	Composition
Au1 a	8.0 (62)	331 (10)	liquid CO_2 10–40% H_2O
Au1 b	8.3[a] (76)	315 (37)	liquid CO_2 40–60% H_2O
Au2	34 (171) (halite!)	278 (113)	liquid or gaseous CO_2 75–95% H_2O
Au3	7.3 (26)	215 (49)	aqueous
Au4		128 180 (36)	aqueous

2. Heat source responsible for the deposits is still a matter of discussion. According to Pohl and Günther (1991), tin granites, Table, 2.1, are spatially not related to the gold mineralization. They

are only related in terms of their early tectonic controls i.e. they are both controlled by compressional deformations associated with deep crustal metamorphism. Hence by considering this genetic association, anatectic melt that resulted into the formation of tin granite intrusion (Pohl and Günther, 1991), can be considered as plausible heat source for the transportation gold bearing fluids into structural traps along deep fault corridors. The migrant fluids were later facilitated by continued fracturing within the deformation corridors (dilatancy) causing fluid expulsion (Gibson, 1990). The mechanisms associated with this type of fluid migration are typical of seismic pumping as proposed by (Sibson et al., 1975).

3. Orogenic gold deposits can be hosted in any type of lithological environment extending from the metamorphic terranes, volcano-plutonic to clastic sedimentary units (Goldfarb et al., 2001; Groves et al., 1998). In most cases, the deposits are emplaced during accretion related events (Groves et al., 1998) associated with volcanism, plutonism, metamorphism and deformation (Poulsen et al., 1992). The possible accretion event that is postulated to be responsible for the emplacement of the orogenic gold deposits in the study area is the compressional phase of Lomanian Orogeny between 1000 to 900Ma (Pohl, 1987). At present, the favourable lithologies hosting these deposits are the metasediments including quartzites, sandstones, mudstones, shales and siltstones (Pohl, 1994; Pohl and Günther, 1991).

4. Structurally, most of the deposits occur within or in the vicinity of regional, crustal scale deformation zones associated with extensive hydrothermal plumbing systems (Campbell and Kerrich, 1998). The regional scale deformation zones in the study area appear to be large fault zones postulated to be associated with deeper structural features (Pohl, 1994). These structures are indicative of compressional to transpressional tectonic settings associated with brittle faults to brittle shear zones (Campbell and Kerrich, 1998; Cassidy et al., 1998). In the KAB, gold mineralization is hosted in quartz veins and breccia associated with brittle shearing near or within the synclinoria deformation zones (Pohl, 1987, 1994; Pohl and Günther, 1991). Therefore the responsible compressional-transpressional tectonic regimes responsible for transporting and preserving gold mineralization in the study area include thrust/reverse faults, folds and strike-slip faults. On the other hand, several gold placer deposits exist in the area, whose source is believed to be the gold-bearing quartz veins (primary deposits) and silicified zones (Pohl, 1987) and are altogether postulated to contribute most of the gold exploited in the area.

5. Most of the host rocks associated with orogenic gold deposit have been characteristically metamorphosed. The degree of metamorphism ranges from sub-greenschist and amphibolite to granulite metamorphic facies condition (Campbell and Kerrich, 1998; Groves, 1993). In the KAB, where the study area lies, metamorphic grade is generally low along the synclinoria to amphibolite facies metamorphic grade towards large granitic batholiths and basements highs (Pohl, 1987; Pohl and Günther, 1991).
6. Hydrothermal wall rock alterations associated with orogenic gold mineralization include carbonitization, pyritization, chloritization, sericitization, silicification and tourmalization (Pohl, 1987; Pohl and Günther, 1991).

7. Mineralogically, quartz veins are the dominant host features with substantial amount of chalcedony, tourmaline, muscovite and sulphide minerals (Pohl and Günther, 1991).

These concepts pertaining to the gold mineralization in the study area constitute the general deposit model. Based on the available datasets used in this study i. e. geology, radiometric, magnetic and DEM,

some of these concepts are going to be used as guidelines under GIS environment to extract evidential features in order to predict favourable zones for the occurrence of undiscoverable gold deposits.

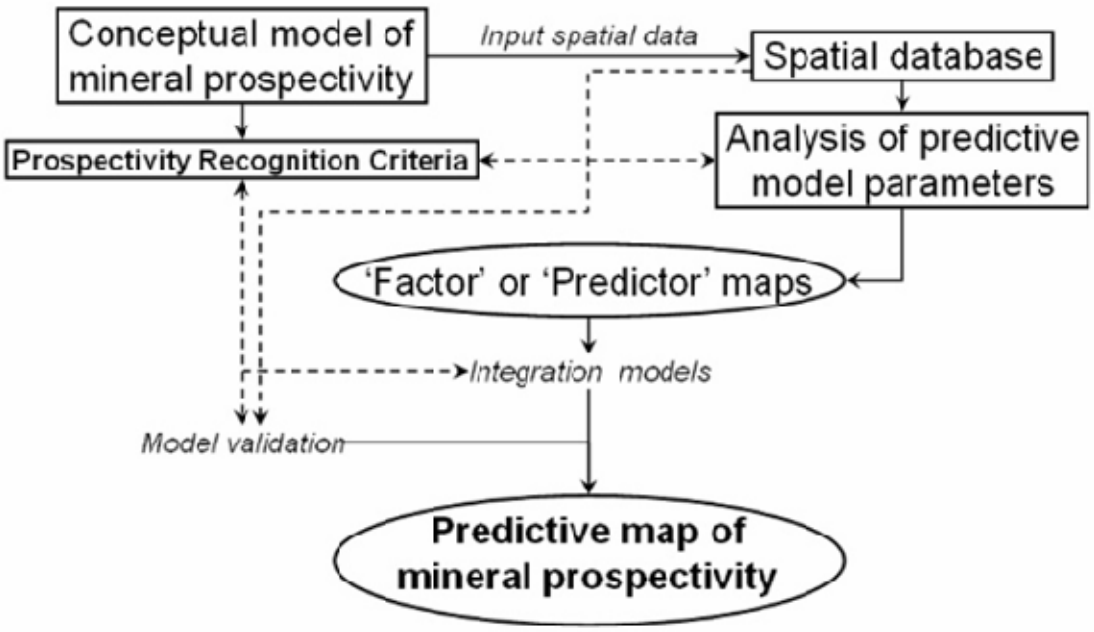

Figure 2.7: Steps towards mineral prospectivity mapping (adopted from Carranza, 2008).

3. DATASETS AND METHODOLOGY

3.1. Datasets

In study area, there are 33 locations of gold occurrences. These mineral deposits can be divided into two sets. The first set is comprised of 11 quartz veins gold deposits. These deposits are considered to be primary and were used to validate the mineral prospectivity map generated. In addition, one deposit out of these 11 was not used in validation. The tectonic framework of this deposit was more of extensional rather than compressional tectonic processes. The later processes are considered to be related to the 10 deposits occurring in the study area. Another set is comprised of 22 placer deposits. These placer deposits are believed to be formed under accumulational rather than insitu processes. Therefore they could not be used for validation. In addition, a scanned 1:100,000 scale geological maps of Rukungiri and Kabale, airborne geophysical and DEM were used to study and extract geological processes/features associated with the primary deposits prior to the identification of favourable zones for the occurrence of undiscovered gold deposits..

3.1.1. Geological Map and Mineral Deposits

Geological features (both structural and lithological units) in the study area were digitized from the scanned 1:100,000 scale geological maps of Rukungiri and Kabale published in 1960 and 1965 are owned by Department of Geological Survey and Mines, Entebbe, Uganda The existing geological maps were helpful towards understanding the geology of the area. On the other hand, the geological map was also used as the baseline for interpretation of the radiometric, magnetic and DEM. Both geological maps are the 1960 and 1965 first published edition of Rukingiri and Kabale respectively. The locations of gold deposits were digitized from these geological maps.

3.1.2. Magnetics and Radiometric Dataset

Aeromagnetic and radiometric surveys have been routinely used to study, understand and evaluate magnetic properties and gamma-radiation levels, respectively related to lithological variations, their age of formation, tectonics and deformation history (Airo, 2002; Blewett et al., 2000). These surveys are the most widely used geophysical methods in mineral exploration (Ghazala, 1993; Grant, 1985a, b; Steenland, 1970). Radiometric surveys represents variations of K, Th and U concentrations in the uppermost 0.3 to 0.5 m of the ground (Airo, 2002; Blewett et al., 2000; Jacques et al., 1997; Schetselaar et al., 2000), which outline surface geochemical processes as well as outcropping solid rocks and their weathered/transported signatures. Based on their capability to measure surface to deeper magnetic signal, magnetic surveys have also been proven to be valuable in areas covered by extensive superficial deposits, surface to subsurface structural information associated with regional and local tectonic frameworks of lithologies and ore-bodies(Airo and Mertanen, 2008; Al-Garni, 2010).

In the study area, the Geological Survey of Uganda has been actively pursuing a program of regional geophysical exploration survey in an attempt to extend knowledge of the basement geology in the context of developing exploration strategy for discovering new mineral deposits. Both magnetic and radiometric data were flown by FURGO: FCR 2417A under the following survey specifications:

Magnetic Data Recording Interval	0.1 seconds
Radiometric Data Recording Interval	1 second
Sensor Mean Terrain Clearance	80 meters
Flight Line Spacing	200 meters
Tie Line Spacing	2000 meters
Flight Line Trend	035 degrees
Tie Line Trend	125 degree
Grid Cell Size	50m

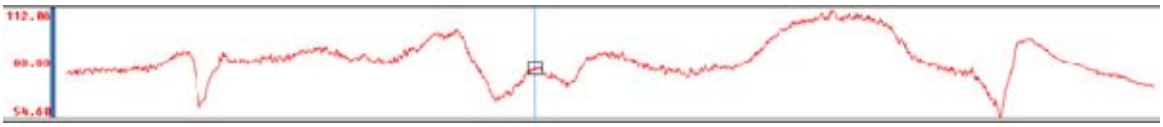

Fig 3.1: Terrain clearance profile of one of the flight survey line

The mean terrain clearance was 80 m, but as shown in Fig. 3.1, there were variations along their paths possibly due to the topography of the area. Based on such topographical variations, it is evident that the mean terrain clearance was not maintained. Therefore such topographical variation can subsequently lead to erroneous results. Therefore, to suffice topographical effect, gradient enhancement technique (Reford, 2006) has been applied to the total magnetic intensity map of the area.

3.2. General Methodology

3.2.1. Airborne Magnetics

Aeromagnetic method (AM) has played and will continue to play a prominent role in geological mapping and in mineral exploration programmes. The method characteristically identifies and map distributions of magnetic minerals that are chiefly dominated by opaque minerals including magnetite (Grant, 1985a, b; Sharma, 1987). The distributions of these minerals and their variations in terms of strength depend entirely on the magmatic differentiation processes associated with the original melt. According to Grant (1985a), two trends are followed during fractional crystallizations of the primary basaltic melt; one maintains oxygen levels, probably through abundant supply of water and the second where oxygen is allowed to drop. The first trend ends up with Fe-Ti oxides and silica enriched liquids, Fig 3.2.1(a), at higher oxidation levels typical of calc-alkaline series of igneous rocks with relatively weaker magnetic properties (Grant, 1985a). The second trend associated with drop of oxygen, is enriched with ferrous iron, Fig. 3.2.1(b) characterized by low silica content at lower oxidation state and is subsequently strong in terms of magnetic properties (Grant, 1985a, b)

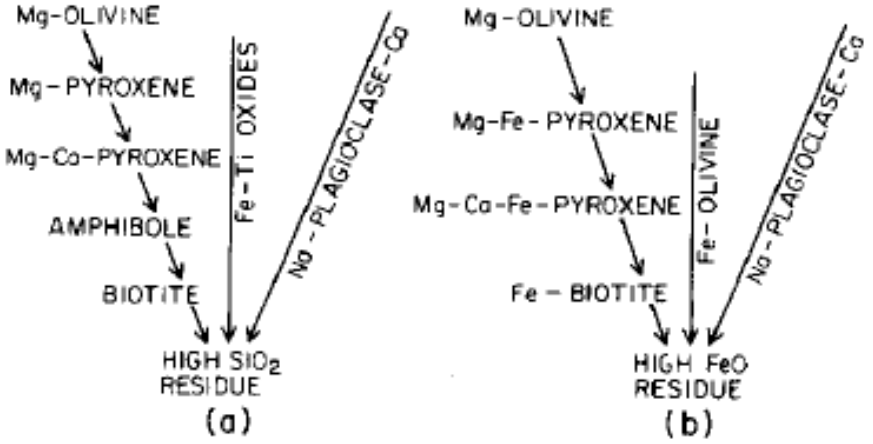

Fig 3.2.1: Magmatic reaction series (adopted from Grant 1985a). QUESTION: Why can you not cite Grant (1985b) here???)

The study area is mostly characterized by the metasediments and to some extent meta-igneous, which are not directly related the magmatic differentiation processes explained above. Hence, the magnetic properties within these rocks are dependent on the pre-metamorphic environment. Magnetization in the metamorphic lithologies apart from other geological parameters, are very much dependent on the original source rocks. Pelitic metasediments (derived from fine grained sedimentary rocks) are more magnetic than psammites (Grant, 1985a). Alternatively, if the source rock were igneous, the resulting magnetic strength of the resultant metamorphic rock would depend on the pre-metamorphic magnetic strength of the respective source rock. Other prominent factors that affect magnetizations in metasediments (in fact, even in other rock units) include: 1) high temperature alterations, 2) repeated metamorphism, 3) low temperature alterations, and 4) granitization (Grant, 1985a). . Hence, direct interpretation of magnetic anomalies resulting from metamorphic terranes pose a significant challenge i.e. similar rock units can give rise to different magnetic anomalies under similar geological processes (Grant, 1985a). However, understanding these geological processes and ground truthing can be helpful towards deducing significant interpretation. In either way, the interpretations should be geologically sensible.

Therefore, based on the knowledge of the geology of the study area and basic principles on which AM works, magnetic data were cautiously used to study, identify and interpret lithological variations and structural controls that are related to geological processes as well as gold mineralization of the area. To achieve this objective, several computer-based processing and enhancement techniques were applied to the airborne magnetic dataset and are discussed below. .

3.2.1.1. Reduced to Pole

Reduction to pole is one of the prevalent enhancement technique used as guideline towards interpreting airborne magnetic dataset. Its main role is to convert magnetic field from the magnetic latitude where the Earth's filed is inclined to the field at magnetic pole where the inducing filed is vertical and subsequently reduce, if not completely remove, the effect of inclination angle of the magnetization vector (Ates et al., 2009; Milligan and Gunn, 1997; Sharma, 1987). In this way, the data appear as if they were acquired through vertical direction of magnetization and subsequently improve the correlation of the anomaly features. In this respect, reduction to pole enhancement technique provides sensible correspondence between the anomaly on the map and their corresponding causative features (i.e., bedrock

geology/geological processes). In other words, the induced anomalies are vertically on top of their sources (Blewett et al., 2000; Milligan and Gunn, 1997; Schetselaar et al., 2000).

In this study, reduced to pole enhancement technique was applied to horizontal gradient enhanced total magnetic intensity (TMI). Apart from improving accuracy and resolution of TMI, including reducing topographical effect, horizontal gradient enhanced technique also provides information of the magnetic anomalies over linear sources that strike obliquely to the survey line (Reford, 2006). Steps towards creating enhanced gradient TMI are demonstrated in Appendix 4 (Nelson, 1994)

3.2.1.2. Analytical Signal

Analytical signal enhancement technique is widely used to interpret anomalies in airborne magnetic dataset. The technique assumes that magnetic bodies of the same geometry result in the same analytical signal anomaly and that analytical signal images are completely independent of direction of magnetization as well as inclination of the Earth's field (Brodie, 2002; Milligan and Gunn, 1997; Reeves, 2005). Several challenges are encountered in interpreting anomaly source from metasedimentary terrain. As mentioned earlier, the magnetic anomalies resulting from metasediments normally depends on the parental rock materials, i.e. similar metasedimentary rock unit derived from different source rock can have different magnetic anomalies. Therefore care should be taken when interpreting these rock units.

3.2.1.3. Vertical Derivative

First vertical derivatives are among the enhancement techniques applied to the total field anomaly map of airborne magnetic data to sharpen the resolution of near-surface features related to short-wavelength information (Jacques et al., 1997; Milligan and Gunn, 1997; Sharma, 1987). These features are important toward studying, understanding and finally locating tectonic zones (weak features) that might have played significant roles as conduits during transportations of gold-bearing fluids and deposition of gold. The type of gold mineralization discussed here is of the orogenic type, characterized mainly by folding and faulting associated with shear zones. Through systematic analysis of first vertical derivative images, deformation features can be outlined and mapped. There are a number of ways to recognize tectonic zones in images of the first vertical derivative of magnetic data. For example, tectonic zones may be recognized from sharp gradients as well as positive and negative closures (Ghazala, 1993). Ghazala (1993) further emphasized that long extended vertical gradients and truncation lines associated with magnetic anomalies are postulated to represent major structural corridors (i.e. fault/shear zones). In summary, tectonic zones can be recognized by (1) offsets of apparently similar magnetic units, (2) sudden discontinuities of magnetic units normally associated with steep gradients and inflections, and (3) a linear narrow anomaly resulting from magnetic low or high caused by weathering (i.e., oxidized magnetic minerals to non-magnetic mineral assemblages) and precipitations of magnetic minerals, in both instances, along those tectonic zones, respectively (Gunn et al., 1997; Milligan and Gunn, 1997).

3.2.1.4. Tilt Derivative (TDR)

TDR is another fundamental enhancement technique used in airborne magnetic data processing. It can be viewed as an effective alternative approach to vertical derivatives in mapping higher frequency anomaly structures that can sometimes be related to shallow basement features. Unlike vertical derivative, TDR represents a unique anomaly contrast that can be used to enhance magnetic fabrics and subsequently map continuity of structures features (Verduzco et al., 2004). Otherwise, the criteria used to recognize these structures features are similar to the ones discussed in section 4.2.1.3 above

3.2.2. Airborne Radiometric

Radiometric survey, as mentioned earlier, is a surface mapping method that is applicable to the top 30-40 cm of the ground. This means that interpretation of the data requires an understanding of surface processes such as weathering and alterations. Other factors to consider during interpretation of radiometric data include relationships between surficial materials and bedrock geology as well as geomorphology. Characteristically, the method relies on the variations, similarities and distributions of K, Th and U radioelement concentrations with respect to their corresponding geological units/processes in terms of age, lithological variations, regolith effects and other related geological processes (Dickson et al., 1996; Jacques et al., 1997; Raghuwanshi, 1992). In this study, ternary image and radioelement band ratioing were used to study surficial geological processes.

3.2.2.1. Ternary Map

In a ternary map, tonal variations are the main features considered in studying surficial lithological variations/processes. Red-Green-Blue colour codes were assigned to K-Th-U radioelement data, respectively, to produce a histogram-equalized ternary map using Oasis Montaj software. To reduce the attenuation effect of vegetation to the radioelements in the area as shown in Appendix 1, the ternary image was fused with Landsat TM band 5 (Schetselaar et al., 2000). Hence, in the fused Tm5-ternary image, areas with elevated concentrations of K appear in red whereas green and blue colours signify elevated concentrations of Th and U, respectively. White colour signify the presence of all three radioelements in elevated concentrations, black represent their absence or very low concentrations whereas yellow colour means the presence of K and Th together in high concentrations (Blewett et al., 2000)

3.2.2.2. Radioelements Band Ratioing

Another widely used enhancement technique in airborne radiometric data is radioelements band ratioing (Jacques et al., 1997). Depending on which individual radioelement one wants to enhance, band rationing of the radioelements becomes indispensable. In this study, the individual processed radioelement concentrations in xyz database format were gridded at 50m pixels size using minimum curvature gridding algorithm. The band ratioing to enhance K radioelement i.e. Th/K and U/K were subsequently created using grid-math expression builder under 7.2 version of Oasis Montaj software. The resultant images were used to demarcate zones enriched in the radioelement sought.

3.2.3. DEM

In this study, a high resolution (33 m) shaded relief DEM images were created from 360, 90 and 135 azimuth angles. The resultant images were later integrated as RGB components for 360, 90 and 135 shaded relief DEMs respectively. The resultant DEM therefore enhances lineaments in multidirectional perspectives. In this respect therefore DEM permits the identification and extracting surficial structural patterns (Jaboyedoff et al., 2009). These surficial structural patterns include anticlines and synclines that are defined by the orientation of layered rocks. Other structural features, such as faults that are exposed to the surface can also be recognized in a DEM by their characteristic offset patterns.

3.2.4. Mineral Prospectivity Modeling (MPM)

The basic concept of mineral prospectivity modeling is based on the understanding of the relationships between known mineral deposit locations and geological features related to their genesis (Carranza, 2008). The success of predicting prospective zones for the occurrence of undiscovered mineral deposits largely depends on: (1) knowledge of mineral deposit locations; 2) knowledge of genetic associations between certain geological features and mineral deposits and 3) selection of suitable method to represent and

integrate those sets of knowledge (Hosseinali and Alesheikh, 2008). Hence, understanding the spatial features related to a specific type of mineral deposit is important towards the identification of favourable zones for undiscovered mineral deposits. These spatial features are typical characteristics of a single type of mineral deposits and are referred to as conceptual model of mineral prospectivity as outlined in section 2.7.

As stated earlier, there are two main approaches to mineral prospectivity mapping in GIS environment, namely, knowledge- and data-driven approaches (Bonham-Carter, 1994). The application of either of these two approaches, knowledge- and data-driven, is based on subjective expert knowledge and geospatial data analysis, respectively. In a data-driven approach, prospective grounds for the occurrence of undiscovered minerals deposits of interests are determined using geo-spatial datasets (Hosseinali and Alesheikh, 2008). Locations of existing mineral deposits and their spatial distributions related to their geological processes are studied and analysed via evidential maps/features extracted from available geo-spatial data sets (i.e., geological, geophysical, geochemical). Carranza (2008) emphasizes that if certain evidential features have more spatial dependence relative to the distribution of the existing mineral deposits of interest than others, the former will have high prospectivity for the occurrence of undiscovered mineral deposits than the latter. Hence, the weighting or rating of geospatial information is not subjective. The weights are quantified though analysis of individual 'evidential features/maps from the datasets used and the deposits sought.

However, applications of data-driven techniques are restricted by the number of already discovered mineral deposits. In the study area, the number of known primary gold deposit is too small to allow them to be used as training and validating sets. Therefore, a knowledge-driven data-guided "wildcat" modeling method for mineral prospectivity mapping, proposed by (Carranza, 2002)) and (Carranza and Hale, 2002a) and later improved by Carranza (2010), is adopted in this study. This method works on the assumptions that: the qualitative geological knowledge of the area with respect to the type of mineral deposits sought is well understood (Carranza, 2010). In this respect, known mineral deposits are considered "non-existing" or undiscovered and the method makes use of the general concept of proximity to geological features to assign 'wildcat' predictor scores and to create wildcat predictor maps (Carranza, 2010). Wildcat predictor maps are integrated to produce a mineral prospectivity map showing zones potential for the occurrence of undiscovered deposits. The map is validated by the known mineral deposits that were assumed to be undiscovered.

4. RESULTS AND INTERPRETATIONS

4.1. Introduction

This chapter describes the results of processing of airborne magnetic, radiometric and DEM datasets, and the interpretations of those results. It should be noted that the existing geological knowledge of the study area, as discussed in section 2.6, provides the basic framework for the interpretation of the results. In addition, based on the new understanding related to the geological processes of the area that emplaced the mineralization as orogenic deposit model, indicative geological processes/features as well as possibility of Kabanga Musongati extension to the area will be sought using airborne magnetic, DEM and geological datasets. Finally the integrated interpretations are discussed and concluded at the end of this chapter.

4.2. Magnetics

Fig 4.1 shows the results of one of the profiles for the gridded images of reduced-to-pole, analytical signal, first vertical derivative and tilt derivative of the gradient enhanced total magnetic intensity of the area (see appendix 5 for the location of the profile). This result has been the base of the interpretation of the filtering techniques employed in this study. Similar anomalies resulting from different filtering techniques were concomitantly analysed and compared. Fig 4.1, therefore, demonstrates the corresponding anomalies at given points along the line. In this way detailed information along the line is gathered (in this case at 8 m interval), analysed, compared and interpreted.

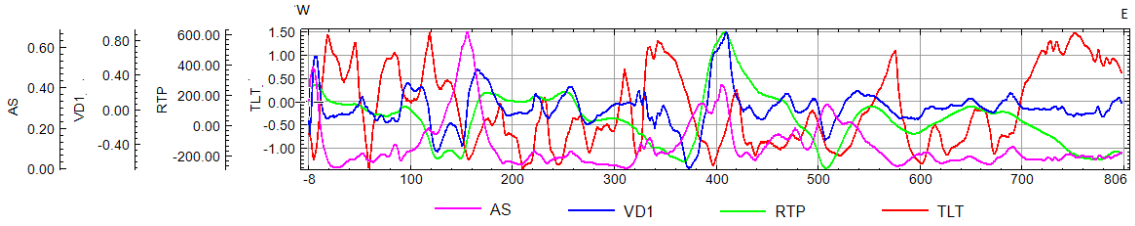

Fig 4.1: Profile along one of the lines demonstrating the corresponding anomalies from AS (analytical signal), VD1 (first vertical derivative), RTP (reduced-to-pole) and TLT (tilt derivative) of the gradient enhanced total magnetic intensity map.

4.2.1. Reduced To Pole

The gradient enhanced total magnetic intensity maps, shaded at 45 and 135 azimuth angles, are presented in Figs 4.2.1 A and 4.2.1B, respectively. Generally, the results show that the north-eastern and south-western parts of the area as separated by line P-R, are characterized by relatively low and high magnetic anomalies, respectively. In addition, few localized high and low magnetic anomalies are also present in the north-eastern and south-western parts of the area, respectively.

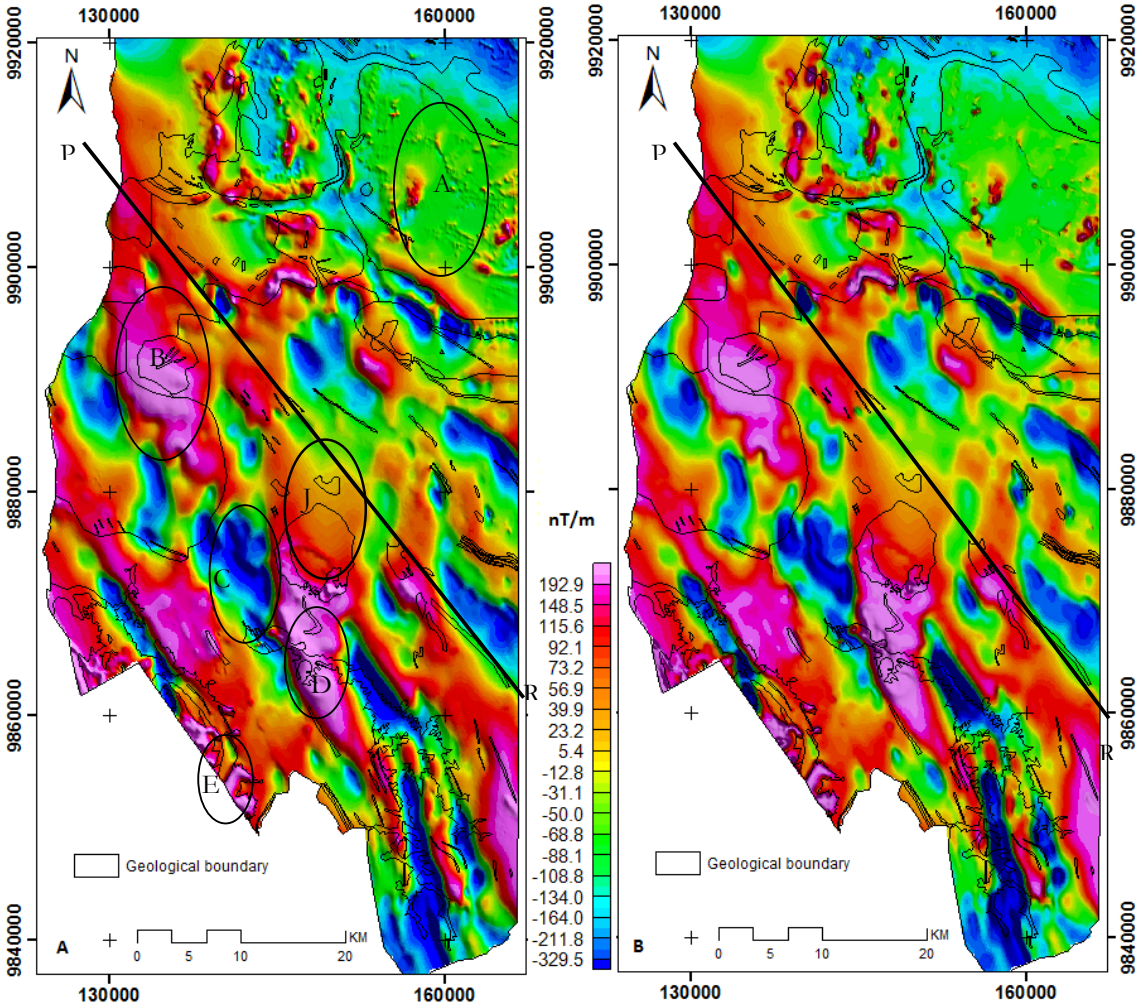

Fig 4.2.1 Gradient enhanced total magnetic intensity map reduced to pole shaded at 45deg (A) and 135deg (B) azimuth angles both overlaid by interpreted geological contacts

Although the images were shaded with different illumination angles, there was no significant change in terms of anomalies orientation. Therefore for consistence, Fig 4.2.1A was used for interpretation. The low magnetic signatures in the north-eastern part of the area are mainly due to biotite gneisses, migmatites, schists and felsic intrusions. The localized high magnetic signatures in that area can be attributed to variations in amounts of magnetite-bearing minerals in the respective lithological units (i.e. biotite in gneisses). Both high (main) and low (localized) magnetic intensities are present over the biotite gneiss. This characteristic suggests that biotite is not uniformly distributed within the gneiss. Biotite has a tendency to be transformed into secondary magnetite especially at low temperature crystallization processes (Grant, 1985a). To this end, there no evidence for the transformation of biotite, but by comparing the anomalies on locations A and B, gneisses can be considered to be derived from protolith of different magnetic properties, therefore, biotite-rich protolith in the gneiss are probably responsible for the local magnetic highs.

Locations C and D on Fig. 4.2.1A are characterized by varied magnetic signatures, both low and high respectively. These locations are underlained predominantly by metasediments. Several factors can be considered to contribute to these variations, including regional metamorphism and source rocks. Regional metamorphism is generally characterized by heating, deformation and cooling. These processes altogether

affect magnetic minerals and cause their re-crystallization into coarser textures/larger grains and subsequent strengthening of magnetic properties (Grant, 1985a; Reeves, 2005). This scenario can justify the higher magnetic zones associated with the metasediments at location D compared to location C within similar geological setting. In addition the presence of high magnetic zones within the metasediments can be attributed by the presence of ironstone lenses that have been mapped and proven to be associated with intercalated quartzites, grits and mudstones of the lower series of the Meso- to Neo-Proterozoic metasedimentary rocks.

Location J at the middle is generally characterized by low to medium magnetic strength. The area is mainly characterized by granitic intrusion. The northen part of the study area, the intrusions are generally associated with low magnetic signatures, suggesting possible age differences of the intrusions. However, the trend of magnetic anomalies associated with the intrusions is low.

Location E on the south-western corner of the study area is characterized by narrow zones with high magnetic anomaly. The area is associated with mafic extrusive rocks (mostly basalt/andesites). One factor for such elevated magnetic zones in the mafic extrusive rocks is alteration (high temperature alteration). Pyroxene is one of the chief minerals in basalts and even andesites, which once altered (e.g., serpentinized) can end up with sufficient amounts of secondary magnetite and, hence, impart in elevated magnetic intensity (Reeves, 2005).

4.2.2. Analytical Signal

The analytical signal images (Fig 4.2.2) show that most of the causative bodies characterizing the area are oriented NW-SE. Based on this dominance trend, NE-SW can therefore be considered to be the main compressive tectonic regime affecting the area. However, upon closer examination of Figs 4.2 2 (A) and (B), heterogeneities in terms of magnetic anomalies within gneiss, schist, and metasediments are noted. Location A is generally considered to have low anomaly, and in this study area it is characterized by the granitic intrusion. Therefore, calc-alkaline magmatic trend can be postulated to be associated with the plutonism of the area. Further to the north at location D, both high and low magnetic anomalies are noted. The dominant rock unit here is the gneiss, considered to be the oldest rock of the area. Hence, the location must have experienced several deformational episodes (Buchwaldt et al., 2008). Therefore, these sporadic deformational processes can affect the magnetic properties and cause variations as noted in this location D. The south western part of the area is generally characterized by high anomalies, i.e. location C. Mafic volcanics occupy this area. Therefore by considering their chemical composition, these mafic volcanics, i.e. basalts is chiefly composed by calc plagioclase, pyroxenes, olivine and magnetite (Hamilton et al., 1995). Hence, although the pathological studies of the basalts have not been done, their general association with magnetite can cause such high magnetic anomalies. The southern part of the study area, at location B is associated with both high and low magnetic anomalies. This can be related to low temperature metamorphism that has affected the metasediments (Pohl, 1987). Location E on the NW part of the area is also associated with both low and high magnetic anomalies. The undifferentiated swamps and other alluvium dominate this location. Therefore, it can be postulated that swamps are overlaying gneiss, and a new lithological unit is proposed.

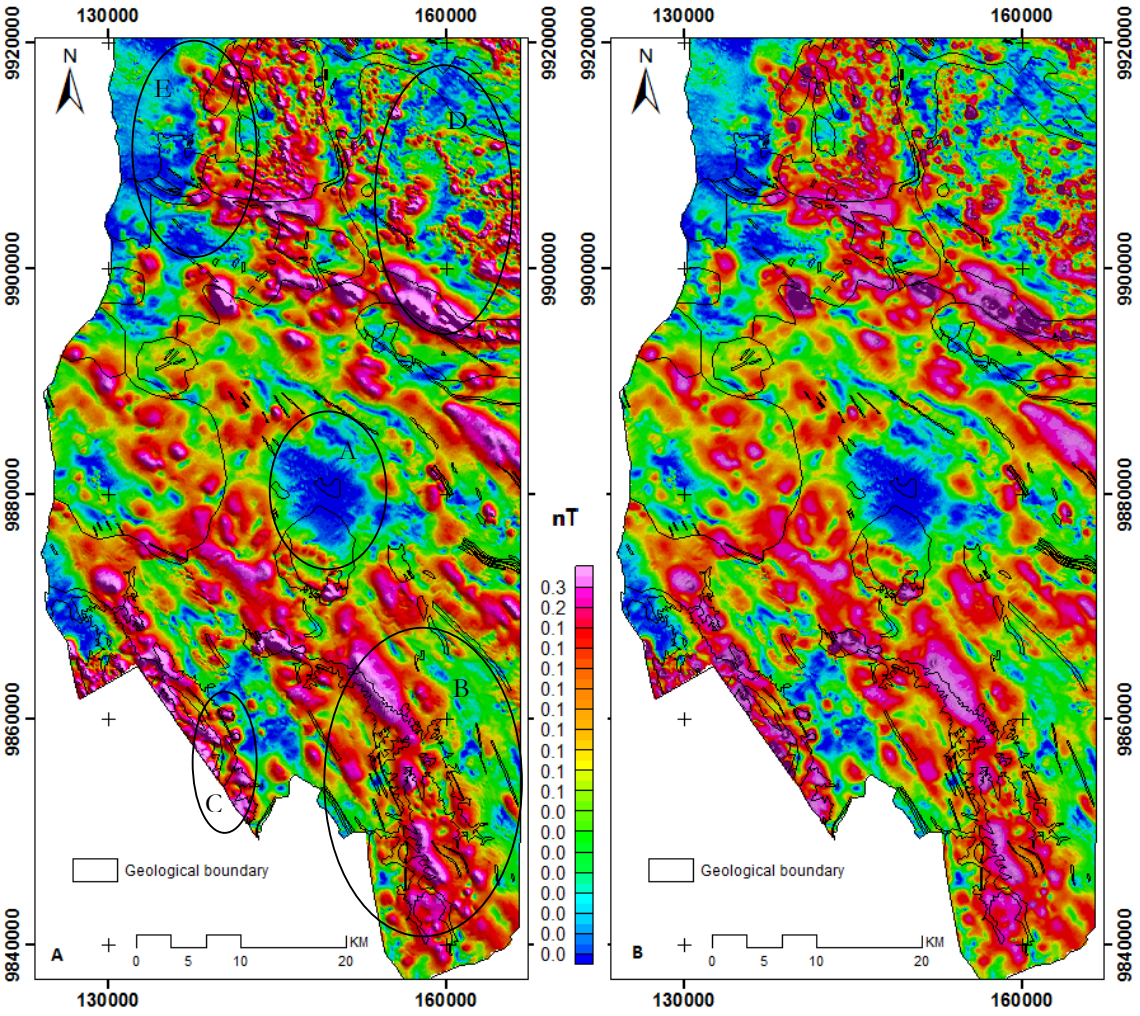

Fig 4.2.2 Analytical signal image shaded at 45 (A) and 135 (B) azimuth angles and overlaid by interpreted geological contacts

4.2.3. Vertical Derivatives

Two prominent trends NW-SE and NE-SW are exhibited by linear features that were interpreted from the image of the first derivative of the horizontal gradient anomaly map (Fig. 4.2.3). These structural features likely represent zones of crustal weakness (Pohl, 1987).

These structural weaknesses are interpreted here as strike-slip faults characterized by either dextral or sinistral sense of movements. Normally strike-slip faults are concomitantly associated with dip-slip faults. Therefore, under continued compressional tectonic regimes associated with orogenic processes, i.e., Lomanian Orogeny that has affected the area at around 1 Ga to 950 Ma (Pohl, 1987), the strike-slip faults might have slided over each other and caused thrusting, Fig 4.2.3A. However, continued thrusting eventually lead to the formation of duplex structures Fig 4.2.3B.

Both strike slip faults and duplex structures are indicative of transpressional tectonic regimes. Transpressional structures settings are the main focus for the gold bearing fluids in orogenic gold deposits (Campbell and Kerrich, 1998; Groves et al., 1998). Therefore in the study area, a number of strike slip

faults are recognized in the study area including locations P, R and U. Otherwise, locations Q, S and T are considered to represent duplex structures. Other linear features are interpreted as joints/fractures.

In addition, most parts of the study area is generally is smooth except the north and north-eastern area, i.e. location A. Location A is associated mainly with the gneiss, which is the oldest rock of the area according to the geological map i.e. Palaeproterozoic. Hence rough texture characterizing those areas suggest that the gneiss might have been significantly be affected by various/prolonged phases of metamorphism and deformations (Buchwaldt et al., 2008). Other features can be related to later magmatic activities, and lithological contacts

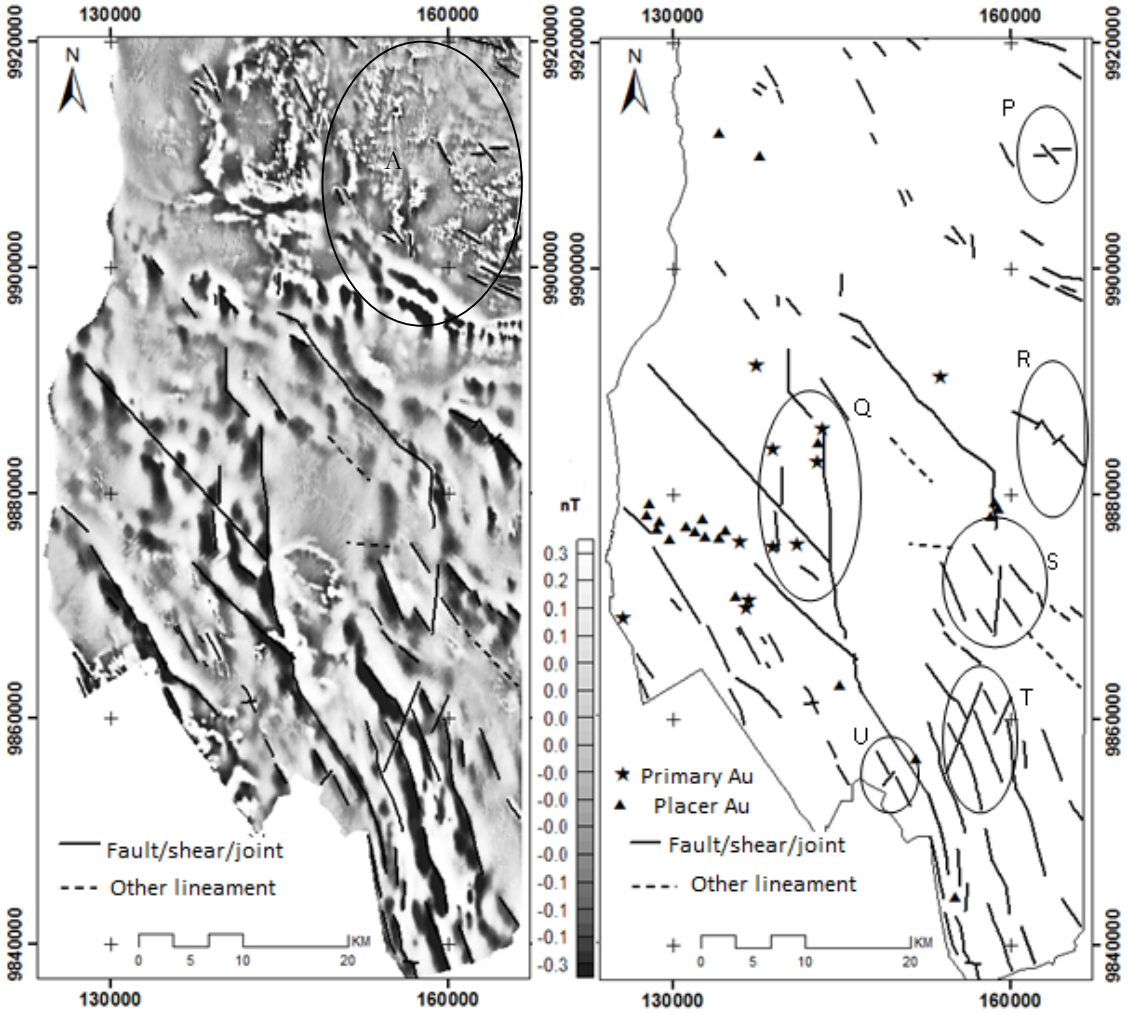

Fig 4.2.3 Structural features interpreted from first vertical derivatives of the gradient enhanced total magnetic intensity anomaly map reduced to pole

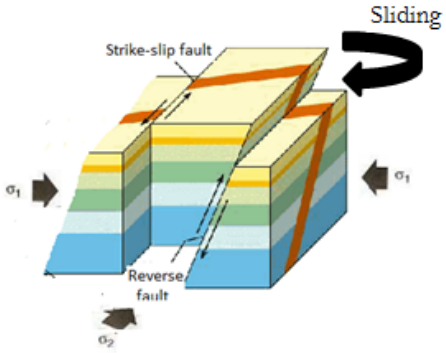

Fig 4.2.3A Structure processes along the EW trending principal stress (James, 1991)

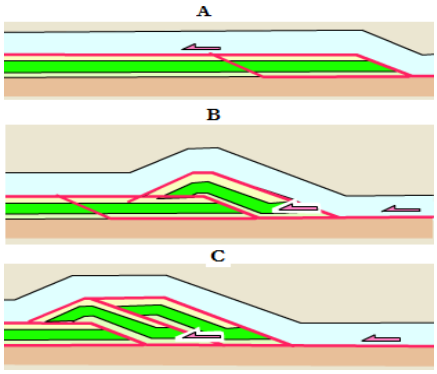

Fig 4.2.3B Duplex structures developing from series of continued thrusting (Butler and Gordon, 2010)

4.2.4. Tilt Derivatives (TDR)

The grey colour of tilt derivative of the horizontal gradient anomaly map reduced-to-pole is presented in Fig. 4.3.4. Similar NW-SE deformation zones have been recognized from the tilt derivatives image. In addition, some NE-SW structural corridors related to fault or shear are also present.

Again, several transpressional tectonic regimes are present. Locations V, T, U, and Z are representative of strike slip faults which are dextral (V and Z) and sinistral at T and U. Location X can be related to duplex structures. Locations W and Y are difficult to interpret. However, location W can be considered to be associated with braided fault zone within strike slip shear regimes. Other linear features can be related to fractures/joints. Lithological contacts and plutonism can be seen at location Q and R respectively on the left image of Fig. 4.2.4.

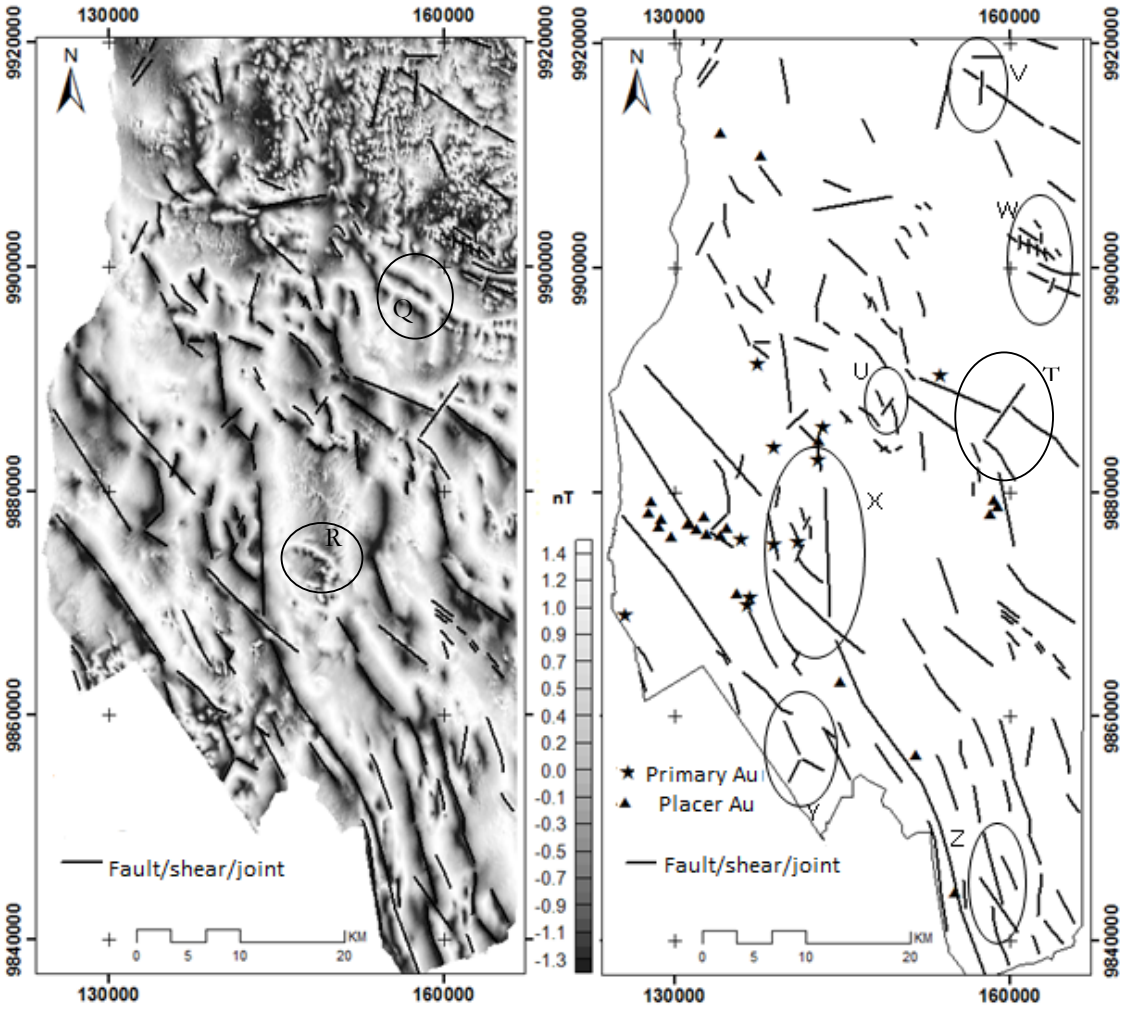

Fig 4.2.4 Structural features interpreted from tilt derivatives of the gradient enhanced total magnetic intensity anomaly map reduced to pole

4.3. DEM

The results of the DEM are presented in Fig. 4.2.5 (a). The results show that the area is characterized by faulting, large scale synclines and anticlines. Other features correspond to stretched quartzitic ridges.

At location A, strike slip faulting i.e. dextral, represent the transpressional tectonics of the area. These deformation zones are manifested along the major NW-SE trending corridors. Other linear features are trending NE-SW and almost E-W are present but not prominent. The structural interpretations i.e. synclines and anticlines, were later validated by the actual ground measurements, Fig. 4.2.5 (b). An intriguing feature is the similar trends of fold axis and fault. One of the reasons for this scenario could be related to the response of the individual rock unit to stress. Normally soft rock i.e. shales respond to stress by bending i. e folding where as others break i.e. faulting. Therefore, under continued stress regime, even soft rocks breaks. Hence under the environment of tight inclined folds, and through continued compressional tectonic regime, the axis of a fold can also break and subsequently its fold axis can be re-oriented into similar trend with the fault. Radulescu (1982 reported the presence of tight folds in the Karagwe-Ankolean System (now KAB) in which the study area lies.

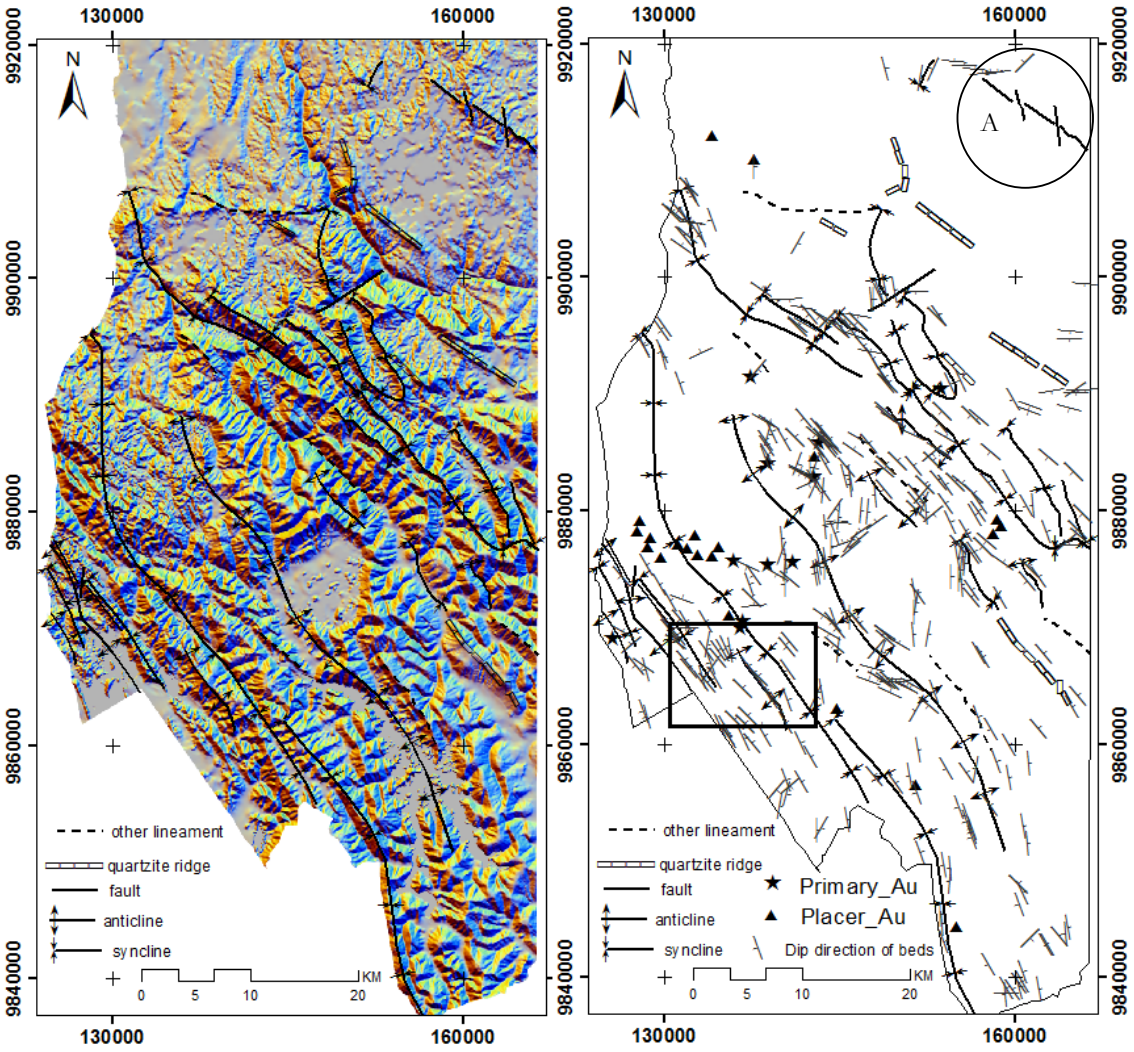

Fig 4.2.5(a) Structural features extracted from DEM generated from 360, 90 and 135 azimuth angles

.

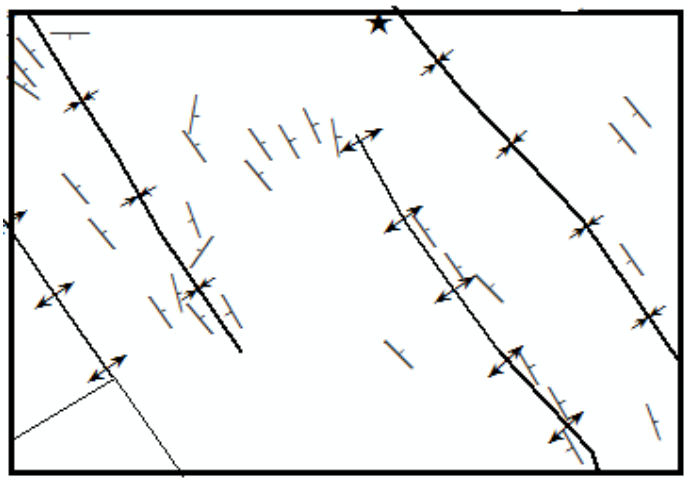

Fig 4.2.5(b) Criteria for structural interpretation from DEM

4.4. Airborne Radiometrics

4.4.1. Ternary and Thorium Maps

Fig 4.3.1(A) and (B) represent, respectively, the ternary image fused with Landsat band 5 and the shaded-relief Th radioelement concentration. In the ternary image, several zones have been demarcated, including K enriched are (red), Th zones (greenish) and U zones (bluish). Other areas are characterized by black/dark and white tonal variation. On the other hand, the Th map, Fig. 4.3.2(B), the area to the east is characterized by reddish tonal variation compared to the western zones.

The area on the north-eastern, location A on Fig 4.3.1A is characterized by green tonal variations indicating elevated concentrations of Th and therefore depletion of K. Several factors can cause such tonal variations. According the 1960 published geological map of Rukungiri, gneiss is oldest rock in this study area (Palaeproterozoic). If this is the case, therefore one could expect the unit to be affected by several phases of geological processes including the Lukamfwa magmatic event at around 1.6 to 1.4Ga (Buchwaldt et al., 2008) associated with deformation, and shearing. In addition, the geological map of Rukungiri categorized some parts of this unit to have no outcrops exposures i.e. weathered, suggesting that erosion and leaching are inevitable. Therefore, K radioelement is very susceptible to these processes and can significantly reduce its presence.

On the other hand, there is a relative depletion of Th and U and K enrichment associated with intebedded schist, as indicated in two locations denoted by B. In nature, schist derived from sedimentary environment, which is the likely case here, are rich in mica. Hence, schist being rich in mica can subsequently be rich in K.

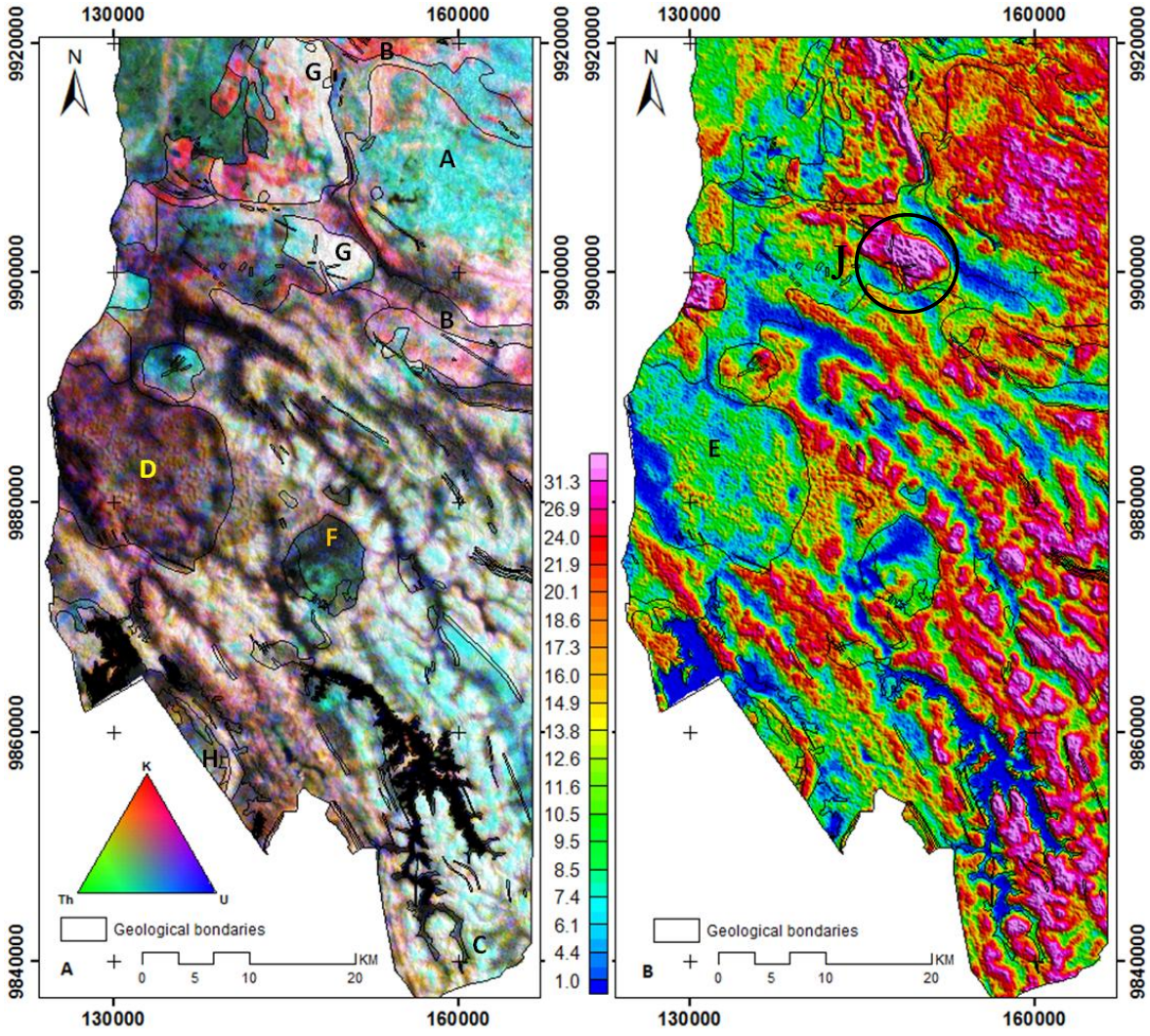

Fig 4.3.1 Spectrometric Radiometric Image with K (Red), Th (Green), U (Blue) Histogram Equalized and Fused with Landsat band 5 (A) and Shaded Th Radioelement Concentrations (B)

There are variations of the radioelement concentrations for the metasediments, which are the dominant rock units in the area, i.e. locations C and D. They are generally characterized by bluish-light greenish on the south-eastern part, C to reddish tonal variation on the western end of the study area, i.e. D. This pattern is not easy to interpret but one thing which is remarkable is that the metasediments are associated with brighter colours. Brighter colours in the ternary image of the radioelements can also be a measure of geomorphic activity indicating areas of active erosions in the upland regions (Jacques et al., 1997). Another distinctive pattern significantly rich in K has been observed on the western side of the area, D. The vegetation index map, Appendix 1, of the area was shows that the area is associated with thicker and impenetrable Bwindi tropical forest. In order to get rid of the vegetation effect, and in fact to reduce the vegetation effect to the radioelements concentration of the whole area, the ternary image was fused with Landsat band 5 (Schetselaar et al., 2000). Landsat TM band 5 reduces the attenuation effect of radioelement by vegetation. Thereafter, zone D was compared with the shaded Th radioelement image at location E, Fig. 4.3.1B. It was noted zone D in Fig 4.3.1A coincide with zone E in Fig 4.3.1B, new K-rich lithological unit, possibly shale, is proposed. This assumption is supported by the fact that earlier studies

made on sedimentary environment suggested that enriched K zones can infer clay related shales (Pliler and Adams, 1962)

At location F, the tonal variation within this intrusion is controversial as it is characterized by green/blue to black/dark tonal variation (absence/very low radioelements concentrations) contrary to the tonal variations of typical acidic intrusions (normally yellow or white). At this location, other processes not directly related to its formation are considered to cause such distinctive variations. Processes that can result into regolith development (i.e. weathering) can be responsible for such black/dark tonal variations. Wilford et al. (1997) emphasized that thicker regolith horizon characterized with quartz/sand rich fragments not only result in radioelement tonal variations that do not necessarily represent underlying bedrock than thinner equivalents. In addition Wilford et al. (1997) further emphasizes that quartz/sand rich fragments are also radioactively barren and in most cases appear black/.dark in ternary images. This situation is recognized at location F in Fig 4.3.1A.

There are two locations denoted by the letter G. These locations have been characterized by white tonal variations, an indication of the presence of all 3 radioelements. The old geological map indicates that these locations are overlain by biotite gneiss. How based on this result, such proposition is refuted. Such tonal variations are typical of acidic intrusion, and the new unit is proposed.

Location H is associated with light green and bluish-reddish-greenish tonal variation respectively. These tonal variations are challenging because the area is overlain by mafic volcanics, were one would expect low radioelement concentration. Such variations are difficult to interpret and may be related to surface processes including weathering and alterations associated in most cases with high Th and U concentrations.

Elevated Th and U concentrations have also been observed associated with the swamps/alluvium on the north-western part of the area. These are relatively lowland areas corresponding to very low erosional activities signified, in most cases, by the dominance of dark colours (including some green colours) (Jacques et al., 1997). Otherwise, based on ternary image interpretation, most of the rivers channels and topographical lowlands have been associated with absence/very low concentrations (dark/black) of the radioelements.

4.4.2. Radioelements Band Ratioing

The results of shaded Th/K and U/K images are presented in Fig. 4.3.2 (A) and (B). The results show that both images show similar pattern related to K-enrichment locations. So for consistence, Fig 4.3.2 (A) has been used for interpretation. Most of the area in the north and south, i.e. location A and B are areas are characterized by depletion of K enrichments whereas locations C and D are relatively associated with high K enrichments.

Therefore based on the nature of lithological units on the ground, these zones can be used to study and deduce bedrock lithology then their resultant weathering/alterations processes. However, understanding the landscape of the area is significantly important. Landscape controls the depth of the regolith materials to be developed (Wilford, 2002). Prolonged development of regolith materials normally result into thicker horizon that do not necessarily represent the underlying bedrock than thinner equivalent can reasonably be assumed to represent either bedrock geology or its resultant geological processes, i.e. weathering, erosion and alteration (Erdi-Krausz et al., 2003; Pickup and Marks, 2000; Wilford et al., 1997).

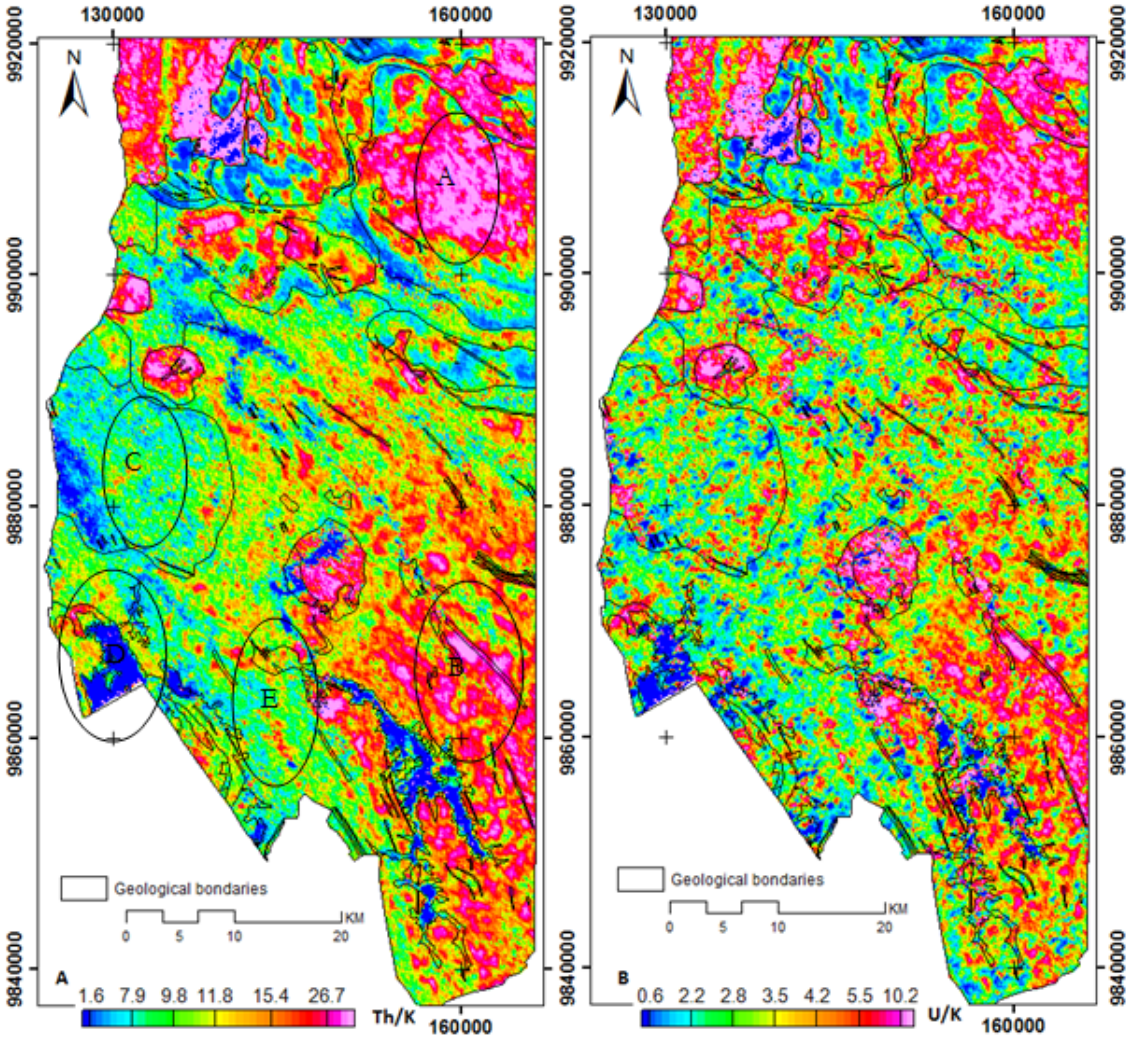

Fig 4.3.2: Thorium-Potassium Ratio (A) and) Uranium-Potassium Ratio (B) Images. Low Values (bluish-green to yellowish) indicating K Enrichment Zones

Therefore, based on the above understanding, radioelements response arising from highland regions i.e. location E, which in this study areas are mostly associated with the metasediments, can be postulated to be directly related to either bedrock geology/geochemistry or its equivalent weathering/alteration products.

Otherwise some location associated with K-enrichments zone i.e. D are spatially coincided with topographically lowland areas characterized with swamps/water bodied, (refer to Fig. 4.3.2 and compare it with Fig. 4.2.5(a) and Fig 2.6). Again, these locations are considered to be more of depositional sites and their response can not necessarily reflect bedrock characteristics as explained above.

4.5. Discussion

The study area is predominantly characterized by the metasediments. Therefore, most of the magnetic anomalies discussed in this chapter are of secondary source (i.e. secondary magnetite). Under such considerations, delineation of new lithological contact/units in the existing geological map was attempted

but with cautions. The reason is that most of the geophysical and radiometric datasets anomalies can be postulated to result from secondary or later processes in such a way that some resulting anomalies i.e. magnetic anomalies, cannot give a direct positive lithological identification of a particular unit but ranges of units (e.g., Grant, 1985b; Gunn et al., 1997). Otherwise, the processes are altogether considered to be associated with faulting, shearing, fracturing, alterations and metamorphism (possibly regional metamorphism). Some of these geological processes are indicative of compressional-transpressional tectonic regimes i.e. faulting. Hence, apart from using the datasets to understand these processes, they were also used to locate them. On the other hand, other aeromagnetic anomalies were perceived to reflect basement tectonics, deep/shallow seated structures and other variations within the individual rocks or series of rocks. Radiometric datasets were mostly utilized to study surface variations.

Variations observed with respect to the tonal variations within the individual datasets were careful incorporated, studied and compared with the corresponding lithological units on the existing geological map. Based on these variations, some units seemed to be quite different. The two lithological units located in the northern part of the study area were found to have distinctive tonal variations in the ternary image (white tonal variations at location G) an indication of presence of all 3 radioelements) contrary to the previous mapped gneiss/migmatite. One could not expect to have such distinctive tonal variations in migmatite/biotite gneiss. Therefore comparisons were made with other data to study their respective responses at these particular locations. In the reduced to pole image the areas are characterized with slightly medium to high magnetic zones and generally low values in both Th/K and U/K ratio images. These are typical characteristics of acidic intrusions (Blewett et al., 2000). When similar locations were compared using shaded Th radioelement concentration image, the pattern does not look very clear. In general, elevated concentration of Th is noted i.e. at location J on Fig 4.3.1B. New lithological units have been proposed, possibly of granodioritic/granitic in composition.

Table 4.5 Principal-component analysis of Th/K, U/K and DEM of the study area

Input Maps	PC1	PC2	PC3
Th/K	0.224	0.655	-0.722
U/K	0.259	0.674	0.692
DEM	-0.94	0.342	0.019
Variance explained (%)	60.75	33.89	5.36

Other typical K enriched zone was recognised within the western part of the area. Th/K and U/K radioelement band ratioing provided zones where K enrichment corridors are present (low Th/K and U/K). In this study, some of the low Th/K and U/K coincided with swamps and water bodies. This could be attributed by the genetic vulnerability nature of K during weathering and pedogenesis (Erdi-Krausz et al., 2003). Alternatively, correlation between K-enrichments zones with elevated regions was made. This correlation was done to deduce if these K enriched zones has spatial association with primary gold deposits. If correlated, these zones could be an indication of alteration zones. Therefore, to understand this relationship, the Th/K, U/K and DEM were integrated using principal component analysis and the result is presented in Table 4.5. In PC1, explaining 60.75% of the total variance represent antipathetic association dominated by DEM. PC2, explaining 33.89% represent positive association dominated by U/K and Th/K. PC3 (explaining 5.36% of the total variance) representing antipathetic association dominated by Th/K and U/K. Of the 3PC's, PC1 is considered most plausible representing K-enrichment zones on elevated areas. Since the relationship is antipathetic, the loadings are negated and equation 1 below was used to create ratio map and is presented in Appendix 6.

$$PC1=-1*((-0.22*Th/K) + (0.259*U/K) + (-0.95*DEM)) \quad 1$$

Still the relationship between the deposit locations and areas representing K enrichment (red) was not clear. Therefore, to firmly understand spatial relationship, the resultant map was discretized into 5 percentile and the map was reclassified at seventy five percentile and presented in appendix 6, right image. The results shows only 2 deposits were spatially correlated with the K enrichment zones.

Furthermore, the areas underlain by swamps/alluvium in the NW part of the study area were careful studied in order to deduce the corresponding bed rock geology underneath. When geophysical anomalies resulting from the swamps/alluvium were compared with those from the extreme NW of the study area being characterized by gneiss, they appear to have related magnetic characteristics. Hence the swamps were considered to overlay gneiss. Similar patterns were examined on other locations associated with the swamps and corresponding bed rock information was deduced.

On the other hand, the intebedded schist, refer to Fig 2.6, has been characterized with relatively low magnetic zones with high K enrichments. Otherwise, as said earlier, the geology of the area is mainly characterized by the metasediments. The old geological map categorized these units as lower, middle and upper units in the Karagwe Ankolean System (now KAB). In addition, no clear boundary has been provided within the map, but rather the classifications of the units were based on rock associations. The metasediments associated with sandstone horizons/conglomerates were classified as Upper units, those associated with resistant quartzitic bands are middle and finally those associated with quartzite and felspathic grit were classified as lower units.

These variations have also been observed in the magnetic data (both reduced to pole and analytical signal images). Although these magnetic variations were not distinct enough to demarcate crisp boundaries, the high magnetic anomalies can be postulated to be associated with the units where shales and mudstones were more prominent (middle and upper units).

Both first vertical and tilt derivatives of the horizontal gradient anomaly map reduced to pole were fundamental towards assessing and identifying zones of structural weakness of the area. The structural patterns from both images were careful examined and compared. It came out that most of the resultant interpreted structures coincided. In order to have a single final structural map, structures resulting from tilt derivatives of the horizontal gradient anomaly map reduced to pole were considered to be the base. In addition, structure corridors that were not extracted from tilt derivatives but were presents in the first vertical derivatives were also added in the final structural map. Similar structural trends were also observed in the first vertical and tilt derivatives of the total magnetic intensity map, but for consistency, were not incorporated in the final structural map.

Furthermore, high resolution DEM has also been very fundamental towards identifying and interpreting surficial deformation zones as well as some exposed faults. These features were also compared with the existing structural features from the geological map. Some of them coincided, others were slightly modified where the evidence were supported in the geological map. For instance, other linear features interpreted from DEM coincided with strike orientation of mapped quartzitic ridges. Off-sets associated with linear features were categorized as faults. Otherwise, these zones are vital in demarcating mineralized zones and are altogether with the interpreted bedrock lithologies are presented in the renewed geological map, Fig 4.4A.

It can be generally perceived that zones resulting from magnetic and radiometric data interpretations are attributed by several causes, some of which can be man-made. It should also be noted that rocks with similar chemical compositions can end up with different magnetic and radiometric properties/signatures (e.g., Grant, 1985a; Wilford et al., 1997). On the other hand, not all the linear features interpreted from the

DEM had direct significant geological processes/features. Therefore, verifications through ground examinations/truthing must be considered (Erdi-Krausz et al., 2003; Gunn et al., 1997) by using structural measurements as well as ground magnetics and portable gamma ray spectrometry to confirm the geological sensibility of the interpretations. This is an important strategy in interpretation of remote sensing data i. e high temperature alterations anomaly result in high magnetic zones, but continued alterations can result into their destructions (Grant, 1985b).

Otherwise, apart from these pitfalls and ambiguities, as well as other difficulties during their acquisitions (Sharma, 1987), the datasets (airborne magnetics and radiometric) coupled with DEM and geological knowledge/information of the area have been fundamental towards understanding geological processes and delineating significant geological units as well as structural features that may probably be associated with gold ore environment. The renewed geological map, with new structural and lithological features of the area is presented in Fig. 4.4A.

4.6. Conclusion

The airborne magnetic and radiometric datasets have provided an insight towards understanding the geological processes/features characterizing the study area. In addition, DEM has been fundamental towards understanding surficial deformation processes affecting the area. The anomalies and tonal variations resulting from magnetics and radiometric dataset were careful studied, compared and comprehended. In addition results from this study were also compared with other similar works already done. The main aim is to extract indicative geological features/processes related to gold mineralization of SW Uganda as presented in the conceptual model. The compressive- transpressional tectonic regimes are considered to be the main deformation phases for the transportation and deposition of gold bearing fluid. The main structural features indicative of transpressional tectonics recognized in the study area include duplex structures, strike slip faults and braided faults. Moreover, several attempts were made in this study to spatially related the K enriched zones with alteration i.e. sericitization Still the results were not satisfactory. Therefore, to this end it is evident that the K enrichments zones associated with elevated regions correspond to bedrock geological processes not directly related to sericitization.

In addition, the results of the analysis unequivocally demonstrated the dominance of the NW-SE structural trend in the area. NE-SW structural trend is also present but not prominent. The presence of mafic lithologies possibly associated with Kabanga Musongati layered complexes is still debatable and has not yet confirmed to occur in the study area.

Therefore, based on the conceptual model generated in section 2.7 of this report, a mineral deposit recognition criterion is going to be established in the next chapter. The recognition criteria are based on the indicative geological features/processes associated with gold mineralization of the study area prior to the generation of mineral potential map of the area.

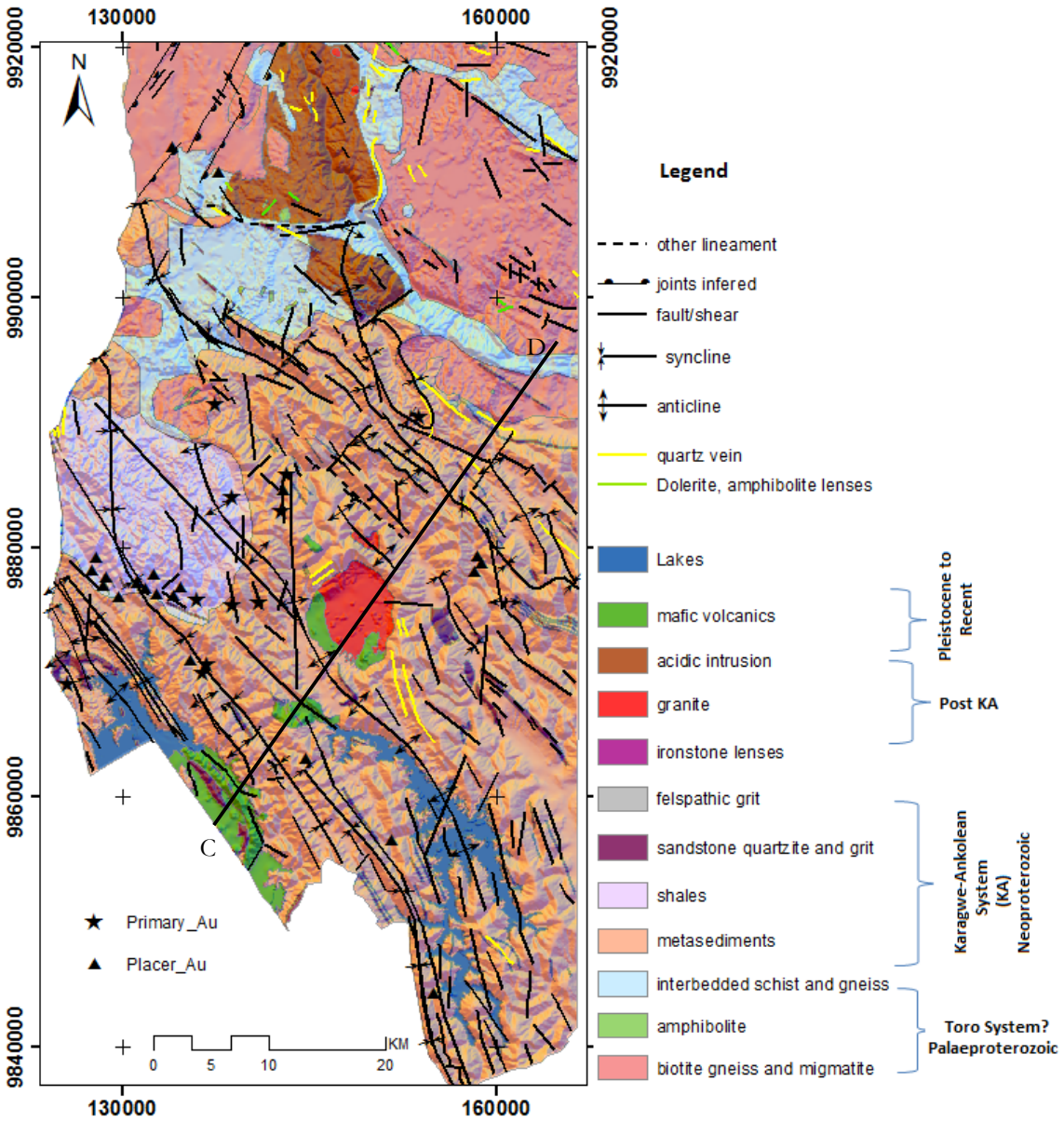

Fig 4.4A Renewed Geological Map of the Study Area

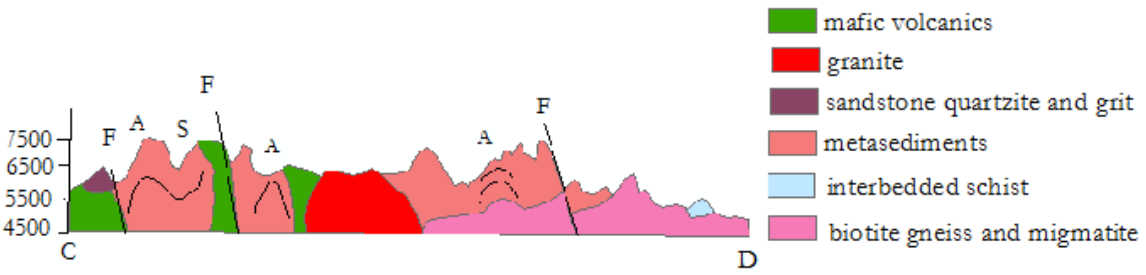

Fig 4.4B: Cross-section along line CD on the geological map Fig 4.4A. F-fault, A-anticline, S-syncline

5. MINERAL PROSPECTIVITY MODELING

5.1. Introduction

This chapter introduces the application of knowledge-driven data-guided wildcat modeling of mineral prospectivity (WMMP) as proposed by Carranza (2002) and Carranza and Hale (2002a) and later improved by Carranza (2010). The method relies on substantial understanding of indicative geological features related to the mineral deposits of interest. It is normally applied in areas with insufficient or less-explored number of known deposits. In such case, known geological knowledge of existing deposits and their spatial associations with respect to related geological processes/features are prime prerequisites (Carranza, 2008, 2010). On the other hand, substantial knowledge in the analysis of geo-spatial distribution of mineral deposits sought is vital and this can be deduced from existing or other similar deposit settings of interest occurring elsewhere.

The geodynamic evolution of the area under which the study area lies (KAB), has been discussed in chapter 2 of this report. Also, based on the mineral system approach, the first two steps i.e. critical and constituents processes (McCuaig et al., 2010) that are considered to be related to the deposit conceptual model have also been discussed in section 2.7. The evidence for the occurrence of these processes (step 3) were later studied, presented and discussed in chapter 4.

In this chapter, spatial association of the indicative geological features controlling mineralization are examined in order to produce predictor maps (step 4 of the mineral system approach) without considering their corresponding mineral deposits, i. e. assumed non-existing. Hence based on the deposit conceptual model (section 2.7), predictor maps are derived using WMMP. These maps are later integrated in order to produce predictive map indicating new favourable zones for the occurrence of new deposits. The viability of the resultant predictive mapping is tested by the number of deposits it predicts and the geological sensibility of the zones it demarcates.

5.2. Deposit Recognition Criteris

Deposit recognition criteria provide a conceptual framework for data extraction, analysis and quantification in GIS based environment. These criteria were formulated based on the conceptual model of mineral deposits under investigation (section 2.7). It should be noted that the proposed deposit recognition criteria in this study constitute the basic understanding of the geological processes/features related to the formation and deposition of the respective deposits and evidenced in the airborne magnetics and radiometric, DEM as well as geological datasets. Based on the limitation of the extraction capabilities of these datasets, not all parameters from the conceptual model were utilized in the deposit recognition criteria. Therefore, the deposit recognition criteria proposed here can be improved prior to the availability of extractable 'technicalities' of evidential layers/features related to mineralization sought under GIS package/environment.

5.2.1. Age of Mineralization

Based on the renewed geodynamic evolution of the KAB (Tack et al., 2010), in which the study are lies, the age of gold mineralization of the study area is considered to be at around 986Ma (Table 2.1). This age is conceived to be post Lomanian Orogeny (Pohl, 1987). According the general geological setting of quartz vein hosted type of gold deposit which is typical of orogenic model, it is apparent that lithological

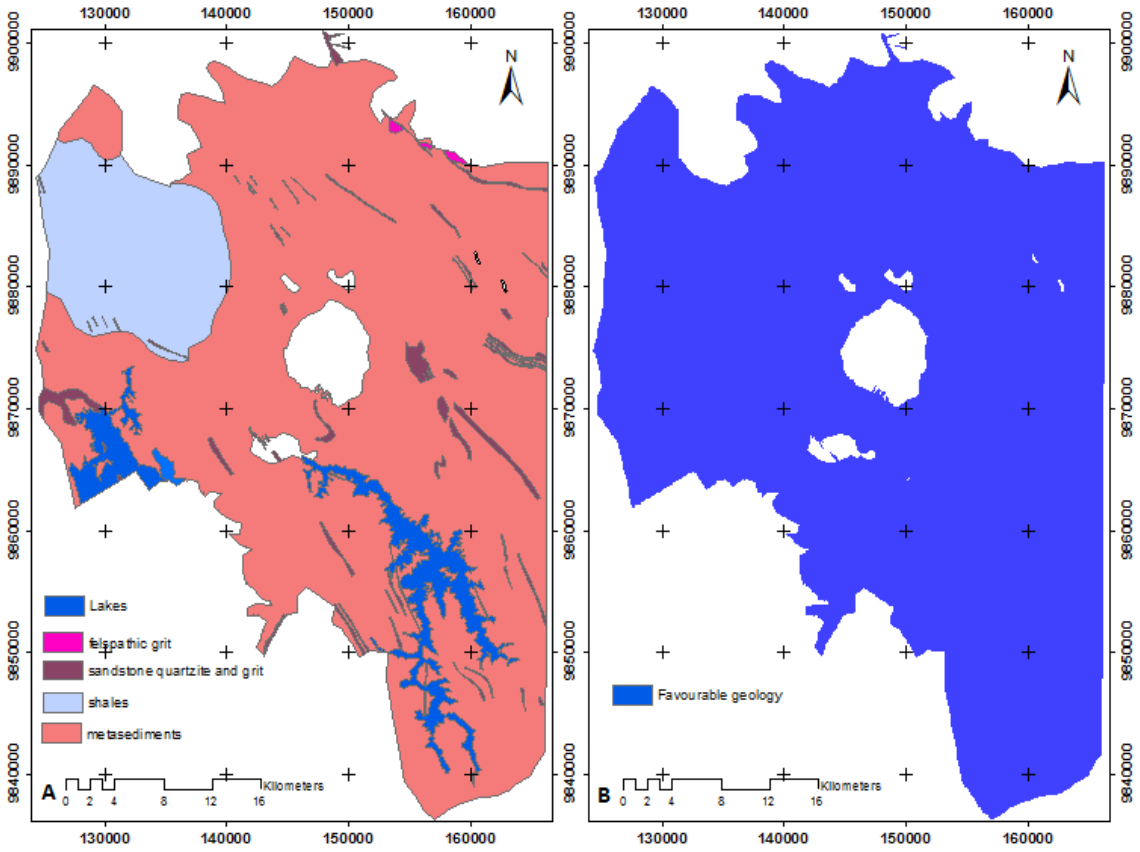

Fig 5.2.1.Evidential feature based on age of mineralization (A) and reclassified (B). Each pixel on (B) is considered prospective – white marks on the middle are granite and metavolcanics. Other on the NE are ironstone lenses (see Fig 4.4A for the units)

parameter cannot be considered as a sensible recognition criteria for controlling the spatial distribution of the respective deposits. Based on the global geological setting, these deposits can occur in any type of geological environment extending from volcano-plutonic, clastic to metamorphic terranes (Goldfarb et al., 2001; Groves et al., 1998). On the other hand, Goldfarb, (2001) emphasizes the correlation of the global thermal events associated with accretionary/collisional orogeny that are related to the formation and preservation orogenic gold deposits. These global tectonic events that are postulated to be associated with orogenic gold deposits occurred episodically: 1) before 3.0Ga, 2) between 2.8-2.5Ga, 3) between 2.1-1.8, 4) some early Neoproterozoic ages (after the growth and stabilization of Rodinian supercontinent at around 1.3 to 1Ga) and 5) during Phanerozoic ages that are associated with the evolution and break up of Pangaea (Goldfarb et al., 2001). Therefore, the type of deposits discussed in this study are conceived to be related to the narrow and confined period of late Neoproterozoic collision thermal events associated with initial phase of Gondwana formation. In the study area, such collisional thermal events coincided with Lormanian Orogeny between 1000 Ma to 950 Ma (Pohl, 1987). The corresponding lithologies that are confined to this event lie within the Karagwe Ankolean System, Fig. 4.4A. Therefore, based on this assumption, pre and post Neoproterozoic units were masked out under GIS environment and presented in Fig 5.2.1A. In addition, one deposit out of the 11 primary deposits present in the area was also considered not to be associated with the Neoproterozoic tectonic settings and was therefore not used in the predictive modelling. Hence, these favourable Neoproterozoic units are considered equally important favourability locations for the occurrence of mineral deposits sought such that all other predictors maps were calculated based on it and are presented as one favourable unit on Fig 5.2.1B.

5.2.2. Presence and Proximity to the Faults/shear and Syncloria Zones

The gold mineralization in the KAB is strongly associated structurally with brittle shearing and faulting as well as narrow syncloria deformation zones (Pohl, 1987, 1994; Pohl and Günther, 1991). The study area lies in the similar geological setting. Therefore, these geological features indicative of gold mineralizations are conceived also to be responsible for the mineralization of the area. These structural elements were extracted from DEM, airborne magnetics and existing geological map. They are considered to have provided channels for the transportation and deposition of fluids containing gold in the study area.

5.3. Application of Wildcat Modeling of Mineral Prospectivity Method (WMMP)

Application of WMMP is based on the understanding geological processes related to the type of deposits sought and proximity of these mineral deposits to their associated geological features. Based on the idealized model that characterize the spatial distribution between deposit location and their corresponding geological features, Fig 5.3, there is strong spatial association between deposit location and proximal zones rather than distal to their respective geological controls on mineralization (Carranza, 2010).

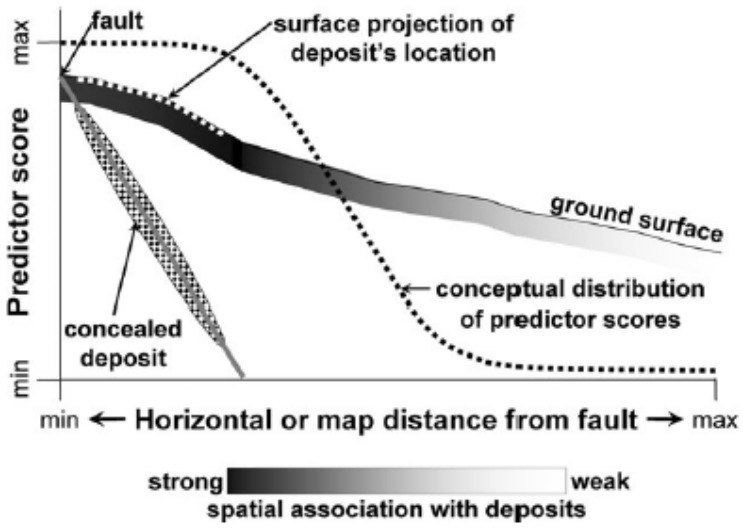

Fig 5.3 Conceptual distribution of mineral deposits, their respective controlling geological features and pattern of predictor scores *(Carranza, 2010)*

According to Carranza (2010), for a given set of geological variables at a given proximities that are conceived to be associated with mineralization sought, the wildcat predictor score, S_c (c = 1, 2… number of proximity classes) is given by:

$$S_c = \frac{1}{\tilde{d}_c} \qquad (2)$$

Where $\tilde{d}_c$ is median distance in each proximity class. Consistence in each individual class width is attained through the use of equal-percentile discretization of distance data (Carranza, 2010). Furthermore, Carranza (2010), emphasizes that equation (2) above can be improved to suffice the conceptual distribution of predictor scores with respect to indicative geological features i.e. fault, Fig 5.3, by estimating an improved wildcat predictor score, IS_C based on the following equation:

$$IS_c = \frac{1}{d_c + e^{-m(S_c - \overline{S}_c)'}} \quad (3)$$

Where c (=1, 2… n number of proximity classes, $\overline{S}_c$ is the median for the set of S_c defined in equation (2) and m an arbitrary integer representing the slope. Several input values of m are applied in the equation (3) to yield given minimum values of IS_c closest but not equal to 0 and maximum is 1 (Carranza, 2010)

In this study, based on the understanding of indicative geological features within the KAB in which the study area lies, the following geological features have been identified to be associated with the quartz vein gold hosted. They include:

1. Presence and proximity to NW-SE to NE-SW trending faults/shear. In addition, few NNW – SSE and NNE-SSW were considered as NW-SE to NE-SW trending faults/shear respectively.
2. Presence and proximity to synclines/anticlines
3. Age of mineralization (Neoproterozoic)

The age of mineralization has already been discussed in section 5.2.1 of this report.

5.3.1. Presence and proximity to NW and NE trending faults/shear

The interpreted faults were rasterized and map distances were calculated form NW and NE trending faults separately using Integrated Land and Water Information System (ILWIS) software. Five-percentile class intervals to the corresponding distances to the NW and NE faults/shear were subsequently generated.

The median of each class, $\tilde{d}_c$ of the twenty classes of 5-percentile interval is calculated and S_c , for each class is also determined using equation 2 prior to the estimations of IS_c in equation 3. The results are presented in Table 5.3.1 below.

When the improved wildcat scores, IS_c , are plotted against their corresponding distances, Fig 5.3.1, a graphical representation similar in terms of patterns to the idealized proximal model presented in Fig.5.3 is attained. Therefore, based on Table 5.3.1 and by examining Fig 5.3.1, the following spatial association between 'invisible' gold deposits to NW and NE trending faults/shear can be postulated as follows: The quartz vein gold hosted deposits are in the study area are 1) within 817.m to NW-SE trending faults/shear and 2) within 3150m to NE-SW trending faults/shear. These postulations are based on IS_c greater than 0.5.

Table 5.3.1 Proximity classes (m), median ($\tilde{d}_c$), wildcat score (S_c) and improved wildcat score (IS_c) for NW and NE trending fault/shear in (A) and (B) respectively. For (A) m=9000 and $\bar{S}_c$ -= 0.001152 whereas for (B) m= 42000 and $\bar{S}_c$ = 0.000303.

Proximity to NW-trending fault/shear				
Distance interval		$\tilde{d}_c$	S_c	IS_c
0-	67.8	33.9	0.029499	1.0000
67.8-	164.6	116.2	0.008606	1.0000
164.6-	242	203.3	0.004919	1.0000
242-	329.1	285.55	0.003502	1.0000
329.1-	406.6	367.85	0.002718	1.0000
406.6-	493.7	450.15	0.002221	0.9999
493.7-	580.8	537.25	0.001861	0.9983
580.8-	667.9	624.35	0.001602	0.9828
667.9-	764.7	716.3	0.001396	0.8998
764.7-	871.2	817.95	0.001223	0.6534
871.2-	977.7	924.45	0.001082	0.3466
977.7-	1093.8	1035.75	0.000965	0.1571
1093.8-	1219.7	1156.75	0.000864	0.0699
1219.7-	1384.2	1301.95	0.000768	0.0306
1384.2-	1548.8	1466.5	0.000682	0.0143
1548.8-	1761.8	1655.3	0.000604	0.0072
1761.8-	2013.4	1887.6	0.000530	0.0037
2013.4-	2352.2	2182.8	0.000458	0.0019
2352.2-	2875	2613.6	0.000383	0.0010
2875-	5904.8	4389.9	0.000228	0.0002
A				

Proximity to NE trending fault/shear				
Distance interval		$\tilde{d}_c$	S_c	IS_c
0-	474.3	237.15	0.004217	1.0000
474.3-	842.2	658.25	0.001519	1.0000
842.2-	1161.6	1001.9	0.000998	1.0000
1161.6-	1471.4	1316.5	0.000760	1.0000
1471.4-	1781.1	1626.25	0.000615	1.0000
1781.1-	2071.5	1926.3	0.000519	0.9999
2071.5-	2371.6	2221.55	0.000450	0.9980
2371.6-	2681.4	2526.5	0.000396	0.9803
2681.4-	2991.1	2836.25	0.000353	0.8901
2991.1-	3310.6	3150.85	0.000317	0.6487
3310.6-	3630	3470.3	0.000288	0.3513
3630-	3949.4	3789.7	0.000264	0.1633
3949.4-	4288.2	4118.8	0.000243	0.0745
4288.2-	4665.8	4477	0.000223	0.0344
4665.8-	5082	4873.9	0.000205	0.0163
5082-	5575.7	5328.85	0.000188	0.0079
5575.7-	6166.2	5870.95	0.000170	0.0038
6166.2-	6911.5	6538.85	0.000153	0.0018
6911.5-	8015	7463.25	0.000134	0.0008
8015-	13242.2	10628.6	0.000094	0.0002
B				

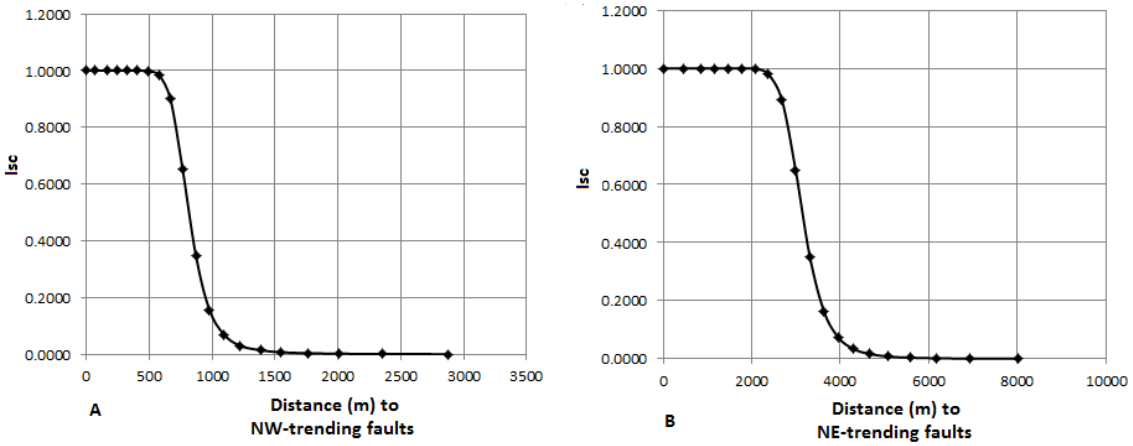

Fig 5.3.1 Graphical representation of improved wildcat predictor scores against their respective distances to NW-trending faults (A) and NE-trending faults/shear (B). Observe similar graphical representation of for conceptual/idealized distribution of predictor scores in Fig 5.3.

5.3.2. Presence and proximity to anticline and syncline

Similar rasterization and distance calculation procedures were executed to calculate $\tilde{d}_c$, S_c and IS_c using 5-percentile proximity classes to anticlines and synclines were created. The 5 percentile proximity classes are maintained in order to have narrow class width. It is postulated that the narrower the class width the higher the number of predicted deposits (Carranza and Hale, 2002a).

Now let us re-examine Fig 5.3. Consider the vertical line representing the IS_c between 0-1 as indicated in Fig 5.3.2 (A) and (B) below. At IS_c 0.5 it intercepts the graph of the conceptual distribution of IS_c score within the horizontal map distances perceived be associated strongly with the occurrence of mineral deposits sought blindly i.e. without knowing its actual location.

Therefore, by considering the favourable IS_c to be greater than 0.5, the following spatial relationship can be presented: Therefore, based on Table 5.3.2 and Fig 5.3.2, the following spatial association between 'invisible' gold deposits a to anticlines and syncline can be postulated as follows: The quartz vein gold hosted deposits are in the study area are 1) within 3842m to anticlines and 2) within 2715m synclines.

Table 5.3.2: Proximity classes (m), median $\tilde{d}_c$ wildcat score (S_c) and improved wildcat score (IS_c) for anticline and syncline in (A) and (B) respectively. For (A) m=50000 and $\overline{S}_c$ = 0.000248 whereas for (B) m= 32000 and $\overline{S}_c$ = 0.00034.

Proximity to anticlines				Proximity to synclines			
Distance interval	$\tilde{d}_c$	S_c	IS_c	Distance interval	$\tilde{d}_c$	S_c	IS_c
0 - 435.6	217.8	0.004591	1.0000	0 - 203.3	101.65	0.009838	1.0000
435.6 - 851.8	643.7	0.001554	1.0000	203.3 - 435.6	319.45	0.003130	1.0000
851.8 - 1258.4	1055.1	0.000948	1.0000	435.6 - 658.2	546.9	0.001828	1.0000
1258.4 - 1665	1461.7	0.000684	1.0000	658.2 - 909.9	784.05	0.001275	1.0000
1665 - 2061.8	1863.4	0.000537	1.0000	909.9 - 1161.6	1035.75	0.000965	1.0000
2061.8 - 2439.4	2250.6	0.000444	0.9999	1161.6 - 1452	1306.8	0.000765	1.0000
2439.4 - 2826.6	2633	0.000380	0.9986	1452 - 1761.8	1606.9	0.000622	0.9999
2826.6 - 3233.1	3029.85	0.000330	0.9839	1761.8 - 2100.6	1931.2	0.000518	0.9966
3233.1 - 3639.7	3436.4	0.000291	0.8968	2100.6 - 2487.8	2294.2	0.000436	0.9550
3639.7 - 4046.2	3842.95	0.000260	0.6508	2487.8 - 2942.7	2715.25	0.000368	0.7092
4046.2 - 4452.8	4249.5	0.000235	0.3492	2942.7 - 3455.8	3199.25	0.000313	0.2908
4452.8 - 4869	4660.9	0.000215	0.1596	3455.8 - 4036.6	3746.2	0.000267	0.0869
4869 - 5314.3	5091.65	0.000196	0.0712	4036.6 - 4714.2	4375.4	0.000229	0.0271
5314.3 - 5769.3	5541.8	0.000180	0.0334	4714.2 - 5459.5	5086.85	0.000197	0.0099
5769.3 - 6272.6	6020.95	0.000166	0.0166	5459.5 - 6224.2	5841.85	0.000171	0.0044
6272.6 - 6834.1	6553.35	0.000153	0.0085	6224.2 - 7047	6635.6	0.000151	0.0023
6834.1 - 7540.1	7187.1	0.000139	0.0044	7047 - 7889.2	7468.1	0.000134	0.0013
7540.1 - 8489.4	8014.75	0.000125	0.0021	7889.2 - 8905.6	8397.4	0.000119	0.0008
8489.4 - 9805.8	9147.6	0.000109	0.0010	8905.6 - 10347.9	9626.75	0.000104	0.0005
9805.8 - 14674.9	12240.35	0.000082	0.0002	10347.9 - 15410.6	12879.25	0.000078	0.0002
A				B			

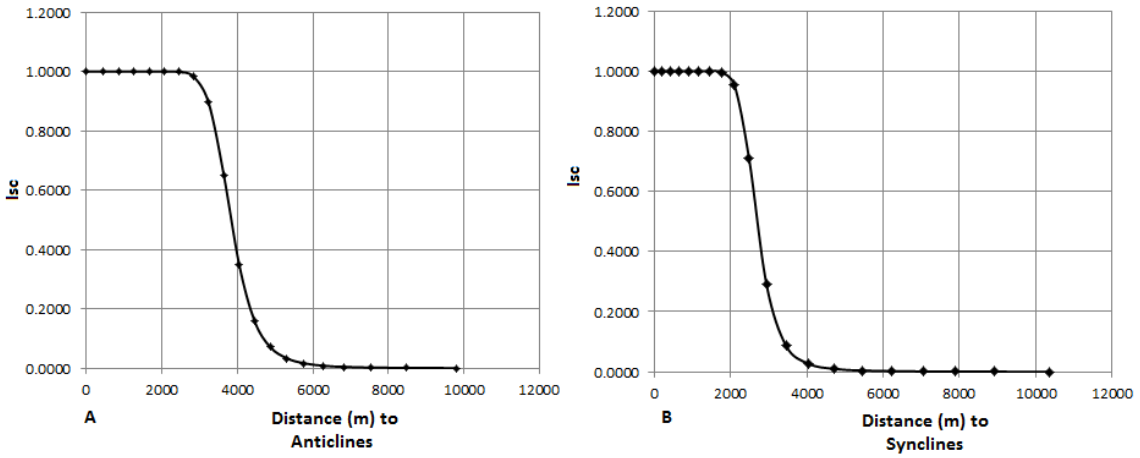

Fig 5.3.2 Graphical representation of improved wildcat predictor scores against their respective distances to anticline (A) and syncline (B). Observe similar graphical representation of for conceptual/idealized distribution of predictor scores in Fig 5.3.

5.4. Integration

As stated earlier in this report, mineral deposits are small manifestation of large scale episodical geological processes. Apart from the fact that these deposits largely depend on these geological processes, not all geological processes are resulting in mineral deposits of economic significance. The approach adopted in this study, (WMMP), created predictor maps based on improved wildcat scores of favourable zones (see section 5.3.1 and 5.3.2 above) of indicative geological features without considering the actual locations of the deposits sought (considering 'non-existing). Therefore the integration of these predictor maps should be online to this consideration.

In this study, the predictor maps generated from improved wildcat predictor scores (IS_c) were integrated using principal component analysis and presented in Table 5.4 below.

Table 5.4 Principal-component analysis of improved wildcat predictor scores of class of proximity classes of indicative geological features of the study area

Isc scores	PC1	PC2	PC3	PC4
Proximity to anticlines	-0.539	0.365	0.634	-0.418
Proximity to synclines	0.569	-0.48	0.644	-0.175
Proximity to NW- trending faults/shear	-0.359	-0.645	-0.324	-0.592
Proximity to NE-trending faults/shear	-0.507	-0.47	0.279	0.667
Variance explained (%)	33.3	28.16	19.96	18.58

Principal component analysis (PCA) is a mathematical procedure that can be used to analyse multivariate data prior to the establishment of their corresponding spatial-association (Geladi et al., 1989; Jimenez-Espinosa et al., 1993). In addition, Principal component can also be used to study and analyse alteration processes (Loughlin, 1991; Ranjbar et al., 2004), that can in turn be used to infer mineralization corridors. Carranza (2010) emphasizes the application of principal component analysis to study, analyse and interpret the multivariate association of predictor maps generated from improved wildcat predictor scores of indicative geological features related to low-sulphidation of epithermal-Au in Aroroy district, Philippines. The approach is adopted in this study.

In this study, four predictor maps are generated based on the improved wildcat scores (IS_c) as presented in Table 5.3.1 and 5.3.2. These predictor maps based on proximity to anticlines, proximity to synclines, proximity to NW-trending faults/shear and proximity to NE-trending faults/shear. The PC's of predictor maps for these geological variables were created in Integrated Land and Water Information Systems (ILWIS) software. The resulting predictor maps were later used as input maps to create PC's

The results of PC's are presented in Table 5.4 above. The PC1, explaining 33.3% of the total variance, is dominated by relative high positive loadings on proximity to synclines, relative high negative loadings on proximity to anticlines and proximity to NE-trending faults/shear. The NW-trending faults/shear has relatively low negative loadings. In PC2 (explaining about 28.16% of the total variance) is dominated by high negative loadings of proximity to NW trending fault/shear. PC3 (explaining 19.96% of the total variance) is mostly dominated by proximity distances to synclines and finally PC4 that explains 18.58% of the total variance is highly characterized by positive loading of proximity to NE trending faults/shear.

When these PC's are further examined, PC3 and PC4 are seen to be dominated by relatively high positive and relatively small negative loadings of both anticlines and synclines respectively. This relationship of

similar signs for anticline and syncline is challenging. In natural, they are supposed to have antipathetic relationship (negative and positive). Such intriguing characteristics be related to earlier tectonic history of the study area. Normally folding is a tectonic process resulting from plastic deformation of relative softer strata (in metasedimentary environment). In the study area the metasediments are composed of both softer and harder strata i.e. shales and limestone respectively. These strata respond differently to stress i.e. harder strata normally respond to stress by breaking/tearing whereas softer ones do not break but rather deform/fold (Lindgren, 1933). In extreme conditions, even softer strata eventually break and are subsequently faulted (Lindgren, 1933) and cause imbrications i.e. toppled over each other and subsequently changes their orientations. The later scenario is supported by the antipathetic dominance of the loadings for proximity to NW-trending faults/shear and proximity to NE-trending faults/shear in PC3 and PC4 respectively. The interpretation based on these PC's is also supported by early deformation history as proposed by Pohl (1987) supporting folding (D1) as the early deformation regime characterizing the area. PC2 can be considered to represent intermediate tectonic regimes as supported by antipathetic association between anticline and syncline.

When the 4 PC's are compared, PC1 is considered to be the most viable multivariate association of predictors based on antipathetic relationship synclines to anticlines, NW-trending faults/shear and NE-trending faults/shear altogether.

However, the loadings in PC1 are antipathetic related. To make the relationship geologically sensible, the loadings are negated and mineral predictive map of the study area was generated based on the aforementioned predictor score maps using the following equation:

$$P=-1*((-0.359*A) + (-0.539*B) + (-0.507*C) + (0.569*D)) \quad (4)$$

Where P is the mineral predictive map of the area, A is the improved wildcat predictor score of NW-trending faults/shear, B is the improved wildcat predictor score of proximity to anticlines and C is the improved wildcat predictor score to NE trending faults/shear (now with high negative loading) and D is the improved wildcat predictor score of proximity to synclines. The prospectivity map resulting from equation 4 was later reclassified based on 5-percentile class interval at 85 percentile class (almost Mean+1SD) and is presented in Fig 5.4 below.

5.5. Discussion

The applied wildcat modeling of mineral prospectivity (WMMP) has been useful in the determination of favourable zones for the occurrence of undiscovered deposits based on the indicative geological features in this study area where there are few existing quartz vein hosted gold deposits. The number of these deposits is significantly few to warrant the application of data-driven approach for mineral prospectivity mapping. Normally data driven approach i.e. weight of evidence, requires sufficient number of point objects (i.e. mineral deposits) to be used as training and validating datasets (Bonham-Carter, 1994). Therefore, WMMP method was employed in this study. Through improved wildcat predictor scores, predictor maps were created using the indicative geological features. In the whole process, the deposits were not used i.e. considered not present. The predictor maps, Appendix 2, were later integrated using principal component analysis in order to produce mineral potential map of the area. The mineral deposits that were previous considered not present were then used to validate the mineral prospectivity map, Fig 5.4

Six zones has been outlined as favourable for the occurrence of new deposits sought as indicated in Fig 5.4, A to F. Location A is the most interesting because almost all of the validating deposits occur. This can be attributed by the presence of duplex structures at this location, refer Fig. 4.2.3 and 4.2.4. Duplex structures are important structural features in transpressional tectonic regimes associated with high shear stress. In orogenic gold deposits, locations characterized by high shear stress are the channels for the transport and deposition of gold-bearing fluids. Similar duplex structures are also characterizing locations B and C. Therefore locations B and C are equally considered as the prime zones for the focus of gold bearing fluids

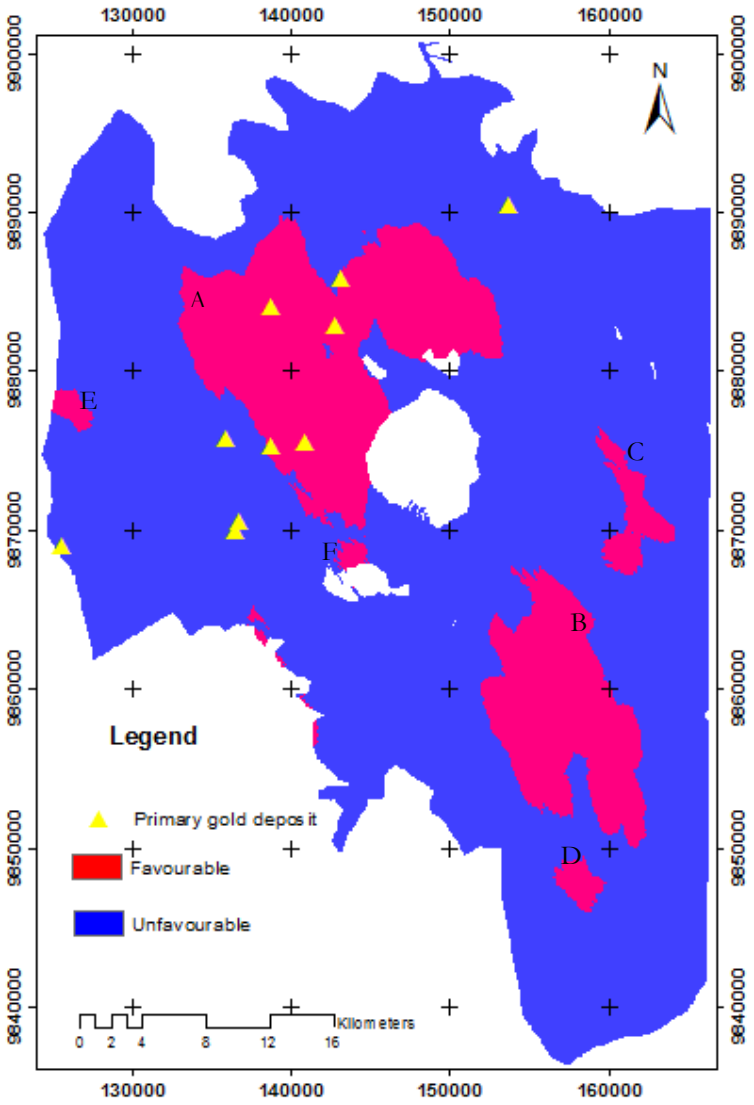

Figure 5.4 Mineral predictive map of the study area

Location D is also considered favourable for the occurrence of undiscovered deposits. This is because the zone is structurally related to suture zones running southwards to northern Rwanda where a number of gold deposits occur. The deposits include the well-studied Miyove deposit. Miyove deposit share similar tectonic controls with the quartz-vein hosted deposit discussed in this report, i.e. formed in tectonically altered region hosted in the quartz-vein and stockworks characterized by steeply dipping shear (Paterson,

2010). In addition, the continuation of regional structural features from the proposed SE favourable zones southward into Rwanda is presented in Fig 4.4A.

To the extreme west of the study area, there has been demarcated favourable zone E. This area is located at impenetrable Ibwindi forest reserve, Appendix 1. However, this zone is also surrounded by a number of placer deposit Appendix 3. Studies have been done elsewhere including in the enormous Circum-Pacific placer fields of the California foothill belt (Goldfarb et al., 1998), suggesting that the orogenic gold deposits can be the source of placer deposits around them.

5.6. Conclusion

Improved wildcat modelling of mineral prospectivity has shown its robustness in the determination of favourable zones for undiscovered deposits from the indicative geological features in the study area where there are few gold deposits existing (10 deposits). The method, being knowledge-guided data-driven (Carranza, 2010), independently (without using knowledge of the existing location of existing deposits) delineate favourable zones for the occurrence of quartz-veined gold deposits using improved wildcat scores Therefore, by assuming that ISc>0.5 (Carranza, 2010), represent favourable zones for the occurrence of quartz-veined gold deposit, the following zones are considered prospective: 1) within 817.m (calculated at 0.6534I) score to NW-trending faults/shear; 2) 3150.m (calculated at 0.6487 score) to NE-trending faults/shear; 3) 3842.m (calculated at 0.6508 ISc score) to anticlines and 4) 2715.m (calculated at 0.7092 score) to synclines.

When these predictor maps were integrated using principal component analysis, PC1 is considered to be the most viable and plausible model for gold mineralization in the study area. Hence these predictor maps were used to generate mineral prospectivity map of the area. 50% of the 10 mineral deposit occurrences tested were correctly predicted. In addition, 20% of the total area (Fig 5.4) is considered prospective. However, ground truthing is proposed to further understand these prospective zones.

6. CONCLUSION AND RECOMMENDATION

6.1. Conclusion

By referring to the research questions presented in chapter one of this report, the following conclusions are made

Q1. *How can geophysical and geological spatial variables/features existing in the south western Uganda be used to study, understand and map the evidence the geological processes related to gold mineralization?*

Through application of several filtering technique, airborne magnetic and radiometric datasets provided geological understanding related to the geological processes that have affected area. These geological processes are conceived to be responsible for the formation and preservation of quartz vein hosted gold mineralization.

The reduced to pole of the enhanced total magnetic intensity was fundamental towards understanding the relationship and genetic origin of the intrusion affected the study area. The plutonism, probably of different ages, is associated with relative low magnetic anomaly. This is an indication that the type of plutonism affected the area is of calc alkaline series. This is supported by the newly reconstructed geodynamic evolution of Karagwe Ankole Belt in which the study area lies. Both first VD and Tilt derivatives provided an insight toward understanding the deformation history of the area. Major NW and minor NE structure sutures were depicted. These structural sutures were mostly seen to be characterized by duplex structures, strike slip faults and shears, indicators of transpressional tectonic regimes.

In addition, DEM generated from 90, 135 and 360 azimuth angles of the hillshade, has also been useful towards recognizing zones associated with synclines and anticlines structural features. These features were validated with actual ground measurements digitized from the existing ground measurements from the geological maps.

Furthermore, based on the results of high resolution airborne magnetic method and DEM, in conjunction with the current knowledge of geodynamic evolution of the study area, orogenic gold deposit model is proposed to be typical gold deposit model characterizing the area.

Q2. *How can the current knowledge of geological processes/features associated with gold mineralization in SW Uganda be used to determine and predict viable and plausible sites potential for the undiscovered deposits?*

Based on the current geological understanding of the gold mineralization in SW Uganda, improved wildcat modeling of mineral prospectivity can be used to determine and predict viable and plausible sites potential for the occurrence of undiscovered gold deposits. Due to the fact that the area has got few existing deposits, the method independently (without using locations of target quartz veined mineral deposits) created predictor maps based on proximity to synclines, favourable proximity to anticlines, favourable proximity to NW-trending structures as well as favourable proximity to NE-trending faults/shear. These favourable proximities to the occurrence of gold deposits were then integrated using principal component analysis prior to the generation of mineral prospectivity map of the study area. The result of the integration shows proximity to NW-trending faults/shear, proximity to NE-trending faults/shear and proximity to anticlines are the most plausible and viable indicative geological features controlling gold

mineralization of the area. In addition, 50% of the 10 mineral deposits validated were correctly predicted. 20% of the tested area, Fig 5.4, is considered prospective (132265 out of 661085 pixels).

6.2. Recommendation

1. A follow up ground geological, structural and stream sediments mapping of the proposed favourable zones is recommended. To start, emphasis should be given to zones B and D so as to study the effect of structural extension to Rwanda where a well-studied Miyove deposit occurs.
2. A systematic approach is recommended to confirm if the K-enriched corridors delineated by both Th/K and U/K ratio images are related to sericitization. This will ultimately improve the mineral prospectivity map of the area.
3. Quantitative analysis of the magnetic anomalies is proposed to infer their depths. This will be significantly important to deduce if these anomalies are related to either deeper or surficial geological processes. In case they are related to deeper tectonic processes, their relation to the basement geology/plutonism can be clarified.

LIST OF REFERENCES

Airo, M.L., 2002, Aeromagnetic And Aeroradiometric Response To Hydrothermal Alteration: Surveys in Geophysics, v. 23, p. 273-302.

Airo, M.L., and Mertanen, S., 2008, Magnetic signatures related to orogenic gold mineralization, Central Lapland Greenstone Belt, Finland: Journal of Applied Geophysics, v. 64, p. 14-24.

Al-Garni, M.A., 2010, Magnetic survey for delineating subsurface structures and estimating magnetic sources depth, Wadi Fatima, KSA: Journal of King Saud University - Science, v. 22, p. 87-96.

Arehart, G.B., 1996, Characteristics and origin of sediment-hosted disseminated gold deposits: a review: Ore Geology Reviews, v. 11, p. 383-403.

Asadi, H.H., and Hale, M., 2001, A predictive GIS model for mapping potential gold and base metal mineralization in Takab area, Iran: Computers & Geosciences, v. 27, p. 901-912.

Ates, A., Büyüksaraç, A., Bilim, F., Bektas, Ö., Sendur, Ç., and KomanovalI, G., 2009, Spatial correlation of the aeromagnetic anomalies and seismogenic faults in the Marmara region, NW Turkey: Tectonophysics, v. 478, p. 135-142.

Bennett, D.G., and Barker, A.J., 1992, High salinity fluids: The result of retrograde metamorphism in thrust zones: Geochimica et Cosmochimica Acta, v. 56, p. 81-95.

Blewett, R.S., Wellman, P., Ratajkoski, M., and Huston, D.L., 2000, Atlas of North Pilbara: Australian Geological Survey, v. 4, p. 36.

Bonham-Carter, G.F., 1994, Geographic Information Systems for Geoscientisr: Modelling with GIS, Pergamon, 398 p.

Brinckmann, J., Lehmann, B., and Timm, F., 1994, Proterozoic gold mineralization in NW Burundi: Ore Geology Reviews, v. 9, p. 85-103.

Brodie, R.C., 2002, Airborne and Ground Magnetics: Geoscience Australia, v. ACT 2601, p. 13.

Buchwaldt, R., Toulkeridis, T., Todt, W., and Ucakuwun, E.K., 2008, Crustal age domains in the Kibaran belt of SW-Uganda: Combined zircon geochronology and Sm-Nd isotopic investigation: Journal of African Earth Sciences, v. 51, p. 4-20.

Butler, R., and Gordon, C., 2010, Duplexes and thrust sequences (http://www.see.leeds.ac.uk/structure/assyntgeology/geology/thrusts/what/duplexes.htm).

Campbell, M.T., and Kerrich, R., 1998, P--T--t--deformation--fluid characteristics of lode gold deposits: evidence from alteration systematics: Ore Geology Reviews, v. 12, p. 381-453.

Carranza, E.J.M., 2002, Geologically-constrained mineral [potential mapping (examples from the Philippines): PhD-Thesis, Delft University of Technology, The Netherlands. ITC- University of Twente. , Enschede, v. Publication No. 86, p. 480p.

Carranza, E.J.M., 2008, Geochemical anomaly and mineral prospectivity mapping in GIS: Amsterdam, Elsevier, 366 p.

Carranza, E.J.M., 2010, Improved wildcat modelling of mineral prospectivity: In: Resource geology, 60(2010)2, pp. 129-149.

Carranza, E.J.M., and Hale, M., 2002a, Wildcat mapping of gold potential, Baguio district, Philippines: Transactions of the Institution of Mining and Metallurgy : Section B : Applied earth science, v. 111.

Cassidy, K.F., Groves, D.I., and McNaughton, N.J., 1998, Late-Archean granitoid-hosted lode-gold deposits, Yilgarn Craton, Western Australia: Deposit characteristics, crustal architecture and implications for ore genesis: Ore Geology Reviews, v. 13, p. 65-102.

Cox, S.F., Wall, V.J., Etheridge, M.A., and Potter, T.F., 1991, Deformational and metamorphic processes in the formation of mesothermal vein-hosted gold deposits -- examples from the Lachlan Fold Belt in central Victoria, Australia: Ore Geology Reviews, v. 6, p. 391-423.

Dickson, B.L., Fraser, S.J., and Kinsey-Henderson, A., 1996, Interpreting aerial gamma-ray surveys utilising geomorphological and weathering models: Journal of Geochemical Exploration, v. 57, p. 75-88.

Eisenlohr, B.N., Groves, D., and Partington, G.A., 1989, Crustal-scale shear zones and their significance to Archaean gold mineralization in Western Australia: Mineralium Deposita, v. 24, p. 1-8.

Erdi-Krausz, G., Matolin, M., Minty, B., Nicolet, J.P., Reford, W.S., and Schetselaar, E.M., 2003, Guidelines for radioelement mapping using gamma ray spectrometry data: International Atomic Energy Agency (IAEA), p. 173.

Fan, H.R., Zhai, M.G., Xie, Y.H., and Yang, J.H., 2003, Ore-forming fluids associated with granite-hosted gold mineralization at the Sanshandao deposit, Jiaodong gold province, China: Mineralium Deposita, v. 38, p. 739-750.

Geladi, P., Isaksson, H., Lindqvist, L., Wold, S., and Esbensen, K., 1989, Principal component analysis of multivariate images: Chemometrics and Intelligent Laboratory Systems, v. 5, p. 209-220.

Ghazala, H.H., 1993, Geological and structural interpretation of airborne surveys and its significance for mineralization, South Eastern Desert, Egypt: Journal of African Earth Sciences, v. 16, p. 273-285.

Gibson, R.G., 1990, Nucleation and growth of retrograde shear zones: an example from the Needle Mountains, Colorado, U.S.A: Journal of Structural Geology, v. 12, p. 339-350.

Goldfarb, R.J., Groves, D.I., and Gardoll, S., 2001, Orogenic gold and geologic time: a global synthesis: Ore Geology Reviews, v. 18, p. 1-75.

Goldfarb, R.J., Phillips, G.N., and Nokleberg, W.J., 1998, Tectonic setting of synorogenic gold deposits of the Pacific Rim: Ore Geology Reviews, v. 13, p. 185-218.

Grant, F.S., 1985a, Aeromagnetics, geology and ore environments, I. Magnetite in igneous, sedimentary and metamorphic rocks: An overview: Geoexploration, v. 23, p. 303-333.

Grant, F.S., 1985b, Aeromagnetics, geology and ore environments, II. Magnetite and ore environments: Geoexploration, v. 23, p. 335-362.

Groves, D., 1993, The crustal continuum model for late-Archaean lode-gold deposits of the Yilgarn Block, Western Australia: Mineralium Deposita, v. 28, p. 366-374.

Groves, D.I., Goldfarb, R.J., Gebre-Mariam, M., Hagemann, S.G., and Robert, F., 1998, Orogenic gold deposits: A proposed classification in the context of their crustal distribution and relationship to other gold deposit types: Ore Geology Reviews, v. 13, p. 7-27.

Gunn, P.J., Maidment, D., and Milligan, P.R., 1997, Interpreting Aeromagnetic Data in Areas of Limited Outcrop: AGSO Journal of Australian Geology and Geophysics, v. 17, p. 175-185.

Hamilton, W.R., Woolley, A.R., and Bishop, A.C., 1995, Hamlyn guide : minerals, rocks and fossils: London etc., Hamlyn, 320 p.

Hedenquist, J.W., and Lowenstern, J.B., 1994, The role of magmas in the formation of hydrothermal ore deposits: Nature, v. 370, p. 519-527.

Hester, B., Boberg, W., Tuhumwire, J.T., Odida, J., Katto, E., and Nyakaana, J., 2006, Opportunities for mining investiment in Uganda: Entebe, Ministry of Energy and Mineral Develop[ment of Uganda through Brian W. Hester Inc, p. 68p.

Hinde, C., and Peters, T., 2007, Uganda-Introduction and country overview: Mining Journal special publication, p. 8p.

Holden, E.-J., Dentith, M., and Kovesi, P., 2008, Towards the automated analysis of regional aeromagnetic data to identify regions prospective for gold deposits: Computers & Geosciences, v. 34, p. 1505-1513.

Hosseinali, F., and Alesheikh, A.A., 2008, Weighting Spatial Information in GIS for Copper Mining Exploration: American Journal of Applied Sciences, v. 5, p. 1187-1198.

Jaboyedoff, M., Couture, R., and Locat, P., 2009, Structural analysis of Turtle Mountain (Alberta) using digital elevation model: Toward a progressive failure: Geomorphology, v. 103, p. 5-16.

Jacques, A.L., Wellman, P., Whitaker, A., and Wyborn, D., 1997, High-Resolution Geophysics in Modern Geological Mapping: AGSO Journal of Australian Geology and Geophysics, v. 17, p. 159-173.

James, P.D., 1991, Plate Tectonic Theory (http://www.drjpdawson.com/pelgnet/pelchap3/Chap3.html), Volume 2011.

Jimenez-Espinosa, R., Sousa, A.J., and Chica-Olmo, M., 1993, Identification of geochemical anomalies using principal component analysis and factorial kriging analysis: Journal of Geochemical Exploration, v. 46, p. 245-256.

Knox-Robinson, C.M., and Wyborn, L.A.I., 1997, Towards a holistic exploration strategy: Using Geographic Information Systems as a tool to enhance exploration: Australian Journal of Earth Sciences: An International Geoscience Journal of the Geological Society of Australia, v. 44, p. 453 - 463.

Kogre, C.A., and Afilaka, J.O., 1988, Review of Africa's solid mineral resource potential: Journal of African Earth Sciences, v. 7, p. 589-600.

Lang, J., and Baker, T., 2001, Intrusion-related gold systems: the present level of understanding: Mineralium Deposita, v. 36, p. 477-489.

Lindgren, W., 1933, Mineral deposits: McGraw-Hill, New York and London, p. 930p.

Loughlin, W.P., 1991, Principal Component Analysis for Alteration Mapping: Photogrammetric Engineering and Remote Sensing, v. 57, p. 1163-1169.

McCuaig, T.C., Beresford, S., and Hronsky, J., 2010, Translating the mineral systems approach into an effective exploration targeting system: Ore Geology Reviews, v. In Press, Corrected Proof.

Milligan, P.R., and Gunn, P.J., 1997, Enhancement and Presentation of Airborne Geophysical Data: AGSO Journal of Australian Geology and Geophysics, v. 17, p. 63-75.

Nelson, J.B., 1994, Leveling total-field aeromagnetic data with measured horizontal gradients: Geophysics, v. 59, p. 1166-1170.

Pal, N., and Mishra, B., 2002, Alteration geochemistry and fluid inclusion characteristics of the greenstone-hosted gold deposit of Hutti, Eastern Dharwar Craton, India: Mineralium Deposita, v. 37, p. 722-736.

Paterson, G.W.L., 2010, A Report prepared for Rwanda Geology and Mines Authority (OGMR): OGMR Reference N°: 10/02/09, p. 50.

Pickup, G., and Marks, A., 2000, Identifying large-scale erosion and deposition processes from airborne gamma radiometrics and digital elevation models in a weathered landscape: Earth Surface Processes and Landforms, v. 25, p. 535-557.

Pliler, R., and Adams, J.A.S., 1962, The distribution of thorium, uranium, and potassium in the Mancos shale: Geochimica et Cosmochimica Acta, v. 26, p. 1115-1135.

Pohl, W., 1987, Metallogeny of the northeastern Kibaran belt, Central Africa: Geological Journal, v. 22, p. 103-119.

Pohl, W., 1994, Metallogeny of the northeastern Kibara belt, Central Africa--Recent perspectives: Ore Geology Reviews, v. 9, p. 105-130.

Pohl, W., and Günther, M.A., 1991, The origin of Kibaran (late Mid-Proterozoic) tin, tungsten and gold quartz vein deposits in Central Africa: a fluid inclusions study: Mineralium Deposita, v. 26, p. 51-59.

Poulsen, K.H., Card, K.D., and Franklin, J.M., 1992, Archean tectonic and metallogenic evolution of the superior province of the canadian shield: Precambrian Research, v. 58, p. 25-54.

Radulescu, J., 1982, Mineralization in the Karagwe-Ankolean system of East Africa/Burundi: The Development Potential of Precambrian Mineral Deposits, v. UN Department of Techical Cooperation and Development, p. 217-225.

Raghuwanshi, S.S., 1992, Airborne gamma-ray spectrometry in uranium exploration: Advances in Space Research, v. 12, p. 77-86.

Ranjbar, H., Honarmand, M., and Moezifar, Z., 2004, Application of the Crosta technique for porphyry copper alteration mapping, using ETM+ data in the southern part of the Iranian volcanic sedimentary belt: Journal of Asian Earth Sciences, v. 24, p. 237-243.

Reeves, C.V., 2005, Aeromagnetic Surveys: Principles, Practice and Interpretation Geosoft, 155 p.

Reford, S., 2006, Gradient enhancement of the total magnetic field: The Leading Edge, v. 25, p. 59-66.

Rumvegeri, B.T., 1991, Tectonic significance of Kibaran structures in Central and Eastern Africa: Journal of African Earth Sciences (and the Middle East), v. 13, p. 267-276.

Schetselaar, E.M., Chung, C.-J.F., and Kim, K.E., 2000, Integration of Landsat TM, Gamma-Ray, Magnetic, and Field Data to Discriminate Lithological Units in VegetatedGranite-Gneiss Terrain: Remote Sensing of Environment, v. 71, p. 89-105.

Scott, M., 2000, GIS, Modern mineral potential modeling and quantitative resource assessment: Implications for the Geological Survey of QUEENSLAND: AIG Journal – Applied geoscientific research and practice in Australia, v. 2, p. 16.

Sewell, D.M., and Wheatley, C.J.V., 1994, The Lerokis and Kali Kuning submarine exhalative gold-silver-barite deposits, Wetar Island, Maluku, Indonesia: Journal of Geochemical Exploration, v. 50, p. 351-370.

Sharma, P.V., 1987, Magnetic method applied to mineral exploration: Ore Geology Reviews, v. 2, p. 323-357.

Sibson, R.H., Moore, J.M.M., and Rankin, A.H., 1975, Seismic pumping--a hydrothermal fluid transport mechanism: Journal of the Geological Society, v. 131, p. 653-659.

Sillitoe, R.H., 1997, Characteristics and controls of the largest porphyry copper-gold and epithermal gold deposits in the circum-Pacific region: Australian Journal of Earth Sciences: An International Geoscience Journal of the Geological Society of Australia, v. 44, p. 373 - 388.

Steenland, N.C., 1970, Recent developments in aeromagnetic methods: Geoexploration, v. 8, p. 185-204.

Tack, L., De Paepe, P., Liégeois, J.P., Nimpagaritse, G., Ntungicimpaye, A., and Midende, G., 1990, Late Kibaran magmatism in Burundi: Journal of African Earth Sciences (and the Middle East), v. 10, p. 733-738.

Tack, L., Liégeois, J.P., Deblond, A., and Duchesne, J.C., 1994, Kibaran A-type granitoids and mafic rocks generated by two mantle sources in a late orogenic setting (Burundi): Precambrian Research, v. 68, p. 323-356.

Tack, L., Wingate, M.T.D., De Waele, B., Meert, J., Belousova, E., Griffin, B., Tahon, A., and Fernandez-Alonso, M., 2010, The 1375 Ma "Kibaran event" in Central Africa: Prominent emplacement of bimodal magmatism under extensional regime: Precambrian Research, v. 180, p. 63-84.

Verduzco, B., Fairhead, J.D., Green, C.M., and MacKenzie, C., 2004, New insights into magnetic derivatives for structural mapping: The Leading Edge, v. 23, p. 116-119.

Wilford, J., 2002, Airborne gamma-ray spectrometry: Cooperative Research Centre for Landscape Envirionments and Mineral Exploration, Commonwealth Scientific and Industrial Research Organization, Bertley, WA, Australia. Open File Rep, v. 144.

Wilford, J.R., Bierwirth, P.N., and Craig, M.A., 1997, Application of airborne gamma-ray spectrometry in soil/regolith mapping and applied geomorphology: AGSO Journal of Australian Geology and Geophysics, v. 17, p. 201-216.

Zhu, Y., Zhou, J., and Zeng, Y., 2007, The Tianger (Bingdaban) shear zone hosted gold deposit, west Tianshan, NW China: Petrographic and geochemical characteristics: Ore Geology Reviews, v. 32, p. 337-365.

APPENDIX

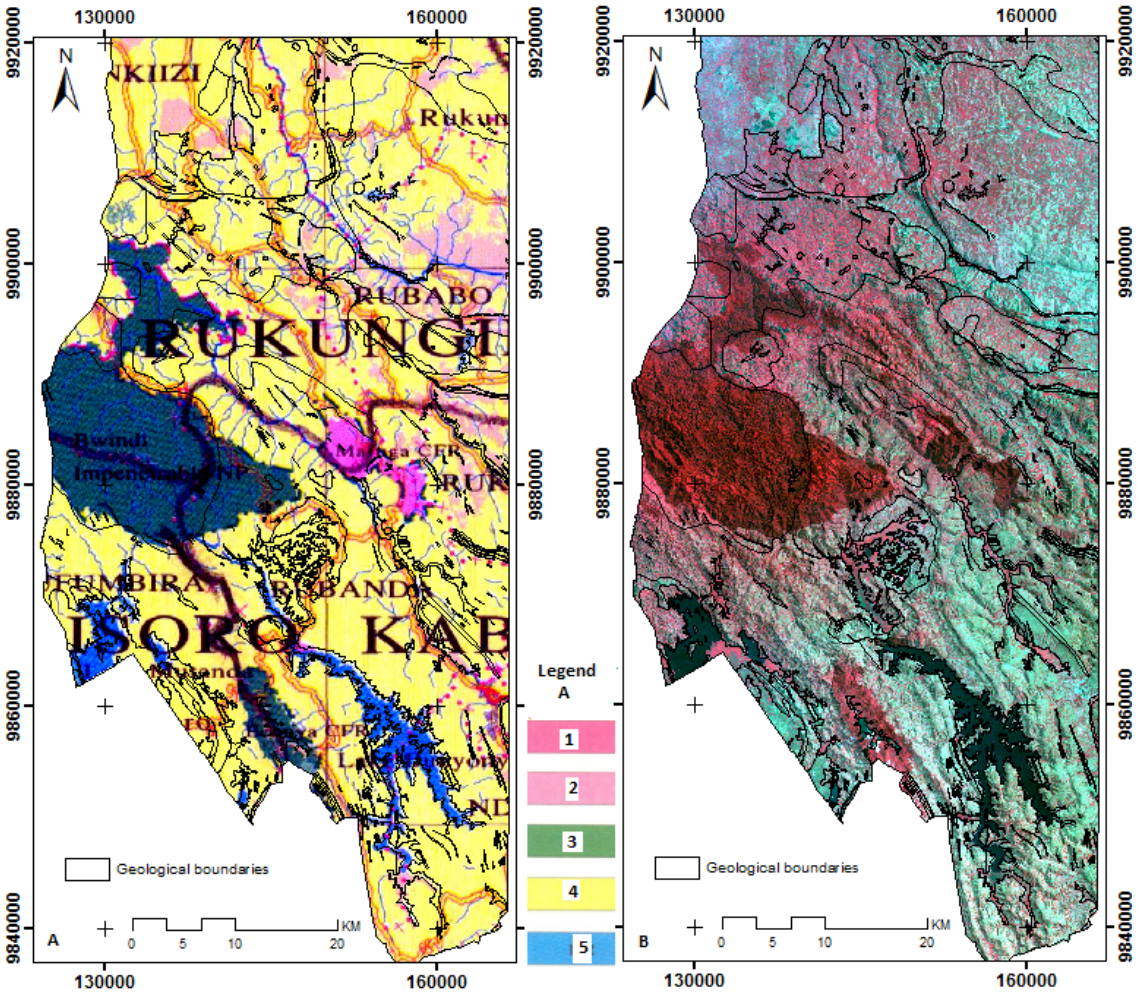

Appendix 1: Vegetation index map of the study area (A) - (adopted from Uganda Department of Forest, 1996), supported by Landsat TM R:G:B 4:3:2. Observe the 'impenetrable Bwindi Tropical Forest' to the west of the area. 1=broadleaved trees, 2=coferious plantations, 3=fully stocked tropical forest, 4= farmland 5= open water

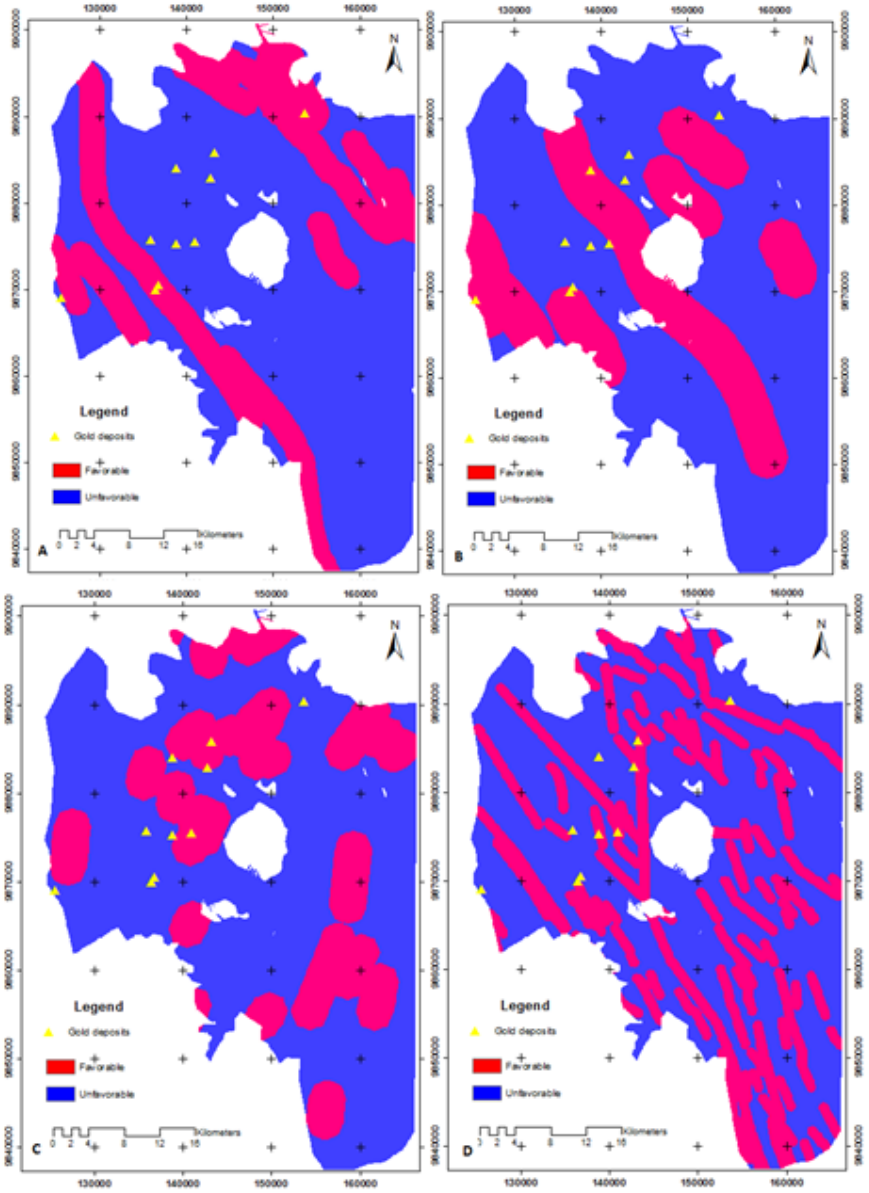

Appendix.2 Predictor maps based on improved wildcat scores-created from 5-percentile classes and reclassified above 75-percentile for (A) synclines and (B) anticlines (C) NE trending faulta/shear and (D) NW-trending faults/shear. 3 deposits were correctly predicted by predictor score map (A) and 5deposits from predictor score from maps (B), (C) and (D).

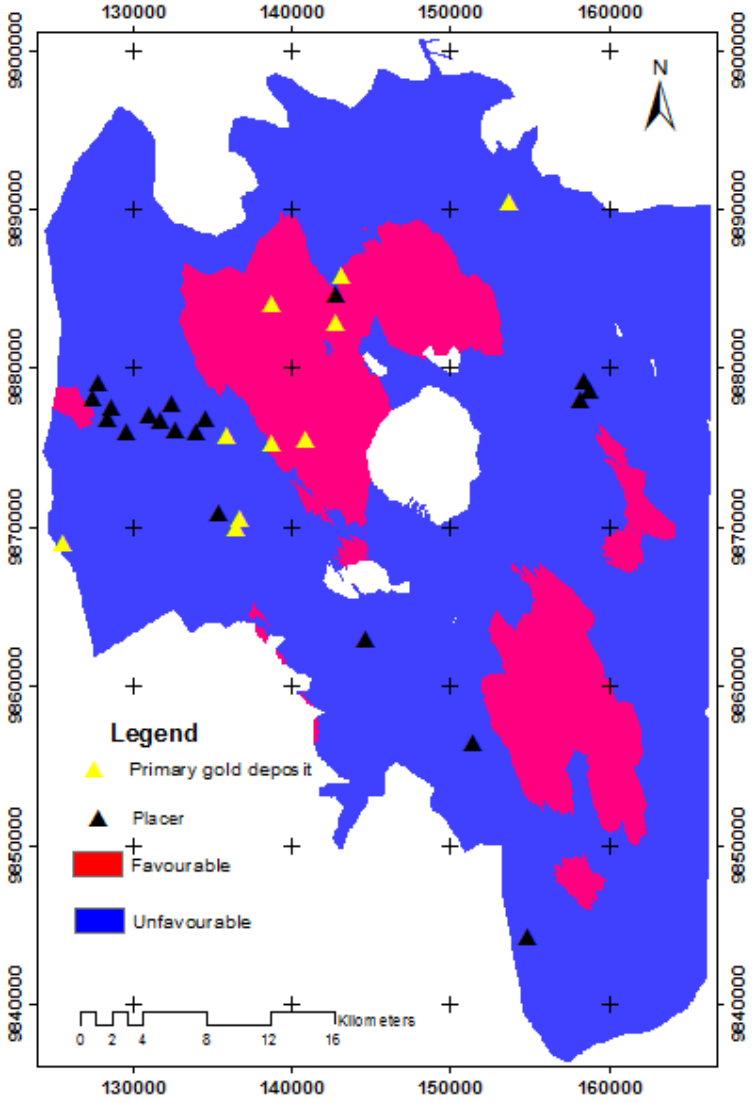

Appendix 3 Prospectivity Map of the area showing primary and placer gold deposits

Step 1:
Launch the tool (Project Manager|Menu **Filtering > Horizontal Gradient TMI Enhancement** (previously **Horizontal Gradient Gridding**)
Step 2:

Specify the X component grid. This corresponds to the across-track gradient (**G_transverse**).

Step 3:
Choose **Next**. INTREPID displays the next page
Step 4:
Specify the grid band number (Specify 1 for single band grids)
Step 5:
Choose **Next**. INTREPID displays the next page
Step 6:

Specify the X component grid. This corresponds to the across-track gradient (**G_longitudinal**).
Step 7:
Choose **Next**. INTREPID displays the next page.
Step 8:

Specify the grid band number (Specify 1 for single band grids).
Step 9
Choose **Next**. INTREPID displays the next page.

Step 10

(If you want INTREPID to calculate the vertical derivative):

- Check the **Optional Vertial Differentiation** checkbox
- Specify the **Order of Differentiation**

Step 11

Specify the output grid in the **Save the reconstructed grid as** text box.
Step 12
Choose **Finish**

Appendix 4: Steps towards creating enhanced gradient TMI

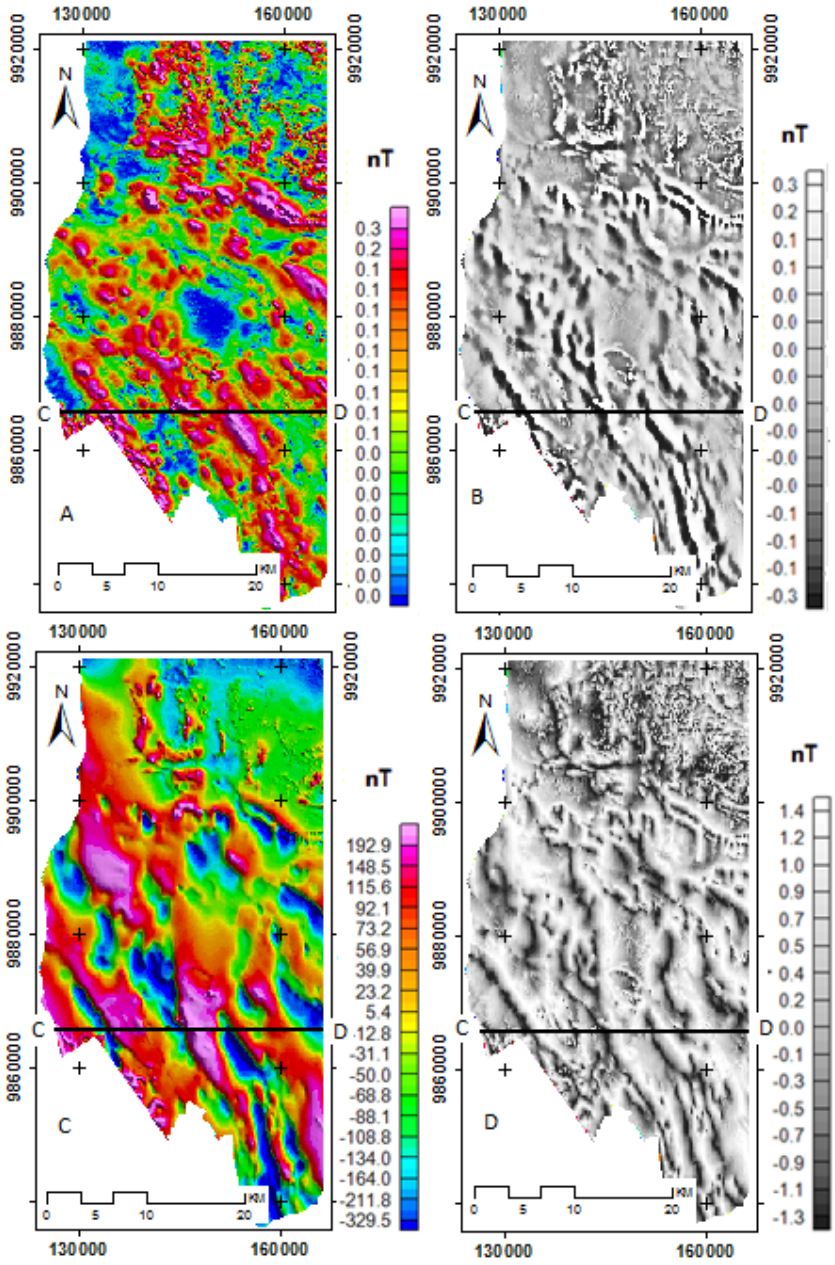

Appendix 5: Geophysical datasets with profile location displayed in Fig 4.1. A-Analytical signal, B-first vertical derivatives, C- Reduced to pole and D- tilt derivatives

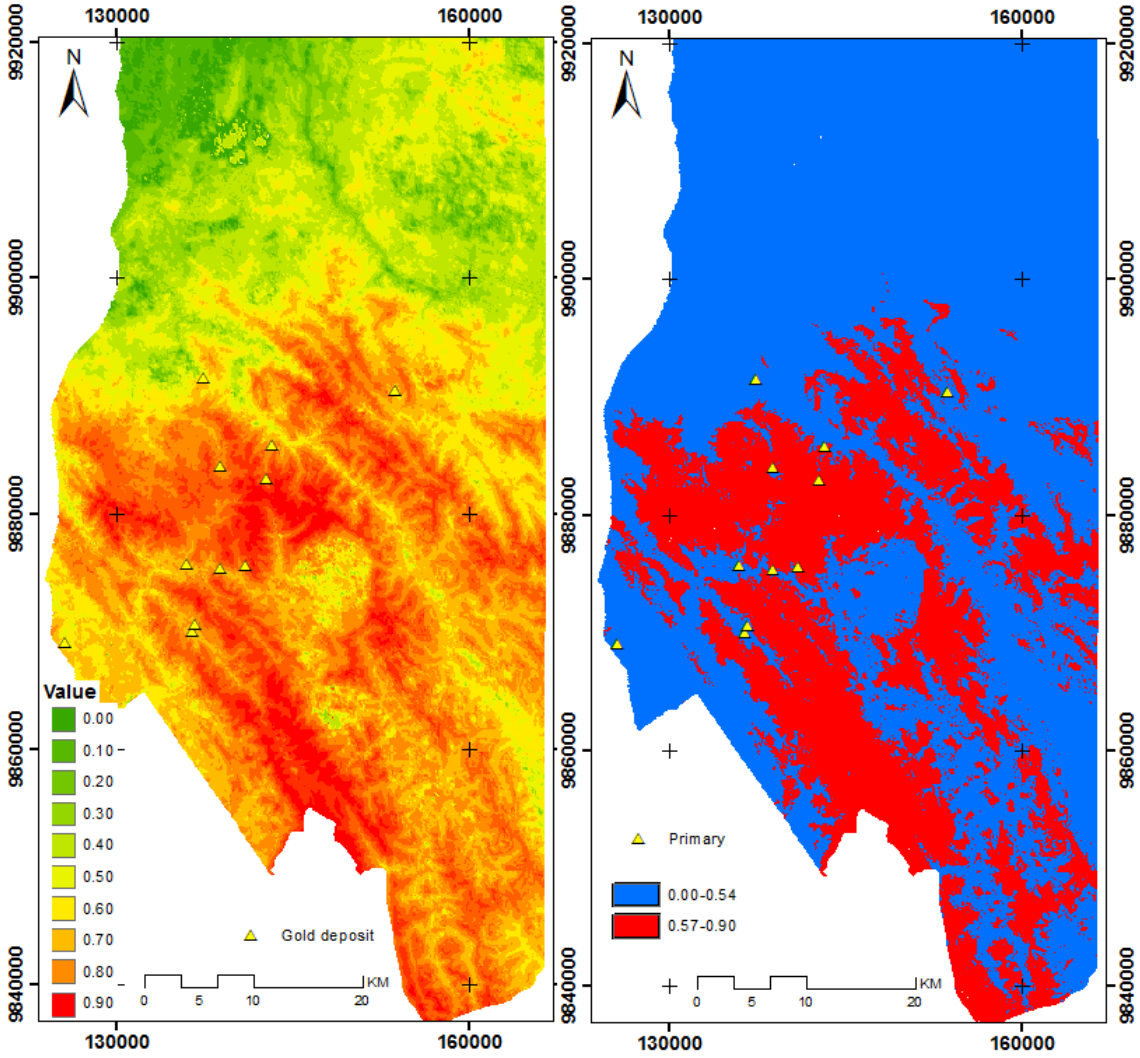

Appendix 6: PC1 analysis of Th/K, U/K and DEM-left and its 75 percentile image on the right